MOTOR NEURONS ARE ESSENTIAL FOR VASCULAR PATHFINDING

by

Amy H. Lim

A dissertation submitted to the faculty of
The University of Utah
in partial fulfillment of the requirements for the degree of

Doctor of Philosophy

Department of Neurobiology and Anatomy

The University of Utah

December 2011

The University of Utah Graduate School

STATEMENT OF DISSERTATION APPROVAL

The dissertation of **Amy H. Lim**

has been approved by the following supervisory committee members:

Chi-Bin Chien	, Chair	**2011-08-11** Date Approved
Dean Y. Li	, Member	**2011-06-23** Date Approved
Richard Dorsky	, Member	**2011-07-21** Date Approved
Mark M. Metzstein	, Member	**2011-07-21** Date Approved
Monica L. Vetter	, Member	**2011-07-21** Date Approved

and by **Monica L. Vetter**, Chair of the Department of **Neurobiology and Anatomy**

and by Charles A. Wight, Dean of The Graduate School.

ABSTRACT

The nervous and vascular systems are highly branched cellular networks and track along parallel pathways throughout the body. The similarities between these two systems extend beyond the gross anatomical level all the way to the molecular level, as cells in both networks respond to common guidance cues during development. Netrin, one of the first neural guidance cues to be identified, is an example of one of these shared guidance molecules. In the nervous system, Netrin can attract or repel axons, depending on the type of receptors expressed by its leading structure, the growth cone. Here, I set out to define the effect of Netrin on the developing vasculature. It has been previously demonstrated that Netrin1a is required for the formation of a specific vascular structure in zebrafish, the parachordal chain (PAC). Muscle pioneers have further been identified as the source of Netrin1a required for PAC formation. However, the receptor(s) by which Netrin1a signals to regulate PAC formation had not yet been defined. Furthermore, it is unknown if the effect of Netrin on PAC formation is direct or indirect.

In this dissertation, I show that Netrin1a's effect on zebrafish vascular development is mediated by at least the effect of two known Netrin receptors: Unc5b and deleted in colorectal cancer (DCC). First, I show that embryos depleted of Unc5b do not form a PAC, phenocopying Netrin1a morphants, suggesting that Unc5b is a receptor that

mediates Netrin1a's effect on PAC formation. Second, I demonstrate that the effect ofNetrin1a on PAC development is due at least partly to a requirement for motor neuron axon guidance at the horizontal myoseptum (HMS), which is mediated through DCC. The ongoing controversy about whether Netrin1a is attractive or respulsive for endothelial cells appears most in the case of the PAC, where Netrin1a acts on lymphendothelial cells only indirectly, through motor neuron axons. I show that DCC is expressed in motor neurons whose axons track along the HMS, and that depletion of Netrin1a or DCC disrupts motor neuron axon turning at the HMS. Using genetic and surgical approaches, I further demonstrate that motor axons are necessary for PAC formation at the HMS. These observations provide the first evidence that axons can guide vessel formation and pathfinding.

TABLE OF CONTENTS

ACKNOWLEDGEMENTS

I would like to thank the many people who contributed to the work described in this dissertation. These include: members of the Chien lab, especially Chi-Bin Chien and Arminda Suli; members of the Li lab, especially Dean Li, Joshua Wythe, Frédéric Larrieu-Lahargue, Kirk Thomas, Aubrey Chan, Nyall London and Matthew Smith; Karina Yaniv and Brant Weinstein; Laura Hale, Sarah Hutchinson and Judith Eisen; Nathan Lawson and members of his lab; Michael Granato and members of his lab; Chris Rodesch and Keith Carney at the Cell Imaging Core, Gretchen King and the staff at the Centralized Zebrafish Core Facility, and Diana Lim. I would also like to thank my parents, Alice and Brant Lim, my sister, Christine Lim, and my brother, Daniel Lim.

CHAPTER 1

INTRODUCTION

Overview

The vascular consists of arteries, veins and lymphatic cells. The vascular system can be divided into the circulatory system and the lymphatic system. Arteries and veins are part of the circulatory system, which is required for delivery of nutrients, gases, and hormones, as well as cells, throughout the entire body. The lymphatic system functions to absorb excess fluid, aid in the absorption of fat and defend the body against pathogens. These cells form complex networks, which extends into every part of the body. Precise formation of the vascular network is critical for proper body perfusion, arterial/venous connections, and blood flow in the animal, and thus is essential for long-term survival. It is of great interest how this complex system forms.

One of the challenges in understanding vascular development is deciphering how endothelial cells communicate with their environment and navigate properly to distal targets during vasculo or angiogenesis. This process involves signals that mediate attraction, growth, and survival. However, cues that stimulate repulsion or apoptosis of nascent vessels that fail to find their final target organ are also important for proper network formation. Here, we specifically address what cues guide vessels to their target,

from what tissues are these cues are derived. Additionally, what are the receptors expressed by the endothelial cells that mediate the response to these cues?

Background

Given that guidance molecules are shared between the nervous and vascular systems, it is not surprising to find that both axons and vessels have analogous specialized pathfinding structures: axons have growth cones and endothelial cells have tip cells. Both growth cones and tip cells express an array of receptors and continuously extend cellular projections into their surroundings, sampling the environment for guidance cues that provide a molecular road map to direct the axon or vessel to their final target (Figure 1.1).

Several centuries ago, the anatomist Andreas Versailles made the observation that nerves and vessels are both highly branched networks that follow parallel trajectories. From this observation, two hypotheses can be made: axons and vessels could follow the same guidance cues and therefore the same path, or they could guide each other (axons secrete molecules that guide vessels or vice versa). There is evidence supporting the first model of axons and vessels following the same guidance cues in the developing quail forelimb, where nerves and vessels are both repelled by Sema3A/Nrp1 signaling (Bates et al., 2003). The latter has also been shown: a subset of axonal projections from the superior cervical ganglion are specifically attracted by Endothelin3 secreted by the external carotid artery (Makita et al., 2008). Conversely, peripheral nerve-derived VEGF has been shown to drive arteriogenesis in mouse skin (Mukouyama et al., 2005). However, this last example does not provide direct evidence of axons guiding vessels, rather axons could be regulating arterial differentiation. Indeed, no observations

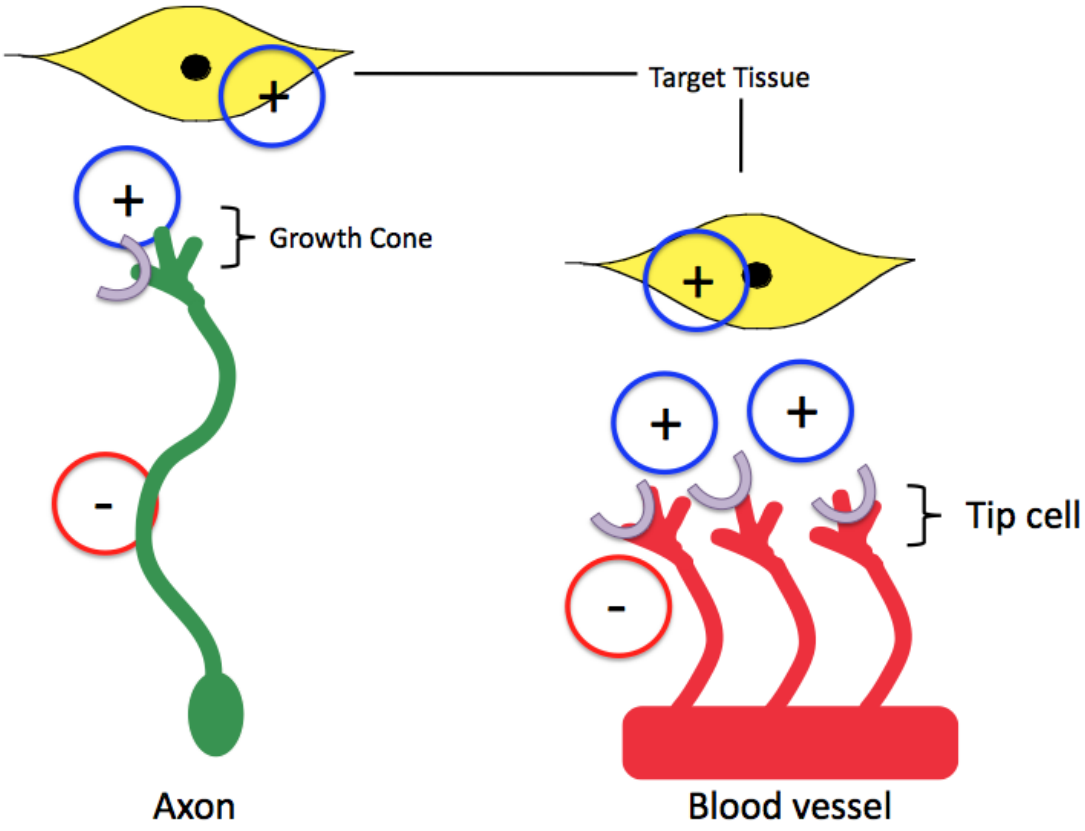

Figure 1.1 Axons and vessels have analogous structures that function to guide them to their target tissue. Axons have a growth cone and endothelial cells have tip cells (indicating brackets). These structures express receptors (purple semi-circles) that help axons and vessels navigate through their environment, growing away from negative (red circle) cues and towards positive cues (blue circles) to reach their final target (e.g., a muscle fiber shown in yellow).

supporting a direct role of axons in vascular patterning has so far been made.

It was soon realized that almost every family of major axon guidance molecules played some role in vascular patterning or function. Interestingly, although these molecules were initially discovered to influence axon guidance and axons are known to influence vascular patterning, few studies investigating common cues in vascular guidance have searched for a primary defect in axon guidance. This is critical as the primary defect may be in axon guidance, with the vascular defect unrelated to the common cue, but instead secondary to the axon guidance defect. Testing this possibility is not necessary in all cases as axons and vessels do not always develop in close association and the timing of development of the vasculature along a certain pathways may occur before axons are present.

Much of what is known about guidance cues and receptors important for vascular guidance were first identified as having roles in axon guidance. The axon guidance field itself began with a simple observation. In 1892, Ramon y Cajal observed that axons take precise courses during development, and hypothesized that axons were guided by diffusible cues from target cells. He noted that axons had specialized structures at their tips, which he named growth cones, hypothesizing that they act as the navigators for axons. He proposed chemotropism as the process by which growth cones responded to these cues. Over a century later, Ramon y Cajal's model of chemotaxis was validated in a novel collagen co-culture assay in which it was shown that a population of neurons were directly attracted by their peripheral targets (Lumsden and Davies, 1983). Soon after, using the same *in vitro* approach, additional examples of targets attracting populations of axons using *in vitro* assays were identified (Tessier-Lavigne et al., 1988).

It was soon discovered that the diffusible factors from target tissues could act not only as attractive cues, but could also be repulsive (Pini, 1993).

These initial observations paved the way for the isolation and identification of several families of attractive and repulsive guidance cues. Notable and well-studied conserved families of axon guidance molecules, which have been shown to also play a role in the formation of the vascular system are Slits, Semaphorins, Ephrins and Netrins (Figure 1.2). Notably, these guidance cues are not strictly attractive or repulsive in axon guidance. Rather, the growth cone's response to extracellular cues depends on a variety of factors including the particular combination of receptors expressed and the intracellular secondary messengers involved (Ming et al., 1997). It is yet known whether the same downstream regulatory factors as formed in axons, play a similar role in modulating endothelial cell responses to guidance cues.

Slit/Robo

The first slit was identified as a repulsive guidance cue at the midline of the nervous system in a Drosophila screen for commissural axon pathfinding defects (Hummel et al., 1999; Seeger et al., 1993). Slits are secreted proteins and act as midline repellents for axons expressing one transmembrane receptor Robo (Brose et al., 1999; Kidd et al., 1999). In vertebrates, there are three slit proteins, Slit 1-3, and four Robo proteins, Robo1-4. Robo4 is the only Robo known to be expressed in the endothelium (Huminiecki et al., 2002). The ligand for Robo4 remains under debate. It has been proposed that Slit2 is a ligand for Robo4 based on *in vitro* binding assays by Robo4-Slit dependent effects on cell migration, tube formation and hyperpermeability assays (Jones et al., 2008; Park et al., 2003; Zhang et al., 2009a); however, Biacore analysis failed to

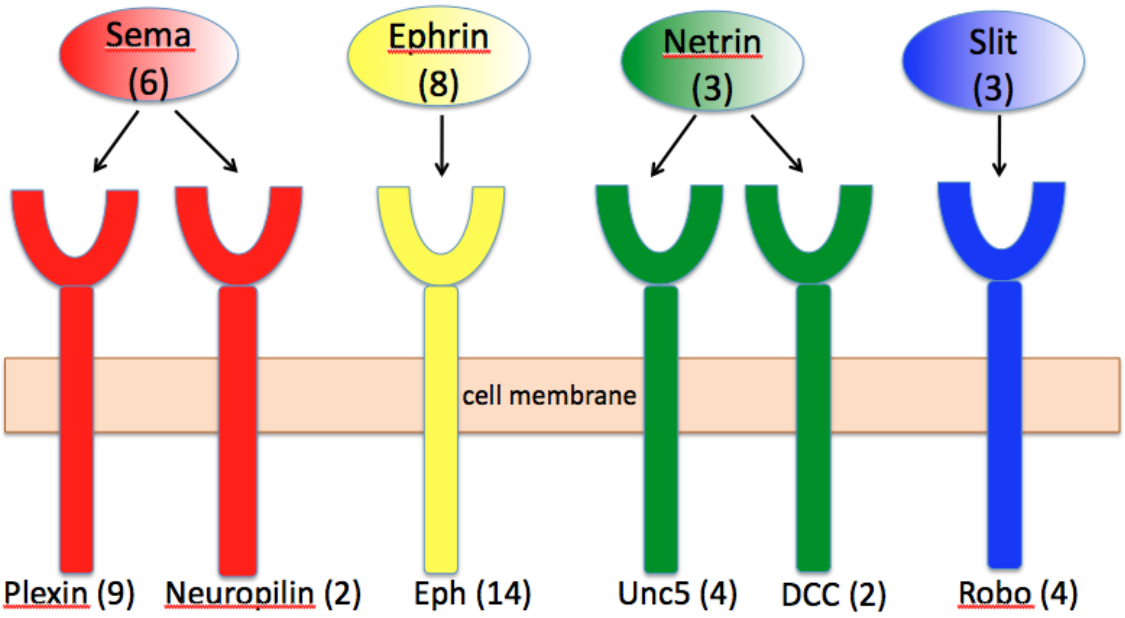

Figure 1.2 Diagram of the major classes of axon guidance ligands and their receptors. The numbers in brackets refer to the number of known genes in mammals (Carmeliet and Tessier-Lavigne, 2005). Sema;Semaphorin.

detect a direct binding of Slit2 to Robo4 (Suchting et al., 2005).

Surprisingly, even though Robo4 is expressed throughout the endothelium, no major vascular guidance defects were observed in Robo4 knockout mice (Jones et al., 2008). Instead, Robo4 was shown to be required to maintain blood vessel integrity by inhibiting VEGF-induced vascular leak: Robo4$^{-/-}$ endothelial cells display hyperpermeability in a VEGF-induced retinal permeability assay and hypervascularization in oxygen-induced retinopathy. In contrast to Robo4$^{-/-}$ mice, it has been suggested that knocking down Robo4 in zebrafish results in severe vascular guidance defects, although we have not been able to reproduce these results (Bedell et al., 2005) . The different phenotypes observed in Robo4 deficient mouse and zebrafish suggest Robo4 is a critical factor for vascular system development and integrity. Since Robo4 expression is restricted to the endothelium, it is unlikely that the defects observed are secondary to an axon guidance phenotype. However, since the Robo4 phenotype in zebrafish was a result of total knock down, and there was no tissue specific rescue performed to confirm that the vascular guidance phenotype was endothelial cell autonomous. Robo4 is expressed in the spinal cord of the zebrafish in addition to the endothelium, so it is possible that that the vascular guidance defects are due to primary defects in axon pathfinding, particularly of axons or projections out of the spinal cord into the trunk, the misguidance of which then affect the vasculature.

Semaphorin/Neuropilin/Plexin

Semaphorins are a large family of molecules which can be secreted, transmembrane, or membrane-anchored. Semaphorins signal through the receptors Plexins and Neuropilins and are generally thought to act as repulsive cues in the context

of axon guidance. Similarly, Semaphorins also have a repulsive effect in vascular guidance. In mice, endothelial specific deletion of PlexinD1 recapitulates the vascular aspect of the PlexinD1 null phenotype, which is characterized by vascular, heart, and skeletal defects (Zhang et al., 2009b). Further, Sema3E knockout mice show severe vascular guidance defects (Gu et al., 2005). These data together suggest a role for Sema3E-PlexinD1 signaling in vascular guidance. Confirming this hypothesis, knocking down PlexinD1 in zebrafish induces severe trunk vascular defects (Torres-Vazquez et al., 2004). PlexD1 is expressed in the growing vessels, tracking within the somitic boundaries, while ligands Sema3A1 and Sema3A2 are expressed in the somites. When either Sema3A1 or Sema3A2 is down-regulated, growing vessels stray into adjacent somites, suggesting that the Semaphorins acts as "guard rails" to keep the vessels within the somitic boundaries. The same phenotype is observed in the absence of PlexinD1, suggesting that Semaphorin-Plexin signaling, as in axon guidance, acts as a repulsive signal for endothelial cells. It is unknown if the axons near the developing trunk vasculature are affected in PlexinD1, Sema3A1 or 3A2 mutants. Additionally, it has not been specifically tested if restoring PlexinD1 specifically to endothelial cells can rescue the defect or specifically knocking out PlexinD1 in endothelial cells results in the defect, which would confirm an endothelial cell autonomous role in vascular guidance. These experiments are critical as they would rule out secondary defects due to misguided axons.

Ephrin/Eph

Ephrins are transmembrane or glycosylphosphatidylinositol (GPI) anchored proteins present at the cell surface that bind to Eph receptors, a large family of receptor tyrosine kinases (Boyd and Lackmann, 2001; Dodelet and Pasquale, 2000; Flanagan and

Vanderhaeghen, 1998; Klein, 2001). Interestingly, Ephs and Ephrins are capable of both forward and reverse signaling: Ephs can signal to Ephrin expressing cells and Ephrins can signal to Eph expressing cells.

One of the most characterized processes in the nervous system known to be regulated by Eph-Ephrins signaling pathway is the establishment of the retinocollicular map (Flanagan and Vanderhaeghen, 1998). Eph-Ephrin also regulate guidance at the midline, where ephrinB3 prevents corticospinal neurons expressing EphA4 from recrossing (Kullander et al., 2001). Several Ephrins and Ephs are expressed in the vascular system and EphrinB2 and EphB4 knockout mice have embryonic vascular defects (Adams et al., 1999; Gerety and Anderson, 2002; Gerety et al., 1999; Wang et al., 1998). Moreover, EphrinB2-EphB4 signaling has been shown to be necessary for arterial-venous identity (Wang et al., 1998). The molecular mechanism by which Ephs and Ephrins regulate vascular development is unclear, as bidirectional signaling complicates the interpretation of the data.

Netrin/Unc5/DCC

Netrins were the first family of axon guidance cues to be identified. Netrins constitute a family of highly conserved proteins, structurally related to laminins (Tessier-Lavigne and Goodman, 1996). Netrin-1 was first isolated from chick brain and shown to be a diffusible factor that promotes the outgrowth of commissural axons (Kennedy et al., 1994; Serafini et al., 1994). Three secreted Netrins have been identified in mammals (Netrin1, 2, and 4). Due to a genome duplication in zebrafish, there are four Netrin family members consisting of Netrin1a, Netrin1b, Netrin2 and Netrin4 (Park et al., 2005). Netrin guidance effects on axons are principally mediated primarily by two families of

receptors, the UNC5 family and the deleted in colorectal cancer (DCC)/neogenin family (Ackerman et al., 1997; Hedgecock et al., 1990{Leonardo, 1997 #26; Keino-Masu et al., 1996; Leonardo et al., 1997). Both of these families belong to the immunoglobulin superfamily (Chan et al., 1996; Livesey, 1999). Other known Netrin receptors include Down Syndrome cell adhesion molecule (DSCAM) and integrin $\alpha6\beta4/\alpha3\beta1$ (Andrews et al., 2008; Cirulli and Yebra, 2007; Liu et al., 2009; Ly et al., 2008; Yebra et al., 2003).

Several groups have shown that Netrin can act as an attractive or repulsive cue, depending on the combination of receptors expressed by the neuronal growth cone. Loss of function of DCC (UNC-40 in *C. elegans* and Frazzled in *Drosophila*) causes misrouting of axons that are normally attracted to a Netrin source (Chan et al., 1996; Keino-Masu et al., 1996; Kolodziej et al., 1996). These results suggest that Netrin acts as an attractive cue, and that this attractive signal is mediated by DCC. Conversely, studies in *C. elegans* reveal that axons that normally grow away from Netrin no longer respond in an Unc5 loss-of-function background (Hedgecock et al., 1990). Additionally, forced expression of Unc5 in axons that do not respond to Netrin, or that normally grow toward Netrin, causes these axons to grow away from the source (Hamelin et al., 1993), suggesting that Unc5 regulates the repulsive activity of Netrin1a. Collectively, these studies demonstrate a critical role of receptor expression in determining a growth cone's response to Netrin.

Of the Netrin receptors, DCC is the best-studied, mediating many Netrin-dependent axon guidance decisions at the midline in the vertebrate spinal cord. It was first identified as the receptor necessary for axon crossing at the midline (Keino-Masu et al., 1996). Netrin is expressed by the floor plate and induces an attractive response of DCC-

expressing axons. Netrin-DCC signaling has since been shown to be important in many other axon guidance events. So far, there have not been any reports of a role for DCC in vascular development.

While the effect of Netrin on Unc5-expressing growth cones has been widely established as repulsive (Bouvree et al., 2008; Hong et al., 1999; Larrivee et al., 2007; Rajasekharan and Kennedy, 2009), the effect of Netrin and Unc5 in vascular development is still being debated. An antiangiogenic role for Netrin through Unc5b has been suggested by Larrivee et al., 2007 and Lu et al., 2004, while we and our collaborators proposed a proangiogenic effect for this signaling pathway (Navankasattusas et al., 2008; Park et al., 2004; Wilson et al., 2006). These divergences of interpretation might result from different genetic strategies, as one of the mice used has a gene trap deletion of the *Unc5b* gene, whereas the other is a vascular-specific conditional *Unc5b* knockout. However, divergent conclusions about the role of Netrin-Unc5b signaling in vascular development have also been drawn from zebrafish studies.

Our observations suggest that this pathway is proangiogenic due to the spatiotemporal expression of Netrin1a relative to a missing endothelial structure (the PAC) in Netrin1a and Unc5 depleted zebrafish embryos (Navankasattusas et al., 2008; Wilson et al., 2006). In contrast, Larrivee et al. found that zebrafish embryos lacking Netrin1a or Unc5 have excess endothelial cell sprouting, suggesting an antiangiogenic role for Netrin1a. Given the difficulty in matching morpholino doses between experimenters, this difference could be explained by a dose-dependent phenotype or off-target effect. Although it is difficult at this time to reconcile these two opposite observations without further experimentation, it is at least apparent from both that

Netrin1 and Unc5b are important for vascular development. It remains however unclear whether Unc5b mediates a proangiogenic or antiangiogenic effect (Larrivee et al., 2007; Lu et al., 2004; Navankasattusas et al., 2008).

In this work, we focus on the common guidance cue Netrin and its receptors, Unc5 and DCC. While a former graduate student, Arminda Suli, has shown the requirement for Netrin1a, Unc5, and DCC in zebrafish vascular development for the formation of the parachordal chain (PAC) (Navankasattusas et al., 2008; Wilson et al., 2006), I am specifically interested in understanding how Netrin-DCC signaling mediates PAC formation. DCC is not known to be expressed in endothelial cells, suggesting that Netrin-DCC signaling in PAC formation is not acting endothelial cell autonomously, but perhaps indirectly through the patterning of axons that are subsequently necessary for this vascular structure to develop.

Zebrafish trunk vascular development

The PAC is a string of endothelial cells located at the horizontal myoseptum (HMS) (Figure 1.3). Development of trunk vasculature in zebrafish begins with the formation of the dorsal aorta (DA) and posterior cardinal vein (PCV). The DA and the PCV are the major central axis artery and vein, respectively, and form via vasculogenesis. Two waves of angioblast migration occur from the lateral plate mesoderm toward the trunk midline beginning at ~15 hpf. The first wave of angioblasts contributes mainly to the DA, while the second wave contribute mainly to the PCV (Torres-Vazquez et al., 2003). Subsequent to DA and PCV formation, sprouts originate between somites from the DA at 22 hpf. These intersegmental vessels (ISVs) grow dorsally, and eventually anastomose at the dorsal midline to form the dorsal longitudinal anastomotic vessel (DLAV) at 30 hpf. By

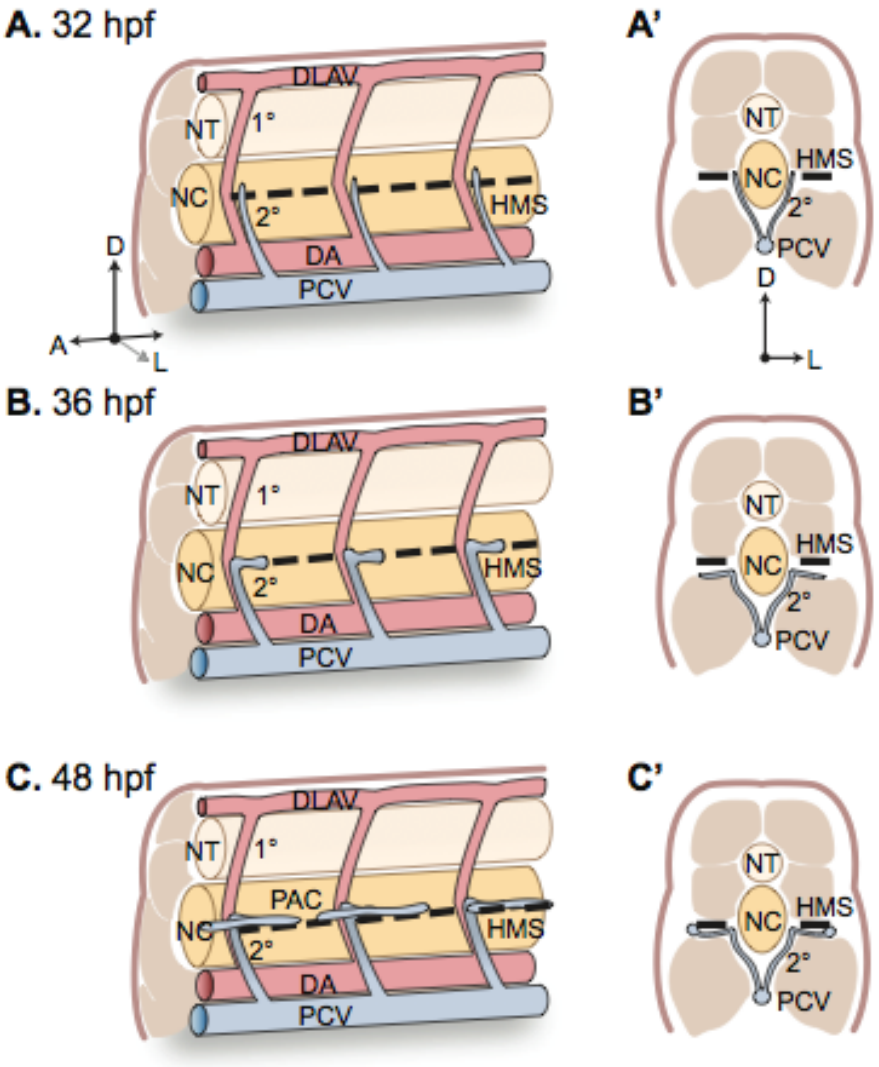

Figure 1.3. Zebrafish trunk vascular development. (A-C) Oblique lateral views of parachordal chain (PAC) formation, showing dorsal aorta (DA) and dorsal longitudinal vessel (DLAV) (*red*); posterior cardinal vein (PCV, *blue*); horizontal myoseptum (HMS, *dashed line*); primary intersomitic vessels (1°, *red*); and secondary sprouts (2°, *blue*). (A'- C') Corresponding transverse views. Dorsal aorta and primary sprouts omitted for clarity. (A, A') Secondary sprouts emerge from the PCV around 32 hpf and grow dorsally to the HMS. (B, B') Dorsal growth stops at the HMS and sprouts turn and grow laterally. (C) Lateral growth stops at the lateral-most aspect of the muscle, and sprout then turns anteriorly and posteriorly to form the PAC (Lim, 2011).

approximately 32 hpf.

Zebrafish motor neuron axon development

Motor neurons extend axons along a trajectory immediately adjacent to that of the future PAC (Beattie, 2000; Eisen et al., 1986; Pike and Eisen, 1990) (Figure 1.4). The close apposition of axonal projections at the HMS along the path of the PAC offers an opportunity to dissect the contribution of neurons and endothelial cells to zebrafish lymphatic patterning and development. There are three primary motor neurons in each somite, the Caudal primary motor neuron (CaP), Middle primary motor neuron (MiP) and Rostral primary motor neuron (RoP), named after their relative cell body position in the spinal cord. The motor neuron that is intimately associated with the developing PAC is RoP. After exiting the spinal cord, RoP's axon grows ventrally to the HMS, branches to the medial and lateral aspects of the muscle, and then grows anteriorly and posteriorly along the HMS. RoP's axon and branches reside where the future PAC will form.

Here, we take advantage of zebrafish as a model organism to study the role of Netrin and its receptors Unc5b and DCC in vascular development. These animals can survive vascular defects for days, allowing sufficient time for analysis, while the same defects would be embryonic lethal for mice. Due to the unparalleled optical clarity in these animals and their external development, the developing zebrafish vascular system can be directly visualized and imaged using confocal microscopy. Further, knocking down gene expression is a fairly simple, rapid method in zebrafish consisting of injecting morpholino oligonucleotides (MOs) that specifically bind to transcripts and prevent their

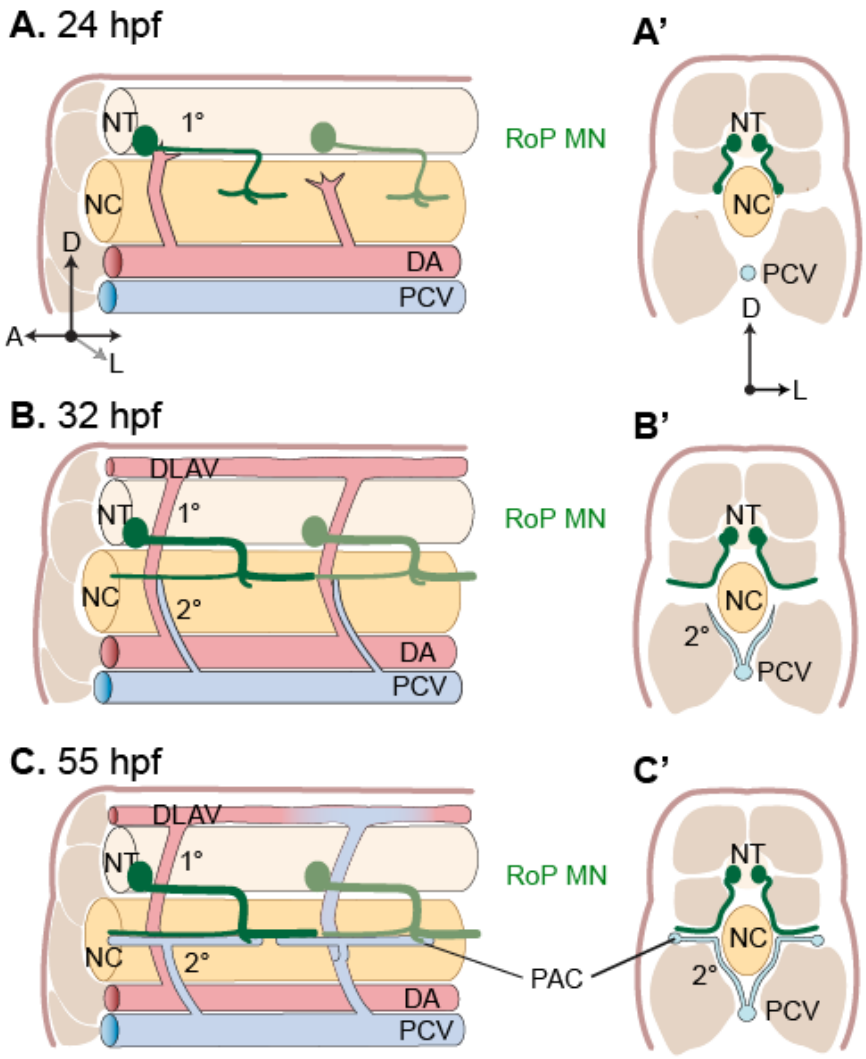

Figure 1.4. Model of motor neuron axon and parachordal chain (PAC) formation. (A-C) Oblique lateral view of trunk. For clarity, only rostral primary motor neuron (RoP) motor neuron is shown. (A', B', C') Transverse view of trunk. Dorsal aorta (DA) and primary sprouts are omitted for clarity. (A, A') RoP motor neuron axons (Bates et al.) exit the spinal cord and extend ventrally toward the HMS at 24 hpf. (B, B') Secondary sprouts (*blue*) grow dorsally to the HMS. (C, C') The axons at the HMS are required for secondary sprouts to grow laterally at the HMS and then turn anteriorly and posteriorly along the HMS to form the PAC. A, anterior; D, dorsal; L, lateral; DLAV, dorsal longitudinal vessel; DA, dorsal aorta; PCV, posterior cardinal vein; PAC, parachordal chain; HMS, horizontal myoseptum; NT, neural tube; NC, notochord; 1°, primary sprouts; 2°, secondary sprouts. Taken from Lim (2011).

splicing or translation. Taking advantages of these properties, we used zebrafish to investigate the role of the axon guidance cue, Netrin1, and its receptors Unc5 and DCC in vascular guidance. Our major discovery was to unravel for the first time an essential role of axons in guiding vessel formation and pathfinding during development.

References

Ackerman, S. L., Kozak, L. P., Przyborski, S. A., Rund, L. A., Boyer, B. B. and Knowles, B. B. (1997). The mouse rostral cerebellar malformation gene encodes an UNC-5-like protein. *Nature* **386**, 838-42.

Adams, R. H., Wilkinson, G. A., Weiss, C., Diella, F., Gale, N. W., Deutsch, U., Risau, W. and Klein, R. (1999). Roles of ephrinB ligands and EphB receptors in cardiovascular development: demarcation of arterial/venous domains, vascular morphogenesis, and sprouting angiogenesis. *Genes Dev* **13**, 295-306.

Andrews, G. L., Tanglao, S., Farmer, W. T., Morin, S., Brotman, S., Berberoglu, M. A., Price, H., Fernandez, G. C., Mastick, G. S., Charron, F. et al. (2008). Dscam guides embryonic axons by Netrin-dependent and -independent functions. *Development* **135**, 3839-48.

Bates, D., Taylor, G. I., Minichiello, J., Farlie, P., Cichowitz, A., Watson, N., Klagsbrun, M., Mamluk, R. and Newgreen, D. F. (2003). Neurovascular congruence results from a shared patterning mechanism that utilizes Semaphorin3A and Neuropilin-1. *Dev Biol* **255**, 77-98.

Beattie, C. E. (2000). Control of motor axon guidance in the zebrafish embryo. *Brain Res Bull* **53**, 489-500.

Bedell, V. M., Yeo, S. Y., Park, K. W., Chung, J., Seth, P., Shivalingappa, V., Zhao, J., Obara, T., Sukhatme, V. P., Drummond, I. A. et al. (2005). roundabout4 is essential for angiogenesis in vivo. *Proc Natl Acad Sci U S A* **102**, 6373-8.

Bouvree, K., Larrivee, B., Lv, X., Yuan, L., DeLafarge, B., Freitas, C., Mathivet, T., Breant, C., Tessier-Lavigne, M., Bikfalvi, A. et al. (2008). Netrin-1 inhibits sprouting angiogenesis in developing avian embryos. *Dev Biol* **318**, 172-83.

Boyd, A. W. and Lackmann, M. (2001). Signals from Eph and ephrin proteins: a developmental tool kit. *Sci STKE* **2001**, re20.

Brose, K., Bland, K. S., Wang, K. H., Arnott, D., Henzel, W., Goodman, C. S., Tessier-Lavigne, M. and Kidd, T. (1999). Slit proteins bind Robo receptors and have an evolutionarily conserved role in repulsive axon guidance. *Cell* **96**, 795-806.

Carmeliet, P. and Tessier-Lavigne, M. (2005). Common mechanisms of nerve and blood vessel wiring. *Nature* **436**, 193-200.

Chan, S. S., Zheng, H., Su, M. W., Wilk, R., Killeen, M. T., Hedgecock, E. M. and Culotti, J. G. (1996). UNC-40, a C. elegans homolog of DCC (Deleted in Colorectal Cancer), is required in motile cells responding to UNC-6 netrin cues. *Cell* **87**, 187-95.

Cirulli, V. and Yebra, M. (2007). Netrins: beyond the brain. *Nat Rev Mol Cell Biol* **8**, 296-306.

Dodelet, V. C. and Pasquale, E. B. (2000). Eph receptors and ephrin ligands: embryogenesis to tumorigenesis. *Oncogene* **19**, 5614-9.

Eisen, J. S., Myers, P. Z. and Westerfield, M. (1986). Pathway selection by growth cones of identified motoneurones in live zebra fish embryos. *Nature* **320**, 269-71.

Flanagan, J. G. and Vanderhaeghen, P. (1998). The ephrins and Eph receptors in neural development. *Annu Rev Neurosci* **21**, 309-45.

Gerety, S. S. and Anderson, D. J. (2002). Cardiovascular ephrinB2 function is essential for embryonic angiogenesis. *Development* **129**, 1397-410.

Gerety, S. S., Wang, H. U., Chen, Z. F. and Anderson, D. J. (1999). Symmetrical mutant phenotypes of the receptor EphB4 and its specific transmembrane ligand ephrin-B2 in cardiovascular development. *Mol Cell* **4**, 403-14.

Gu, C., Yoshida, Y., Livet, J., Reimert, D. V., Mann, F., Merte, J., Henderson, C. E., Jessell, T. M., Kolodkin, A. L. and Ginty, D. D. (2005). Semaphorin 3E and plexin-D1 control vascular pattern independently of neuropilins. *Science* **307**, 265-8.

Hamelin, M., Zhou, Y., Su, M. W., Scott, I. M. and Culotti, J. G. (1993). Expression of the UNC-5 guidance receptor in the touch neurons of C. elegans steers their axons dorsally. *Nature* **364**, 327-30.

Hedgecock, E. M., Culotti, J. G. and Hall, D. H. (1990). The unc-5, unc-6, and unc-40 genes guide circumferential migrations of pioneer axons and mesodermal cells on the epidermis in C. elegans. *Neuron* **4**, 61-85.

Hong, K., Hinck, L., Nishiyama, M., Poo, M. M., Tessier-Lavigne, M. and Stein, E. (1999). A ligand-gated association between cytoplasmic domains of UNC5 and DCC family receptors converts netrin-induced growth cone attraction to repulsion. *Cell* **97**, 927-41.

Huminiecki, L., Gorn, M., Suchting, S., Poulsom, R. and Bicknell, R. (2002). Magic roundabout is a new member of the roundabout receptor family that is endothelial specific and expressed at sites of active angiogenesis. *Genomics* **79**, 547-52.

Hummel, T., Schimmelpfeng, K. and Klambt, C. (1999). Commissure formation in the embryonic CNS of Drosophila. *Dev Biol* **209**, 381-98.

Jones, C. A., London, N. R., Chen, H., Park, K. W., Sauvaget, D., Stockton, R. A., Wythe, J. D., Suh, W., Larrieu-Lahargue, F., Mukouyama, Y. S. et al. (2008). Robo4

stabilizes the vascular network by inhibiting pathologic angiogenesis and endothelial hyperpermeability. *Nat Med* **14**, 448-53.

Keino-Masu, K., Masu, M., Hinck, L., Leonardo, E. D., Chan, S. S., Culotti, J. G. and Tessier-Lavigne, M. (1996). Deleted in Colorectal Cancer (DCC) encodes a netrin receptor. *Cell* **87**, 175-85.

Kennedy, T. E., Serafini, T., de la Torre, J. R. and Tessier-Lavigne, M. (1994). Netrins are diffusible chemotropic factors for commissural axons in the embryonic spinal cord. *Cell* **78**, 425-35.

Kidd, T., Bland, K. S. and Goodman, C. S. (1999). Slit is the midline repellent for the robo receptor in Drosophila. *Cell* **96**, 785-94.

Klein, R. (2001). Excitatory Eph receptors and adhesive ephrin ligands. *Curr Opin Cell Biol* **13**, 196-203.

Kolodziej, P. A., Timpe, L. C., Mitchell, K. J., Fried, S. R., Goodman, C. S., Jan, L. Y. and Jan, Y. N. (1996). frazzled encodes a Drosophila member of the DCC immunoglobulin subfamily and is required for CNS and motor axon guidance. *Cell* **87**, 197-204.

Kullander, K., Croll, S. D., Zimmer, M., Pan, L., McClain, J., Hughes, V., Zabski, S., DeChiara, T. M., Klein, R., Yancopoulos, G. D. et al. (2001). Ephrin-B3 is the midline barrier that prevents corticospinal tract axons from recrossing, allowing for unilateral motor control. *Genes Dev* **15**, 877-88.

Larrivee, B., Freitas, C., Trombe, M., Lv, X., Delafarge, B., Yuan, L., Bouvree, K., Breant, C., Del Toro, R., Brechot, N. et al. (2007). Activation of the UNC5B receptor by Netrin-1 inhibits sprouting angiogenesis. *Genes Dev* **21**, 2433-47.

Leonardo, E. D., Hinck, L., Masu, M., Keino-Masu, K., Ackerman, S. L. and Tessier-Lavigne, M. (1997). Vertebrate homologues of C. elegans UNC-5 are candidate netrin receptors. *Nature* **386**, 833-8.

Lim, A. H., Suli, A., Yaniv, K, Weinstein, B., Li, D.Y., Chien, C.B. (2011). Motoneurons are essential for vascular pathfinding. *Development* **138**, 3847-3857.

Liu, G., Li, W., Wang, L., Kar, A., Guan, K. L., Rao, Y. and Wu, J. Y. (2009). DSCAM functions as a netrin receptor in commissural axon pathfinding. *Proc Natl Acad Sci U S A* **106**, 2951-6.

Livesey, F. J. (1999). Netrins and netrin receptors. *Cell Mol Life Sci* **56**, 62-8.
Lu, X., Le Noble, F., Yuan, L., Jiang, Q., De Lafarge, B., Sugiyama, D., Breant, C., Claes, F., De Smet, F., Thomas, J. L. et al. (2004). The netrin receptor UNC5B

mediates guidance events controlling morphogenesis of the vascular system. *Nature* **432**, 179-86.

Lumsden, A. G. and Davies, A. M. (1983). Earliest sensory nerve fibres are guided to peripheral targets by attractants other than nerve growth factor. *Nature* **306**, 786-8.

Ly, A., Nikolaev, A., Suresh, G., Zheng, Y., Tessier-Lavigne, M. and Stein, E. (2008). DSCAM is a netrin receptor that collaborates with DCC in mediating turning responses to netrin-1. *Cell* **133**, 1241-54.

Makita, T., Sucov, H. M., Gariepy, C. E., Yanagisawa, M. and Ginty, D. D. (2008). Endothelins are vascular-derived axonal guidance cues for developing sympathetic neurons. *Nature* **452**, 759-63.

Ming, G. L., Song, H. J., Berninger, B., Holt, C. E., Tessier-Lavigne, M. and Poo, M. M. (1997). cAMP-dependent growth cone guidance by netrin-1. *Neuron* **19**, 1225-35.

Mukouyama, Y. S., Gerber, H. P., Ferrara, N., Gu, C. and Anderson, D. J. (2005). Peripheral nerve-derived VEGF promotes arterial differentiation via neuropilin 1-mediated positive feedback. *Development* **132**, 941-52.

Navankasattusas, S., Whitehead, K. J., Suli, A., Sorensen, L. K., Lim, A. H., Zhao, J., Park, K. W., Wythe, J. D., Thomas, K. R., Chien, C. B. et al. (2008). The netrin receptor UNC5B promotes angiogenesis in specific vascular beds. *Development* **135**, 659-67.

Park, K. W., Crouse, D., Lee, M., Karnik, S. K., Sorensen, L. K., Murphy, K. J., Kuo, C. J. and Li, D. Y. (2004). The axonal attractant Netrin-1 is an angiogenic factor. *Proc Natl Acad Sci U S A* **101**, 16210-5.

Park, K. W., Morrison, C. M., Sorensen, L. K., Jones, C. A., Rao, Y., Chien, C. B., Wu, J. Y., Urness, L. D. and Li, D. Y. (2003). Robo4 is a vascular-specific receptor that inhibits endothelial migration. *Dev Biol* **261**, 251-67.

Park, K. W., Urness, L. D., Senchuk, M. M., Colvin, C. J., Wythe, J. D., Chien, C. B. and Li, D. Y. (2005). Identification of new netrin family members in zebrafish: developmental expression of netrin 2 and netrin 4. *Dev Dyn* **234**, 726-31.

Pike, S. H. and Eisen, J. S. (1990). Identified primary motoneurons in embryonic zebrafish select appropriate pathways in the absence of other primary motoneurons. *J Neurosci* **10**, 44-9.

Pini, A. (1993). Chemorepulsion of axons in the developing mammalian central nervous system. *Science* **261**, 95-8.

Rajasekharan, S. and Kennedy, T. E. (2009). The netrin protein family. *Genome Biol* **10**, 239.

Seeger, M., Tear, G., Ferres-Marco, D. and Goodman, C. S. (1993). Mutations affecting growth cone guidance in Drosophila: genes necessary for guidance toward or away from the midline. *Neuron* **10**, 409-26.

Serafini, T., Kennedy, T. E., Galko, M. J., Mirzayan, C., Jessell, T. M. and Tessier-Lavigne, M. (1994). The netrins define a family of axon outgrowth-promoting proteins homologous to C. elegans UNC-6. *Cell* **78**, 409-24.

Suchting, S., Heal, P., Tahtis, K., Stewart, L. M. and Bicknell, R. (2005). Soluble Robo4 receptor inhibits in vivo angiogenesis and endothelial cell migration. *Faseb J* **19**, 121-3.

Tessier-Lavigne, M. and Goodman, C. S. (1996). The molecular biology of axon guidance. *Science* **274**, 1123-33.

Tessier-Lavigne, M., Placzek, M., Lumsden, A. G., Dodd, J. and Jessell, T. M. (1988). Chemotropic guidance of developing axons in the mammalian central nervous system. *Nature* **336**, 775-8.

Torres-Vazquez, J., Gitler, A. D., Fraser, S. D., Berk, J. D., Van, N. P., Fishman, M. C., Childs, S., Epstein, J. A. and Weinstein, B. M. (2004). Semaphorin-plexin signaling guides patterning of the developing vasculature. *Dev Cell* **7**, 117-23.

Torres-Vazquez, J., Kamei, M. and Weinstein, B. M. (2003). Molecular distinction between arteries and veins. *Cell Tissue Res* **314**, 43-59.

Wang, H. U., Chen, Z. F. and Anderson, D. J. (1998). Molecular distinction and angiogenic interaction between embryonic arteries and veins revealed by ephrin-B2 and its receptor Eph-B4. *Cell* **93**, 741-53.

Wilson, B. D., Ii, M., Park, K. W., Suli, A., Sorensen, L. K., Larrieu-Lahargue, F., Urness, L. D., Suh, W., Asai, J., Kock, G. A. et al. (2006). Netrins promote developmental and therapeutic angiogenesis. *Science* **313**, 640-4.

Yebra, M., Montgomery, A. M., Diaferia, G. R., Kaido, T., Silletti, S., Perez, B., Just, M. L., Hildbrand, S., Hurford, R., Florkiewicz, E. et al. (2003). Recognition of the neural chemoattractant Netrin-1 by integrins alpha6beta4 and alpha3beta1 regulates epithelial cell adhesion and migration. *Dev Cell* **5**, 695-707.

Zhang, B., Dietrich, U. M., Geng, J. G., Bicknell, R., Esko, J. D. and Wang, L. (2009a). Repulsive axon guidance molecule Slit3 is a novel angiogenic factor. *Blood* **114**, 4300-9.

Zhang, Y., Singh, M. K., Degenhardt, K. R., Lu, M. M., Bennett, J., Yoshida, Y. and Epstein, J. A. (2009b). Tie2Cre-mediated inactivation of plexinD1 results in congenital heart, vascular and skeletal defects. *Dev Biol* **325**, 82-93.

CHAPTER 2

THE NETRIN RECEPTOR UNC5B PROMOTES ANGIOGENESIS IN SPECIFIC VASCULAR BEDS

The following chapter was reprinted with permission from The Company of Biologists. In addition to myself, the other authors were Sutip Navankasattusas, Kevin Whitehead, Arminda Suli, Lise Sorenson, Jia Zhao, Kye Won Park, Joshua Wythe, Kirk Thomas, Chi-Bin Chien and Dean Li. It was originally published in Development, 2008 Feb;135(4):659-67. I participated in the design, execution and interpretation of data related to the *in vivo* zebrafish phenotype (Figure 4).

Development 135, 659-667 (2008) doi:10.1242/dev.013623

The netrin receptor UNC5B promotes angiogenesis in specific vascular beds

Sutip Navankasattusas[1,*], Kevin J. Whitehead[1,2,*], Arminda Suli[3], Lise K. Sorensen[1], Amy H. Lim[3], Jia Zhao[1], Kye Won Park[1,†], Joshua D. Wythe[1,4], Kirk R. Thomas[1,5], Chi-Bin Chien[3,6,‡] and Dean Y. Li[1,2,4,‡]

There is emerging evidence that the canonical neural guidance factor netrin can also direct the growth of blood vessels. We deleted the gene encoding UNC5B, a receptor for the netrin family of guidance molecules, specifically within the embryonic endothelium of mice. The result is a profound structural and functional deficiency in the arterioles of the placental labyrinth, which leads first to flow reversal in the umbilical artery and ultimately to embryonic death. As this is the only detectable site of vascular abnormality in the mutant embryos, and because the phenotype cannot be rescued by a wild-type trophectoderm, we propose that UNC5B-mediated signaling is a specific and autonomous component of fetal-placental angiogenesis. Disruption of UNC5B represents a unique example of a mutation that acts solely within the fetal-placental vasculature and one that faithfully recapitulates the structural and physiological characteristics of clinical uteroplacental insufficiency. This pro-angiogenic, but spatially restricted requirement for UNC5B is not unique to murine development, as the knock-down of the *Unc5b* ortholog in zebrafish similarly results in the specific and highly penetrant absence of the parachordal vessel, the precursor to the lymphatic system.

KEY WORDS: Angiogenesis, Netrin, Placenta, UNC5B, Zebrafish, Mouse

INTRODUCTION

Guidance cues were first identified by their ability to direct axonal projections along specific trajectories. Many of these cues and their cognate receptors have since been shown to play similar roles during angiogenesis, either promoting or directing the growth of growing vessels. A prime example of this is the netrin family, the founding member of which, netrin 1, was originally purified as a secreted guidance cue capable of stimulating growth of commissural axons and attracting them towards the midline (Kennedy et al., 1994; Serafini et al., 1994). Reports from our group and others have shown that netrins can also play a similar role in the vasculature, promoting developmental and therapeutic angiogenesis in a number of in vitro and in vivo systems (Nguyen and Cai, 2006; Park et al., 2004; Wilson et al., 2006).

Netrin signaling is complex, however, and is not always attractive/stimulatory. In mammals there are three netrins and at least eight potential netrin receptors: DCC, neogenin, UNC5A-D, and α6β4 and α3β4 integrins (Cirulli and Yebra, 2007; Huber et al., 2003; Tessier-Lavigne and Goodman, 1996; Yebra et al., 2003). Additional netrin receptors have been postulated, and efforts to identify them are ongoing. Although netrins are the prototypic neural attractants, they can also act as repulsive guidance signals under the appropriate cellular context. One receptor, UNC5B, was identified as a mediator of the repulsive response in neurons (Leonardo et al., 1997), and it is the only known netrin receptor with prominent endothelial expression (Engelkamp, 2002; Lu et al., 2004).

Unc5b is expressed in the endothelium of developing mouse embryos beginning at embryonic day 8.5 (Engelkamp, 2002; Lu et al., 2004). A published study concluded that the axon-repulsive activity mediated by UNC5B is mirrored by an anti-angiogenic role for netrin 1-UNC5B signaling in both mice and zebrafish (Lu et al., 2004). This conclusion was based on observations that the mutation of *Unc5b* resulted in increased sprouting within developing arterial beds, which was interpreted as an indicator of reduced repulsion. This report also postulated that the excessive vascular sprouting caused by the global absence of UNC5B during murine embryogenesis precipitated greater resistance to circulation, resulting in heart failure and fetal demise.

In contrast to the conclusions of Lu and colleagues, our previous analysis of netrin signaling in the vasculature (Park et al., 2004; Wilson et al., 2006) suggested a starkly different situation. We found that the addition of netrins stimulated angiogenesis both in vivo and in vitro, and that the knock-down of *netrin1a* in zebrafish inhibited growth of the parachordal vessel (PAV), a blood vessel that has recently been found essential for lymphatic development (Yaniv et al., 2006).

In an attempt to resolve these different interpretations, we have made use of non-invasive imaging technologies to examine mice carrying a conditional mutant allele of the *Unc5b* gene. Although the vascular-restricted deletion of *Unc5b* indeed causes embryonic lethality, we could find no evidence of either low or high-output heart failure prior to abrupt death at embryonic day 12. Instead, our data showed a previously unappreciated and essential role for UNC5B in promoting placental arteriogenesis. In zebrafish we found a similar pro-angiogenic role, where knocking down *unc5b*, like knocking down *netrin1a*, prevents formation of the PAV.

[1]Program in Human Molecular Biology and Genetics, [2]Division of Cardiology, Department of Internal Medicine, [3]Department of Neurobiology and Anatomy, [4]Department of Oncological Sciences, [5]Division of Hematology, Department of Internal Medicine and [6]Brain Institute, University of Utah, Salt Lake City, UT 84112, USA.

*These authors contributed equally to this work
[†]Present address: Department of Pathology and Laboratories Medicine, UCLA, Los Angeles, CA 90095, USA
[‡]Authors for correspondence (e-mails: chi-bin.chien@neuro.utah.edu; dean.li@hmbg.utah.edu)

Accepted 21 November 2007

MATERIALS AND METHODS

Mouse strains

Generation of the *Unc5b* alleles has been described (Wilson et al., 2006). *R26R1*, *Tie2-Cre*, *Vav1-Cre* and *Netrin1:lacZ* mice were generously provided by Phil Soriano, Masashi Yanagisawa, Matthias Stadtfeld and Lindsay Hinck, respectively. *SM22-Cre* (*Tagln-Cre*), *Nestin-Cre* and *Wnt1-Cre* mice were obtained from The Jackson Laboratory. Genotypes were determined by PCR analysis of genomic DNA isolated from either ear biopsies or yolk sacs; amplification used primers and conditions previously described for *Tie2-Cre* (Kisanuki et al., 2001), *SM22-Cre* (Holtwick et al., 2002), *Nestin-Cre* (Sclafani et al., 2006), *Vav1-Cre* (Stadtfeld and Graf, 2005) and *Rosa26* (Soriano, 1999). For *Wnt1-Cre*, the primers were 5′-AGCAACC-ACAGTCGTCAGAACC and 5′-AAGATAATCGCGAACATCTTCAGG with amplification of 94°C for 30 seconds, 58°C for 30 seconds, and 72°C for 40 seconds. *Unc5b* mice were genotyped with primers: 5′-TAGC-CTCAGGGTCTACTGTCTG; 5′-CTCTCAGACTTCTCAAAGAGATTC; and 5′-CCACTGTATGCCAGACGACATG under conditions of 94°C for 30 seconds, 62°C for 20 seconds and 68°C for 40 seconds.

Histology

Smooth muscle cells were identified by anti-α-smooth muscle actin antibody (Sigma) staining of formaldehyde-fixed, paraffin-embedded tissue sectioned at 10 μm as described previously (Urness et al., 2000). The number of arterioles in the labyrinth was determined by examination of all serial sections from a placental hemisphere. Wild-type and mutant placentas were from paired littermates. β-Galactosidase staining was performed using a standard protocol (Soriano, 1999) with the following modification: the tissues were fixed in PBS containing 2% formaldehyde, 0.2% glutaraldehyde, 0.02% sodium deoxycholate and 0.01% NP-40 for 10-30 minutes. Placentas were hemisected with a razor blade before fixation. The tissues were permeabilized in PBS containing 0.02% sodium deoxycholate and 0.1% NP-40 overnight at 4°C before staining with X-gal.

Staining for PECAM1 was performed on tissues fixed overnight in Dent's fixative (4:1 MEOH: DMSO) at 4°C, followed by bleaching by addition of an equal volume of 37% H_2O_2 for 6-10 hours at room temperature, and storage at –20°C in 100% methanol. Placentas were rehydrated to PBS, hemisected sagittally at the umbilical cord, blocked/permeabilized for 3 hours in PBSMT (PBS+ 0.5% Triton X-100 +2% nonfat milk). Following the addition of 5 μg/ml rat anti-mouse PECAM1 antibody (Pharmingen), samples were incubated overnight at 4°C. Tissues were washed six times in PBSMT and incubated overnight in PBSMT+1:50 anti-rat Ig HRP-conjugate (Pharmingen). HRP staining was performed as previously described (Urness et al., 2000). Tissues were postfixed in 4% paraformaldehyde overnight at 4°C, cleared in 80% glycerol and photographed on a Leica MZ12 stereoscope equipped with a Zeiss Axiocam digital camera.

Hypoxia assay

Pregnant females (30 g) were injected IP with 200 ml of pimonidazole ('Hypoxyprobe' 10 mg/ml in PBS, Chemicon). After 2 hours, mice were killed by cervical dislocation, the embryos were dissected into 4% formaldehyde and the yolk sacs removed for genotyping. Following 16 hours fixation, embryos were serially dehydrated in ethanol, followed by xylene, embedded in paraffin and stored at 4°C. Sections (10 μm) were mounted on glass slides and stained with monoclonal antibodies directed against pimonidazole under conditions provided by the manufacturer. Primary antibody was diluted 200-fold; peroxidase staining for the secondary antibody was for 2 minutes at room temperature. Sections were counterstained with Mayer's hematoxylin prior to photography.

mRNA detection

Whole-mount in situ hybridization was performed as described previously (Urness et al., 2000). Embryos were harvested at E11.5. Decidual tissue was trimmed away and yolk sac fragments were collected from each embryo for genotyping. Placentas were fixed overnight at 4°C in 4% formaldehyde, pH 7.4. Antisense digoxigenin-labeled riboprobe was generated from mouse *Unc5b* DNA using a DIG RNA Labeling Kit (Roche). In situ hybridization was performed overnight at 65°C with rotation in a Hybaid hybridization oven. All comparisons were between sibling pairs.

Tetraploid aggregation

Eight-week old C57Bl6/J mice were superovulated with 5 IU pregnant mares' serum gonadotropin followed after 48 hours with 5 IU human chorionic gonatotropin (hCG); mating with C57Bl6/J males immediately followed the hCG injection. Two-cell stage embryos were flushed at 1.5 days post plug, washed through two drops of M2 medium, four drops of mannitol and fused in mannitol using a Biological Laboratory Equipment BLS CF-150/B Cell Fusion apparatus. Settings were as follows: 40 V, 40 mseconds, enable 1.0. Following fusion, embryos were washed through three drops M2, three drops KSOM (Chemicon) and incubated in a 37°C CO_2 incubator. Most two-cell embryos fused to one cell within 10 minutes. Fused embryos were incubated in KSOM under oil overnight. Morulae (2.5-day old) were flushed from superovulated *Unc5b*$^{+/-}$ mice (mated with *Unc5b*$^{+/-}$ males), washed through Tyrode's (Sigma) to remove the zona pellucida, then washed through three drops M2 medium and three drops KSOM medium. One morula and one fused tetraploid embryo (now four-cell stage) were transferred into each miniwell of KSOM under oil, and incubated overnight. After 16 hours, all miniwells contained one fused blastocyst, which was implanted into 2.5-day pseudopregnant females (C57Bl6/J × CBA F1). Embryos were dissected and analyzed at E13.5.

Echocardiography

Embryos were analyzed and imaged noninvasively in utero using ultrasound biomicroscopy (UBS, Visualsonic Vevo 660) with a 40 MHz transducer and image-guided 23 MHz spectral pulsed-wave (PW) Doppler. Heart rate, blood flow velocities and blood flow volumes were determined from pulsed Doppler waveforms. During scanning, maternal body temperature and heart rate were maintained within normal range, and the duration of anesthesia was less than 1.5 hours (Mu and Adamson, 2006). The hemodynamics of embryos were measured every 6 hours for 36 hours, by which time all of the *Unc5b*-deficient embryos would have died. During each scan, the bladder was used as a reference for the midpoint between the left horn and the right horn of the fallopian uterus, and the relative location of embryos was mapped within the abdomen. After scanning at the final timepoint, a laparotomy was performed and the embryos were scanned a final time to correlate the order of embryo location by ultrasound with anatomic position. The genotype of embryos from previous scans was deduced from the location of embryos relative to each other, especially relative to the location of dead embryos. To confirm correlation between flow reversal and mutant genotype, a number of litters were scanned only until embryos with reversed diastolic flow in the umbilical artery were identified, at which time laparotomy was performed, anatomic correlation was established, and the embryos genotyped.

Umbilical vessel angiogenesis assays

Quantitative three-dimensional umbilical vessel angiogenesis assays were performed according to published methods (Nicosia et al., 2005) with minor modifications. Umbilical cord sections from murine embryos from *Unc5b*$^{+/-}$ × *Unc5b*$^{+/-}$ matings were harvested at E10.5. Immediately prior to harvest, three-dimensional collagen gels (0.25 ml/well) consisting of 2 mg/ml purified rat tail collagen I (Trevigen), 2.34 mg/ml $NaHCO_3$ in 2× concentrated EBM-2 (Lonza) medium supplemented with 1 μg/ml ascorbic acid and 0.2 μg/ml hydrocortisone with or without 100 ng/ml rmNetrin-1 (R&D Systems) were cast into the center wells of four-well chambered coverglasses (Nunclon) and stored on blue ice blocks to delay polymerization. Each embryo was sterilely dissected in the supplemented EBM-2 medium. A 0.5 mm fragment of yolk sac was retained in lysis buffer (50 mM KCl, 2.5 mM $MgCl_2$, 10 mM Tris-HCl pH 8.5, 0.005% NP-40, 0.05% Tween 20, 0.01% gelatin) for PCR genotyping, and a 1.5 mm section of umbilical vessel (equidistant from placenta and embryo) was dissected and washed in EBM-2 (supplemented as above) prior to plating/polymerizing into the collagen gel. Gels with umbilical vessel explants were polymerized for 30 minutes at 37°C/5% CO_2, and subsequently overlaid with 0.25 ml of the supplemented EBM-2 medium. The following morning the medium was exchanged, and the explants photographed in phase-contrast on a Zeiss Axiovert inverted microscope equipped with a Zeiss Axiocam digital camera to confirm location and condition of the umbilical vessel explants. Thereafter, the medium was exchanged every 3-4 days, and the cultures were re-photographed on the tenth day of culture. The capillary

outgrowths observed around the perimeter of each umbilical vessel photograph were counted, and data presented as the average number of capillary outgrowths per umbilical vessel perimeter. The experiment was performed six times on a total of 36 wild-type and 32 mutant siblings.

Embryo raising and MO injection experiments

Heterozygous Tg(*fli1:egfp*)^{y1} transgenic carriers (Lawson and Weinstein, 2002) were incrossed, and embryos were raised at 28.5°C in E2/GN embryo medium with 0.003% phenylthiourea to inhibit pigment formation and staged by time and overall morphology (Kimmel, 1995). *Unc5b* morphants typically reached the 48 hpf stage 1-2 hours after controls. Three MOs were obtained from Gene Tools: control MO ('standard control'), 5′-CCTCTTACCTCAGTTACAATTTATA-3′; *unc5b*SBMO1 (Lu et al., 2004), 5′- CATTTAACCGGCTCGTACCTGCATG-3′, which binds to 7 bp of exon 1 and 18 bp of intron 1; and *unc5b*SBMO2, 5′-AGGAAGACAATACAGCACCTCAGCA-3′, which binds to 7 bp of exon 4 and 18 bp of intron 4. MOs were diluted, stored and injected at 1 nl nominal volume as described previously (Wilson et al., 2006). RT-PCR was carried out as described previously (Wilson et al., 2006); primer sequences available upon request.

Microscopy and image analysis

fli:egfp-positive embryos were either imaged live or fixed and stained with anti-GFP before imaging (Wilson et al., 2006). Briefly, embryos were mounted laterally in agarose, right side down and confocal *z*-stacks were taken at the level of somites 7-12. *Z*-stacks were used to score the presence of PAVs in four to six hemisegments. We modified our analysis slightly by scoring only the near (right) side of the trunk, which could be imaged most clearly; and by calculating in each embryo the fraction of hemisegments with absent, partial or complete PAVs, then averaging these fractions across embryos. Statistical analysis used two-tailed Mann-Whitney tests (Instat3, Graphpad).

RESULTS

Endothelial restricted ablation of Unc5b causes embryonic lethality

Because of the broad expression pattern of *Unc5b* in the murine embryo, we generated an allele of *Unc5b* (Wilson et al., 2006) that can be inactivated, conditionally, through tissue-restricted expression of CRE recombinase. This allele, *Unc5b*^{flox}, contains *loxP* sites within introns 3 and 13. CRE-mediated deletion of the intervening sequences removes much of the ligand-binding domain, the entire transmembrane domain, and most of the cytoplasmic signaling domain of the mature protein, generating a presumed null allele. To reduce the chance of cis-acting effects, the selectable marker gene used in construction of this allele was removed prior to analysis. We also engineered mice that transmit the deletion allele, *Unc5b*$^{-}$, through the germline. Mice homozygous for this mutation die in utero between 12 and 13.5 days post-fertilization (E12-E13.5). Our preliminary phenotypic characterization of *Unc5b*$^{-/-}$ embryos has been described (Wilson et al., 2006) and, surprisingly, it revealed none of the excessive vascular sprouting described by Lu et al. (Lu et al., 2004).

To systematically inactivate *Unc5b* in a tissue-specific fashion, animals homozygous for the conditional allele (*Unc5b*$^{flox/flox}$) were mated with animals heterozygous for the *Unc5b* null allele (*Unc5b*$^{+/-}$) and carrying one of a variety of *Cre* genes under tissue-restricted control. Deletion of *Unc5b* in neural crest-derived tissues [*Wnt1-Cre* (Jiang et al., 2000)], smooth and cardiac muscle [*Tag1n-Cre* (Holtwick et al., 2002)] in the nervous system [*Nestin1-Cre* (Sclafani et al., 2006)] or in hematopoietic lineages [*Vav1-Cre* (Stadtfeld and Graf, 2005)] resulted in mice that survived to adulthood and that appeared normal (Table 1 and data not shown). When *Unc5b* was deleted by an endothelial-expressed *Cre* transgene, *Tie2-Cre* (Kisanuki et al., 2001), however, no animals of the genotype *Unc5b*$^{-/flox}$; +/*Tg(Tie2-Cre)*, were ever recovered at birth. Embryos of this genotype died in mid-gestation between 12 and 13.5 days post-fertilization and were indistinguishable from homozygous null *Unc5b*$^{-/-}$ embryos (data not shown). The implication from these results is that vascular expression, and only vascular expression, of *Unc5b* is required for viability.

Arteriole reduction in *Unc5b*-deficient placentas

Embryonic death in the E10-E13 period is generally attributed to failures in cardiac function, hematopoiesis or placentation (Papaioannou and Behringer, 2005), and *Tie2-Cre* is expressed in these relevant tissues (Kisanuki et al., 2001). Histological analyses of E12.5 embryos revealed no differences in heart structure or in the morphology of coronary vessels between *Unc5b*$^{+/flox}$; +/*Tg(Tie2-Cre)* and *Unc5b*$^{-/flox}$; +/*Tg(Tie2-Cre)* embryos; blood counts were equivalent, as was the profile of circulating cells; and the vasculature of the somites, neural tube, yolk sac and hindbrain were indistinguishable (data not shown). The only discernible difference between the two genotypes was within the placental labyrinth: fetal-

Table 1. Tissue-specific deletion of Unc5b

Cross	*Unc5b*$^{flox/flox}$ × *Unc5b*$^{+/-}$;+/*Tg(Tie2-Cre)*			
Genotype	*Unc5b*$^{-/flox}$;+/*Tg(Tie2-Cre)*	*Unc5b*$^{+/flox}$;+/*Tg(Tie2-Cre)*	*Unc5b*$^{-/flox}$	*Unc5b*$^{+/flox}$
Number of progeny	0	25	28	24
Cross	*Unc5b*$^{flox/flox}$ × *Unc5b*$^{+/-}$;+/*Tg(Tagln-Cre)*			
Genotype	*Unc5b*$^{-/flox}$;+/*Tg(Tagln-Cre)*	*Unc5b*$^{+/flox}$;+/*Tg(Tagln-Cre)*	*Unc5b*$^{-/flox}$	*Unc5b*$^{+/flox}$
Number of progeny	18	10	7	11
Cross	*Unc5b*$^{flox/flox}$ × *Unc5b*$^{+/-}$;+/*Tg(Nes-Cre)*			
Genotype	*Unc5b*$^{-/flox}$;+/*Tg(Nes-Cre)*	*Unc5b*$^{+/flox}$;+/*Tg(Nes-Cre)*	*Unc5b*$^{-/flox}$	*Unc5b*$^{+/flox}$
Number of progeny	6	12	6	9
Cross	*Unc5b*$^{flox/flox}$ × *Unc5b*$^{+/-}$;+/*Tg(Wnt1-Cre)*			
Genotype	*Unc5b*$^{-/flox}$;+/*Tg(Wnt1-Cre)*	*Unc5b*$^{+/flox}$;+/*Tg(Wnt1-Cre)*	*Unc5b*$^{-/flox}$	*Unc5b*$^{+/flox}$
Number of progeny	4	8	6	3
Cross	*Unc5b*$^{flox/flox}$ × *Unc5b*$^{+/-}$;+/*Tg(Vav-Cre)*			
Genotype	*Unc5b*$^{-/flox}$;+/*Tg(Vav-Cre)*	*Unc5b*$^{+/flox}$;+/*Tg(Vav-Cre)*	*Unc5b*$^{-/flox}$	*Unc5b*$^{+/flox}$
Number of progeny	17	23	14	8

Matings were performed between the genotypes indicated. Progeny were left with their mothers until weaning (3-4 weeks), at which time they were genotyped as described in the Materials and methods.

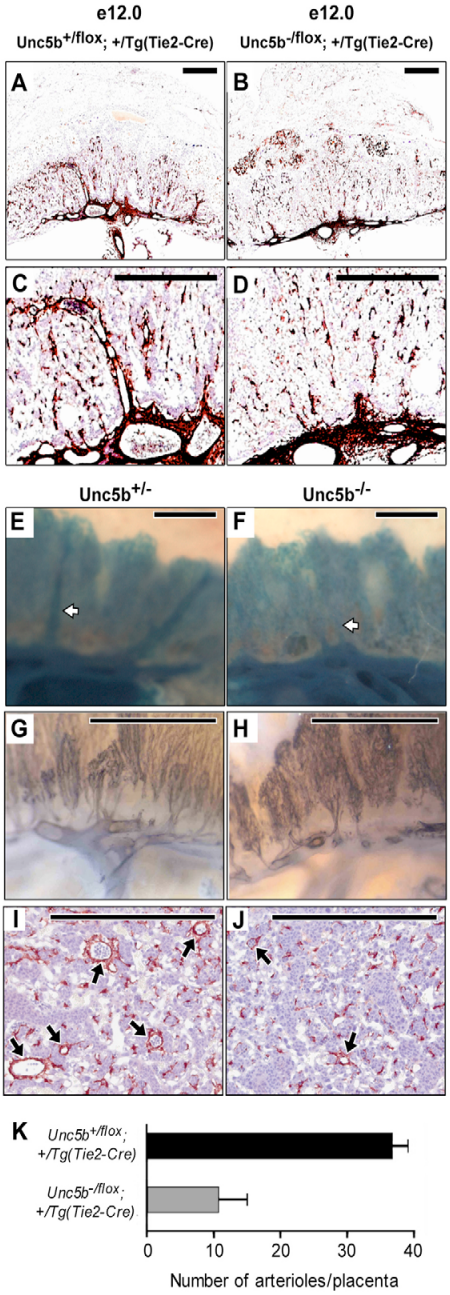

Fig. 1. Vascular ablation of Unc5b impacts labyrinthine arterioles. Embryos were harvested at E12.0 from *Unc5b*$^{flox/flox}$ × *Unc5b*$^{+/–}$; *Tg(Tie2-Cre)/Tg(Tie2-Cre)* (**A-D**), *Unc5b*$^{+/–}$*;R26R* [Rosa26 Reporter (Soriano, 1999)] × *Unc5b*$^{+/–}$; *Tg(Tie2-Cre)/Tg(Tie2-Cre)* (**E**,**F**) or *Unc5b*$^{+/–}$ × *Unc5b*$^{+/–}$ (**G-J**) matings. Placentas were dissected, formalin fixed, hemisected and stained for: smooth muscle actin (anti-smooth muscle actin antibody followed by HRP-conjugated secondary antibody) to identify smooth muscle cells surrounding the arterial bed (A-D); for β-galactosidase activity (X-gal) to identify endothelial expression of *Tie2-Cre* (E,F); and for Pecam I (anti-Pecam1 antibody followed by HRP-conjugated secondary antibody) to highlight the endothelium (G,H). There is a decrease in the number of robust vertical vessel stalks in placentas lacking UNC5B (B,D,F,H) when compared with their littermate controls (A,C,E,G). This is also shown in I,J, which represent 10 μm cross-sections through samples stained for smooth muscle actin. Arterioles are indicated by arrows; scale bars: 0.5 mm. (**K**) The number of arterioles per placenta was determined by serial sectioning (10 μm) of hemisected placentas, staining for smooth muscle actin and visually counting all vessels. Paired littermates (three pairs) representing each of the two genotypes were used for all measurements. Error bars are standard deviation.

derived arterioles, visualized either by smooth muscle or endothelial specific stains, were less numerous in embryos lacking vascular *Unc5b* (Fig. 1).

Defective umbilical blood flow and hypoxia in *Unc5b*-deficient embryos

To determine the functional relevance of this placental defect, Doppler flow analysis was performed on umbilical vessels in utero. Three pregnancies from *Unc5b*$^{flox/flox}$ × *Unc5b*$^{+/–}$; *Tg(Tie2-Cre)/Tg(Tie2-Cre)* crosses were probed at regular intervals from E11.0 to E13.5. At these time points, normal umbilical artery flow is predominantly systolic with a minimal amount of flow in diastole. Beginning at ~E12.0, significant and reversed blood flow in diastole within the umbilical arteries of mutant embryos could be detected in some embryos (Fig. 2A, Table 2A). As pregnancy proceeded, the number of embryos with abnormal flow increased, as did the degree of flow reversal (e.g. –22% to –91%, Fig. 2A). By E13.5, all embryos that had exhibited reversed flow were dead. In another set of identical crosses, embryos were probed at a single time point, E12.5, and subsequently killed and genotyped (Fig. 2B,C). There was a strong genotype/phenotype correlation between the vascular deletion of *Unc5b* and flow reversal. Umbilical artery diastolic flow reversal is a clinical sign of fetal distress and is consistent with an abnormally high resistance within the placenta, a plausible consequence of the reduced number of arterioles. Consistent with this interpretation, physiological and anatomical changes in cardiac function, such as bradycardia and pericardial effusion, were only detected after the onset of umbilical arterial flow reversal and immediately prior to death (Fig. 2A) but not earlier (Fig. 2C).

By E13, the embryo is nutritionally dependent on maternal blood. We thus hypothesized that the defective placenta and the accompanying circulatory abnormality would result in a decrease in available metabolites. As a metabolic indicator, O_2 levels of embryos were assessed by examining the ability of tissues to retain pimonidazole, a compound that shows enhanced protein-binding capacity under hypoxic conditions (Raleigh et al., 1987). At 12.5 days after fertilization, pregnant females were injected with pimonidazole. Two hours later, embryos were removed and apparently viable, outwardly normal, embryos were fixed and sectioned. Bound pimonidazole was then assessed by immunostaining. At E12.5, the majority (4/5) of *Unc5b*$^{–/–}$ embryos exhibited a higher level of pimonidazole immunoreactivity than did their wild-type counterparts (Fig. 2D,E), suggestive of a hypoxic environment and implying a direct link between altered umbilical flow and ultimate death.

UNC5B acts within the embryo proper

The arterioles affected by *Unc5b* loss are derived from the umbilical vessels emanating from the embryo proper, but their patterning depends on signaling from the adjacent extra-embryonic

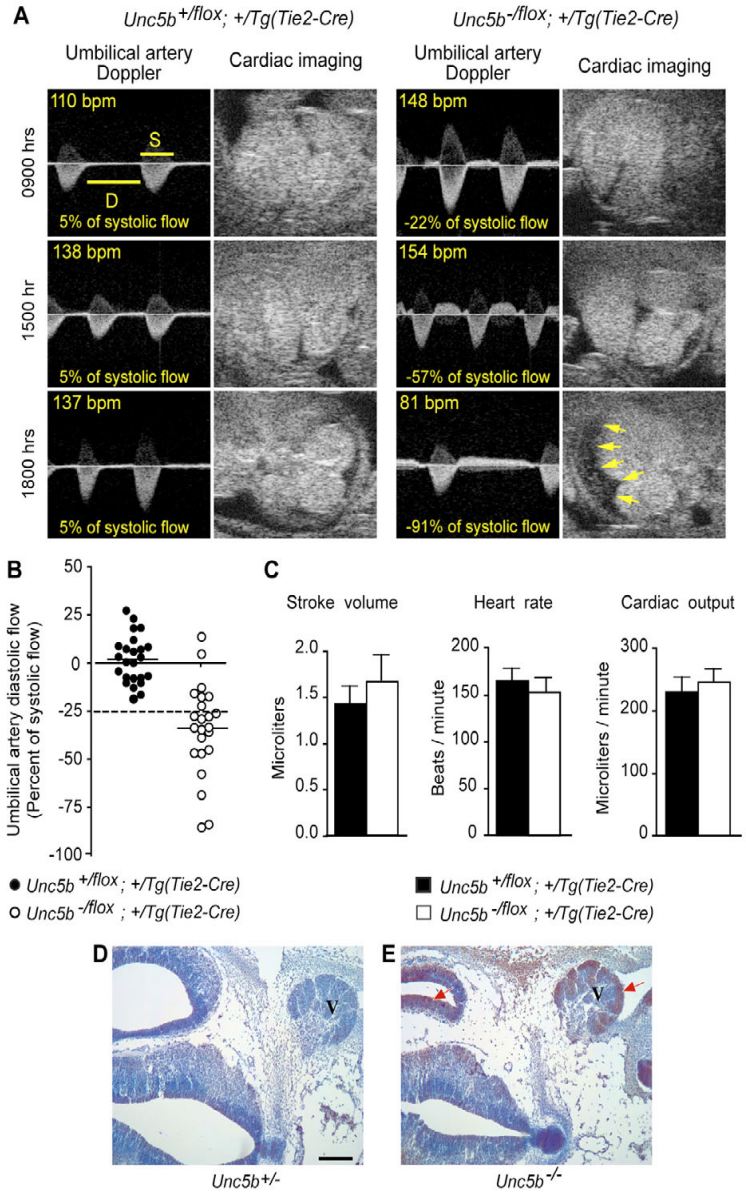

Fig. 2. Physiological assessment of embryos. (**A**) Doppler flow analysis of umbilical arteries and hearts in utero. For longitudinal follow-up of umbilical artery Doppler flow, *Unc5b*$^{+/flox}$; *+/Tg(Tie2-Cre)* and *Unc5b*$^{-/flox}$;*+/Tg(Tie2-Cre)* embryos were monitored on E12 at the time intervals indicated on the left. The ratio of diastolic (D) flow (time velocity integral) over systolic (S) flow is shown as a percentage with a negative number indicative of reverse flow. The ratio decreased progressively over time in the mutant embryo and preceded pericardial effusion (arrows) and bradycardia. (**B**) Quantitation of umbilical artery diastolic flow reversal. The ratio of umbilical diastolic flow (time velocity integral) over systolic flow was used to quantitate the degree of end diastolic reverse flow and the ratio of –25% of systolic flow (broken line) was chosen as a threshold for significant reversal; 24 *Unc5b*$^{+/flox}$; *+/Tg(Tie2-Cre)* and 23 *Unc5b*$^{-/flox}$;*+/Tg(Tie2-Cre)* embryos were sampled at a single time point at E12.5. (**C**) The stroke volume, heart rate and cardiac output were recorded at the onset of significant diastolic reverse flow; data from four *Unc5b*$^{+/flox}$; *+/Tg(Tie2-Cre)* and three *Unc5b*$^{-/flox}$;*+/Tg(Tie2-Cre)* are reported; error bars are standard deviation. (**D**,**E**) Increased hypoxia in *Unc5b*$^{-/-}$embryos. Pregnant females were injected with pimonidazole 2 hours prior to sacrifice and removal of embryos. Sections (10 μm) from the hindbrain region of E12.5 *Unc5b*$^{+/-}$ (D) and *Unc5b*$^{-/-}$ (E) embryos were probed with antibodies directed against pimonidazole and HRP-conjugated secondary antibodies, stained for HRP activity (brown, indicated by arrows) and counterstained with hematoxylin (blue). V, trigeminal ganglion. Scale bar: 100 μm.

trophoblast (Adamson et al., 2002; Cross et al., 2003; Rinkenberger and Werb, 2000; Rossant and Cross, 2001). To understand more specifically the requirement for *Unc5b*, we examined its gene expression in the placenta. Sections of E12.0 placentas of genotypes *Unc5b*$^{+/flox}$; *+/Tg(Tie2-Cre)*; and *Unc5b*$^{-/flox}$; *+/Tg(Tie2-Cre)* were probed with RNA complementary to *Unc5b* mRNA. As

Table 2. Phenotypes of Unc5b deletion

A Diastolic flow reversal in umbilical arteries*

	Unc5b$^{+/flox}$; +/*Tg(Tie2-Cre)*			*Unc5b*$^{-/flox}$; +/*Tg(Tie2-Cre)*		
	Normal	Reversed	Dead	Normal	Reversed	Dead
Age (d.p.c.)	Number of embryos					
12	11	0	1	7	3	3
12.5	11	0	1	2	6	5
13	11	0	1	1	1	11
13.5	11	0	1	0	0	13

B Failure of rescue: *Unc5b*$^{+/-}$ × *Unc5b*$^{+/-}$ (morulae) + *Unc5b*$^{+/+}$ tetraploid (two cell)†

	Unc5b$^{+/+}$		*Unc5b*$^{+/-}$		*Unc5b*$^{-/-}$	
	Dead	Alive	Dead	Alive	Dead	Alive
Age (d.p.c.)	Number of embryos					
13.5	0	20	0	18	11	1

*Three pregnancies from *Unc5b*$^{flox/flox}$ × *Unc5b*$^{+/-}$; *Tg(Tie2-Cre)/Tg(Tie2-Cre)* crosses were probed at 12-hour intervals from E11.0 to E13.5. Umbilical flow and viability were monitored as described in the Materials and methods, and in the legend to Fig.2. At E13.5, the pregnant females were sacrificed and the embryos genotyped.
†Morulae produced from an *Unc5b*$^{+/-}$ intercross were aggregated with tetraploid, wild-type, two-cell stage embryos. The fused embryos were implanted into females and allowed to mature. At E13.5 (relative age of the morulae), embryos were harvested, examined for viability and genotyped.

shown in Fig. 3A,B, binding of this probe was restricted to the labyrinth but could not be detected in placentas in which *Unc5b* had been deleted by endothelial-expressed CRE (Fig. 3A,B). Thus, placental expression of UNC5B is limited to the fetal-derived endothelium. These data suggest a model whereby UNC5B-expressing endothelial cells within the labyrinth respond to signals emanating from the trophectoderm and direct proper vascular development. Consistent with this idea, expression of the secreted guidance factor, netrin 1, an UNC5B ligand, can be detected in the trophoblast giant cells (Fig. 3C,D). Although no placental phenotype has been described in mice deficient for netrin 1 (Salminen et al., 2000; Serafini et al., 1996), the mutations analyzed in those studies were hypomorphic alleles that synthesize detectable levels of wild-type transcript.

This model also predicts that wild-type trophoblast cells should be unable to rescue embryos deficient in *Unc5b* (Nagy et al., 1993). To test this prediction, we aggregated diploid morulae from an *Unc5b*$^{+/-}$ intercross with tetraploid, wild-type, two-cell stage embryos that can contribute only to the extra-embryonic tissues (Nagy et al., 1993). Fused embryos were implanted into foster mothers, harvested at E13.5 and examined for viability and genotype. As summarized in Table 2B, all wild-type and heterozygous embryos were viable, whereas 11/12 *Unc5b*$^{-/-}$ embryos were dead. Examination by PCR of genomic DNA isolated from extra-embryonic tissue of the *Unc5b*$^{-/-}$ embryos showed a significant contribution from wild-type (tetraploid) cells (data not shown). The fact that these cells were incapable of supporting an *Unc5b* mutant embryo implies that the deficiencies resulting from this genotype are within the embryo proper.

Evidence that UNC5B is active within the fetal-placental vasculature was provided by examining the growth of isolated umbilical arteries in vitro. When cultured on a collagen matrix in the absence of serum, umbilical arterial explants isolated from *Unc5b*$^{+/+}$ embryos support a more vigorous netrin 1-dependent outgrowth than do those isolated from their *Unc5b*$^{-/-}$ littermates (Fig. 3E,F).

Knock-down of Unc5b inhibits PAV formation in zebrafish

The role of netrin signaling in zebrafish vascular development is not without controversy. During development of the embryonic trunk vasculature, the zebrafish netrin 1 ortholog, *netrin1a*, is expressed at the horizontal myoseptum (Lauderdale et al., 1997; Wilson et al., 2006), precisely where secondary sprouts growing dorsally from the posterior cardinal vein (PCV) grow laterally and turn anteroposteriorly to form the parachordal vessel (PAV). It has been reported that knocking down either *netrin1a* or *unc5b* using antisense morpholino oligonucleotides (MOs) disrupts intersomitic vessel (ISV) formation and leads to excess vessel branching (Lu et al., 2004). We found, however, that a carefully titrated dose of a splice-blocking MO against *netrin1a* led to a highly penetrant phenotype in which the PAV failed to form (Wilson et al., 2006). ISVs are only very rarely affected at this dose, and overall trunk morphology appears normal, unlike that seen at higher doses (A.S. and C.-B.C., unpublished).

We therefore reexamined formation of the trunk vasculature after *unc5b* knockdown, injecting two different MOs against *unc5b*: *unc5b*SBMO1 [identical to that used by Lu et al. (Lu et al., 2004)] and *unc5b*SBMO2, and using the *fli:egfp* transgene to visualize endothelial cells (Fig. 4). In preliminary dose-response experiments, we chose MO doses (1 ng *unc5b*SBMO1 or 4 ng *unc5b*SBMO2) that yielded embryos with normal trunk morphology (Fig. 4A-D). This was crucial as, even at moderate doses (1.5 ng), *unc5b*SBMO1 caused gross morphological defects (strongly curved tails, hindbrain edema and small eyes), which may reflect off-target effects. At these doses, both MOs were effective, as shown by significant reductions in wild-type *unc5b* mRNA detected by RT-PCR (see Fig. S1 in the supplementary material). Although development of the overall vasculature was normal, including the dorsal aorta, PCV and ISVs, we saw a specific, highly penetrant effect on PAV formation (Fig. 4E-H). PAVs normally form by ~36 hpf. To avoid potential confounding effects of mild developmental delay, we scored PAVs at 48 hpf. The fraction of hemisegments that completely lacked a PAV increased from 1±1% to 46±6% (mean±s.e.m., $P<0.0001$) with *unc5b*SBMO1, and from 2±2% to 70±7% ($P<0.0001$) with *unc5b*SBMO2 (Fig. 4I,J). The concordant results with two nonoverlapping MOs strongly suggests that the lack of PAVs is specifically due to loss of *unc5b* function, rather than an off-target effect. Given the expression of *netrin1a* at the horizontal myoseptum, the most parsimonious explanation is that Ntn1a-Unc5b signaling is pro-angiogenic in this system.

DISCUSSION

We have analyzed the developmental consequences of *Unc5b* mutagenesis in both mouse and zebrafish. Deletion of *Unc5b* within the endothelial cells – and only within the endothelial cells – of the developing murine vasculature leads to a mid-gestational lethality that phenocopies universal ablation of *Unc5b*. The only observed defect in embryos lacking *Unc5b* is a reduction in the number of labyrinthine arterioles within the placenta. This leads to an increase in placental resistance, followed by flow reversal in the umbilical artery, hypoxia, cardiac failure and ultimately death. Morphological analyses of mutant embryos revealed no other defects, and fetal echocardiography showed no signs of high-output or low-output heart failure or lethal arrhythmia predating the onset of structural and physiological placental abnormalities. The reduction in the number of placental arterioles in the absence of *Unc5b* implies a pro-angiogenic role for netrin/UNC5B signaling during development, which is further supported by our observation that umbilical arteries isolated from *Unc5b*-deficient embryos were unable to support vessel outgrowth in vitro. A pro-angiogenic role of UNC5B was also observed in the zebrafish trunk vasculature, where we found that the knockdown of *unc5b* function, using carefully titrated doses of two different MOs, leads to a specific and highly penetrant absence of PAVs. Although we cannot rule out the possibility that UNC5B may play some role in ISV formation that would be revealed by higher doses of MO (Lu et al., 2004), we did not analyze higher doses because of morphological defects that were potentially nonspecific. This issue would be best addressed by isolating mutant alleles for *unc5b*. Furthermore, we note that the morphant images of Lu et al. (Lu et al., 2004) appear to show missing PAVs in some segments; in other segments, secondary sprouts appear to turn normally to form the PAV, but have been interpreted as increased vessel branching. Together with the observations that the PAV forms along the muscle pioneer cells that line the horizontal myoseptum and express *netrin1a*, and that *netrin1a* morphants have very similar phenotypes to *unc5b* morphants (Wilson et al., 2006), these data support an important pro-angiogenic role for Ntn1a/Unc5b signaling in zebrafish lymphatic development.

Though zebrafish do not have placental arterioles and mice do not have a structural equivalent to the PAV, our developmental studies indicate that netrin signaling has evolved to ensure the formation of specific subsets of vessels. Thus, in contrast to VEGF signaling, which has profound effects on virtually all endothelial cells and vascular beds during developmental angiogenesis (Ferrara et al., 2003), guidance cues in general and UNC5B specifically, may provide an additional level of regulation to coordinate the spatial and temporal organization of tissue-specific vascular beds during embryogenesis. Because the first vital requirement for UNC5B is during mid-gestation, the reagents used in this study were unable to ascertain a function in later stages of development or within the adult. Such an assessment requires the use of alternative mutagenesis schemes, which we are vigorously pursuing.

A role for UNC5B in embryonic angiogenesis was originally postulated because of its vascular-specific expression pattern and was supported by the characterization of a mouse mutant in which exons 3 and 4 of *Unc5b* were replaced with 8 kb of exogenous DNA encoding the *lacZ* and alkaline phosphatase genes (Lu et al., 2004). Although embryos homozygous for that allele died at the same time as those containing the exon3-13 deletion allele described in our previous work (Wilson et al., 2006) and in this manuscript, they were characterized as having increased capillary branching in the embryo proper, which the authors hypothesized would raise vascular resistance and precipitate heart failure. However, this study did not report physiological measurements of embryonic cardiac function or any analyses – functional or morphological – of the placenta. It would be interesting to re-examine this allele in the light of our present findings.

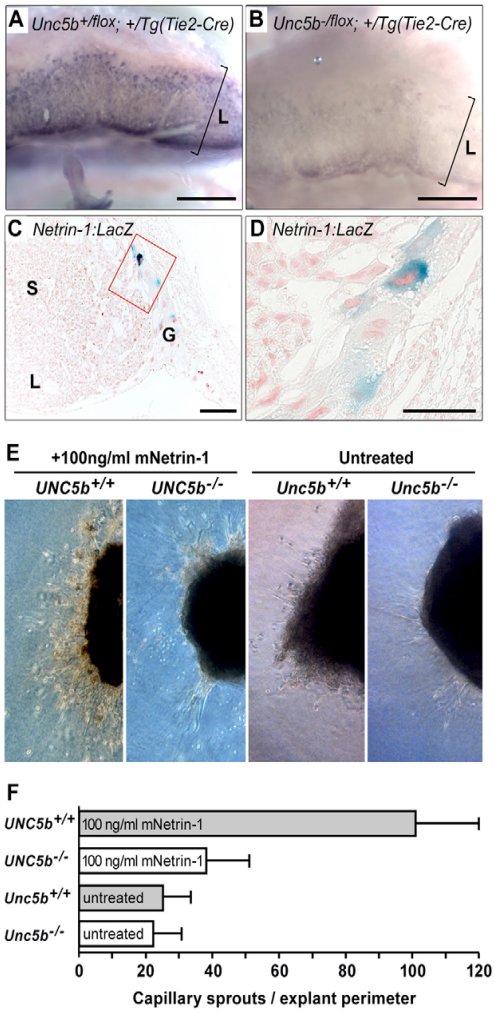

Fig. 3. Unc5b/Netrin signaling in the placenta. (**A**,**B**) *Unc5b* mRNA localization in the labyrinth. Placentas from E12.5 embryos were hemisected and probed with antisense RNA complementary to *Unc5b* mRNA. (A) *Unc5b*$^{+/flox}$;*+/Tg(Tie2-Cre)* and (B) *Unc5b*$^{-/flox}$; *+/Tg(Tie2-Cre)*; L indicates extent of labyrinthine layer. Scale bars: 1 mm. (**C**,**D**) Netrin expression in giant trophoblast cells. Placentas (E12.5) from embryos heterozygous for the *netrin1:lacZ* gene trap (Serafini et al., 1996) were fixed, hemisected and stained with X-gal to detect *lacZ* activity; 10 μm sections were mounted on slides and counterstained with nuclear Fast Red. L, labyrinth; S, spongiotrophoblast; G, giant trophoblast cell layer. Image in D is a 4× magnification of boxed area in C. Scale bars: 200 μm in C; 100 μm in D. (**E**) Growth of umbilical vessels in vitro. Umbilical vessels at E10.5 were explanted into collagen gels and allowed to sprout for 10 days in the presence or absence of netrin 1 protein. Numbers of sprouts were counted under phase contrast. Genotypes and growth conditions are indicated above each frame. (**F**) Quantitation from four pairs of umbilical arteries of each genotype. Error bars are standard deviation.

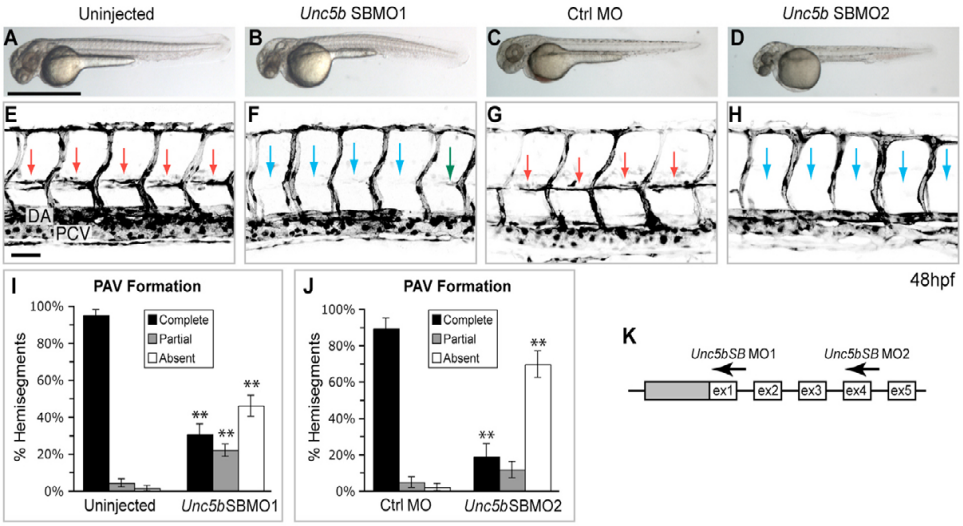

Fig. 4. Knockdown of zebrafish *unc5b* prevents formation of a specific vessel: the PAV. (**A-D**) Bright-field images of live embryos, anterior towards the left. Overall trunk morphology is normal in *unc5b* morphants (1 ng *unc5b*SBMO1 or 4 ng *unc5b*SBMO2) compared with controls (uninjected or 8 ng control MO). (**E-H**) Confocal projections of *fli:egfp* transgenics (reverse contrast) show that *unc5b* knockdown prevents PAV formation. Lateral views of somites 7-11, anterior towards the left; confocal projections through entire trunk. Embryos imaged live (G,H) or fixed after anti-GFP staining (E,F). (E,G) In uninjected embryos or control morphants at 48 hpf, almost every hemisegment is spanned by a PAV at the horizontal myoseptum (red arrows). (F,H) In embryos injected with either of two *unc5b* splice-blocking MOs, PAVs are absent (blue arrows) or only partially span their hemisegment (green arrows). DA, dorsal aorta; PCV, posterior cardinal vein. (**I**,**J**) PAV formation scored as percentage of hemisegments per embryo. In controls, at least 98% of hemisegments have complete or partial PAVs; this fraction is drastically reduced by either *unc5b* MO. *n*=25-30 embryos per condition; ***P*<0.0001. Bars show mean±s.e.m. (**K**) Partial *unc5b* genomic structure (not to scale), showing 5′ UTR (gray box), coding exons (white boxes) and MO targets. Scale bars: 1 mm in A for A-D; 50 μm in E for E-H.

The placenta is one of the more complex vascularized tissues in mammals. It is derived from three distinct sources: maternal tissue, extra-embryonic fetal tissue, and arteries and veins originating from the embryo proper. The fetal-placental vascular system circulates fetal blood and interdigitates with the trophoblast sinuses filled with maternal blood (Cross, 2005; Red-Horse et al., 2004). Assembly of the vasculature within the placental labyrinth requires signaling between the extra-embryonic tissue and the fetal-placental vessels. Mutational analysis has revealed dozens of genes required for this communication, with virtually all reports concluding that these genes exert their effects through the extra-embryonic trophectoderm (Cross, 2005; Rossant and Cross, 2001). In fact, patterning by the trophoblast cells is deemed an essential guide for proper growth of the fetal vessels into and within the labyrinth layer. The specific and autonomous role of *Unc5b* in promoting fetal-placental arteriogenesis emphasizes that vascular signaling pathways on the fetal-placental side of the equation should not be ignored. As the UNC5B-deficient phenotype could not be rescued by a wild-type trophectoderm, we propose that UNC5B-mediated signaling is a specific and autonomous component of fetal-placental angiogenesis, and that *Unc5b* disruption represents a rare, if not the first, example of a mutation acting solely with the fetal placental vasculature.

Abnormal placental vascular development may be etiologically linked to multiple obstetric complications, including early pregnancy loss, intrauterine growth restriction, fetal death and pre-eclampsia, and may have lasting consequences for childhood development (Cross, 2006; Mayhew et al., 2007; Redman and Sargent, 2003). Recent studies have assigned a role for maternal angiogenic signaling pathways in pre-eclampsia (Levine et al., 2006; Wallner et al., 2007). The findings presented herein provide genetic evidence that defects in netrin/UNC5B signaling, which disrupts the fetal contribution to the placental vasculature, should be considered in the pathogenesis of clinical syndromes of uteroplacental insufficiency (Cross, 2003; Levine et al., 2006; Wallner et al., 2007).

We thank the many former and current Li and Chien laboratory members for their support with this project; Diana Lim for help in manuscript preparation; Antonio Frias, Suzanne Mansour, Shannon Odelberg and L. Charles Murtaugh for critique of the manuscript; Antonio Frias for insights into uteroplacental insufficiency; the University of Utah Mouse Core laboratory for assistance with tetraploid aggregation; and Philippe Soriano, Matthias Stadtfeld, Masashi Yanagisawa and Lindsay Hinck for mouse strains. This work was supported by grants to D.Y.L. from the NIH, American Cancer Society, American Heart Association, Flight Attendants Medical Research Institute and the Burroughs Wellcome Fund and by RO1 EY12873 to C.-B.C.

Supplementary material

Supplementary material for this article is available at
http://dev.biologists.org/cgi/content/full/135/4/659/DC1

References

Adamson, S. L., Lu, Y., Whiteley, K. J., Holmyard, D., Hemberger, M., Pfarrer, C. and Cross, J. C. (2002). Interactions between trophoblast cells and the maternal and fetal circulation in the mouse placenta. *Dev. Biol.* **250**, 358-373.

Cirulli, V. and Yebra, M. (2007). Netrins: beyond the brain. *Nat. Rev. Mol. Cell Biol.* **8**, 296-306.

Cross, J. C. (2003). The genetics of pre-eclampsia: a feto-placental or maternal problem? *Clin. Genet.* **64**, 96-103.

Cross, J. C. (2005). How to make a placenta: mechanisms of trophoblast cell differentiation in mice – a review. *Placenta Suppl.* **26**, S3-S9.

Cross, J. C. (2006). Placental function in development and disease. *Reprod. Fertil. Dev.* **18**, 71-76.

Cross, J. C., Baczyk, D., Dobric, N., Hemberger, M., Hughes, M., Simmons, D. G., Yamamoto, H. and Kingdom, J. C. (2003). Genes, development and evolution of the placenta. *Placenta* **24**, 123-130.

Engelkamp, D. (2002). Cloning of three mouse Unc5 genes and their expression patterns at mid-gestation. *Mech. Dev.* **118**, 191-197.
Ferrara, N., Gerber, H. P. and LeCouter, J. (2003). The biology of VEGF and its receptors. *Nat. Med.* **9**, 669-676.
Holtwick, R., Gotthardt, M., Skryabin, B., Steinmetz, M., Potthast, R., Zetsche, B., Hammer, R. E., Herz, J. and Kuhn, M. (2002). Smooth muscle-selective deletion of guanylyl cyclase-A prevents the acute but not chronic effects of ANP on blood pressure. *Proc. Natl. Acad. Sci. USA* **99**, 7142-7147.
Huber, A. B., Kolodkin, A. L., Ginty, D. D. and Cloutier, J. F. (2003). Signaling at the growth cone: ligand-receptor complexes and the control of axon growth and guidance. *Annu. Rev. Neurosci.* **26**, 509-563.
Jiang, X., Rowitch, D. H., Soriano, P., McMahon, A. P. and Sucov, H. M. (2000). Fate of the mammalian cardiac neural crest. *Development* **127**, 1607-1616.
Kennedy, T. E., Serafini, T., de la Torre, J. R. and Tessier-Lavigne, M. (1994). Netrins are diffusible chemotropic factors for commissural axons in the embryonic spinal cord. *Cell* **78**, 425-435.
Kimmel, C. B., Ballard, W. W., Kimmel, S. R., Ullmann, B. and Schilling, T. F. (1995). Stages of embryonic development of the zebrafish. *Dev. Dyn.* **203**, 253-310.
Kisanuki, Y. Y., Hammer, R. E., Miyazaki, J., Williams, S. C., Richardson, J. A. and Yanagisawa, M. (2001). Tie2-Cre transgenic mice: a new model for endothelial cell-lineage analysis in vivo. *Dev. Biol.* **230**, 230-242.
Lauderdale, J. D., Davis, N. M. and Kuwada, J. Y. (1997). Axon tracts correlate with netrin-1a expression in the zebrafish embryo. *Mol. Cell. Neurosci.* **9**, 293-313.
Lawson, N. D. and Weinstein, B. M. (2002). In vivo imaging of embryonic vascular development using transgenic zebrafish. *Dev. Biol.* **248**, 307-318.
Leonardo, E. D., Hinck, L., Masu, M., Keino-Masu, K., Ackerman, S. L. and Tessier-Lavigne, M. (1997). Vertebrate homologues of C. elegans UNC-5 are candidate netrin receptors. *Nature* **386**, 833-838.
Levine, R. J., Lam, C., Qian, C., Yu, K. F., Maynard, S. E., Sachs, B. P., Sibai, B. M., Epstein, F. H., Romero, R., Thadhani, R. et al. (2006). Soluble endoglin and other circulating antiangiogenic factors in preeclampsia. *N. Engl. J. Med.* **355**, 992-1005.
Lu, X., Le Noble, F., Yuan, L., Jiang, Q., De Lafarge, B., Sugiyama, D., Breant, C., Claes, F., De Smet, F., Thomas, J. L. et al. (2004). The netrin receptor UNC5B mediates guidance events controlling morphogenesis of the vascular system. *Nature* **432**, 179-186.
Mayhew, T. M., Manwani, R., Ohadike, C., Wijesekara, J. and Baker, P. N. (2007). The placenta in pre-eclampsia and intrauterine growth restriction: studies on exchange surface areas, diffusion distances and villous membrane diffusive conductances. *Placenta* **28**, 233-238.
Mu, J. and Adamson, S. L. (2006). Developmental changes in hemodynamics of uterine artery, utero- and umbilicoplacental, and vitelline circulations in mouse throughout gestation. *Am. J. Physiol. Heart Circ. Physiol.* **291**, H1421-H1428.
Nagy, A., Rossant, J., Nagy, R., Abramow-Newerly, W. and Roder, J. C. (1993). Derivation of completely cell culture-derived mice from early-passage embryonic stem cells. *Proc. Natl. Acad. Sci. USA* **90**, 8424-8428.
Nguyen, A. and Cai, H. (2006). Netrin-1 induces angiogenesis via a DCC-dependent ERK1/2-eNOS feed-forward mechanism. *Proc. Natl. Acad. Sci. USA* **103**, 6530-6535.
Nicosia, R. F., Zhu, W. H., Fogel, E., Howson, K. M. and Aplin, A. C. (2005). A new ex vivo model to study venous angiogenesis and arterio-venous anastomosis formation. *J. Vasc. Res.* **42**, 111-119.
Papaioannou, V. E. and Behringer, R. R. (2005). *Mouse Phenotypes*. Cold Spring Harbor, NY: Cold Spring Harbor Laboratory Press.
Park, K. W., Crouse, D., Lee, M., Karnik, S. K., Sorensen, L. K., Murphy, K. J., Kuo, C. J. and Li, D. Y. (2004). The axonal attractant Netrin-1 is an angiogenic factor. *Proc. Natl. Acad. Sci. USA* **101**, 16210-16215.
Raleigh, J. A., Miller, G. G., Franko, A. J., Koch, C. J., Fuciarelli, A. F. and Kelly, D. A. (1987). Fluorescence immunohistochemical detection of hypoxic cells in spheroids and tumours. *Br. J. Cancer* **56**, 395-400.
Red-Horse, K., Zhou, Y., Genbacev, O., Prakobphol, A., Foulk, R., McMaster, M. and Fisher, S. J. (2004). Trophoblast differentiation during embryo implantation and formation of the maternal-fetal interface. *J. Clin. Invest.* **114**, 744-754.
Redman, C. W. and Sargent, I. L. (2003). Pre-eclampsia, the placenta and the maternal systemic inflammatory response-a review. *Placenta Suppl.* **24**, S21-S27.
Rinkenberger, J. and Werb, Z. (2000). The labyrinthine placenta. *Nat. Genet.* **25**, 248-250.
Rossant, J. and Cross, J. C. (2001). Placental development: lessons from mouse mutants. *Nat. Rev. Genet.* **2**, 538-548.
Salminen, M., Meyer, B. I., Bober, E. and Gruss, P. (2000). Netrin 1 is required for semicircular canal formation in the mouse inner ear. *Development* **127**, 13-22.
Sclafani, A. M., Skidmore, J. M., Ramaprakash, H., Trumpp, A., Gage, P. J. and Martin, D. M. (2006). Nestin-Cre mediated deletion of Pitx2 in the mouse. *Genesis* **44**, 336-344.
Serafini, T., Kennedy, T. E., Galko, M. J., Mirzayan, C., Jessell, T. M. and Tessier-Lavigne, M. (1994). The netrins define a family of axon outgrowth-promoting proteins homologous to C. elegans UNC-6. *Cell* **78**, 409-424.
Serafini, T., Colamarino, S. A., Leonardo, E. D., Wang, H., Beddington, R., Skarnes, W. C. and Tessier-Lavigne, M. (1996). Netrin-1 is required for commissural axon guidance in the developing vertebrate nervous system. *Cell* **87**, 1001-1014.
Soriano, P. (1999). Generalized lacZ expression with the ROSA26 Cre reporter strain. *Nat. Genet.* **21**, 70-71.
Stadtfeld, M. and Graf, T. (2005). Assessing the role of hematopoietic plasticity for endothelial and hepatocyte development by non-invasive lineage tracing. *Development* **132**, 203-213.
Tessier-Lavigne, M. and Goodman, C. S. (1996). The molecular biology of axon guidance. *Science* **274**, 1123-1133.
Urness, L. D., Sorensen, L. K. and Li, D. Y. (2000). Arteriovenous malformations in mice lacking activin receptor-like kinase-1. *Nat. Genet.* **26**, 328-331.
Wallner, W., Sengenberger, R., Strick, R., Strissel, P. L., Meurer, B., Beckmann, M. W. and Schlembach, D. (2007). Angiogenic growth factors in maternal and fetal serum in pregnancies complicated by intrauterine growth restriction. *Clin. Sci.* **112**, 51-57.
Wilson, B. D., Ii, M., Park, K. W., Suli, A., Sorensen, L. K., Larrieu-Lahargue, F., Urness, L. D., Suh, W., Asai, J., Kock, G. A. et al. (2006). Netrins promote developmental and therapeutic angiogenesis. *Science* **313**, 640-644.
Yaniv, K., Isogai, S., Castranova, D., Dye, L., Hitomi, J. and Weinstein, B. M. (2006). Live imaging of lymphatic development in the zebrafish. *Nat. Med.* **12**, 711-716.
Yebra, M., Montgomery, A. M., Diaferia, G. R., Kaido, T., Silletti, S., Perez, B., Just, M. L., Hildbrand, S., Hurford, R., Florkiewicz, E. et al. (2003). Recognition of the neural chemoattractant Netrin-1 by integrins alpha6beta4 and alpha3beta1 regulates epithelial cell adhesion and migration. *Dev. Cell* **5**, 695-707.

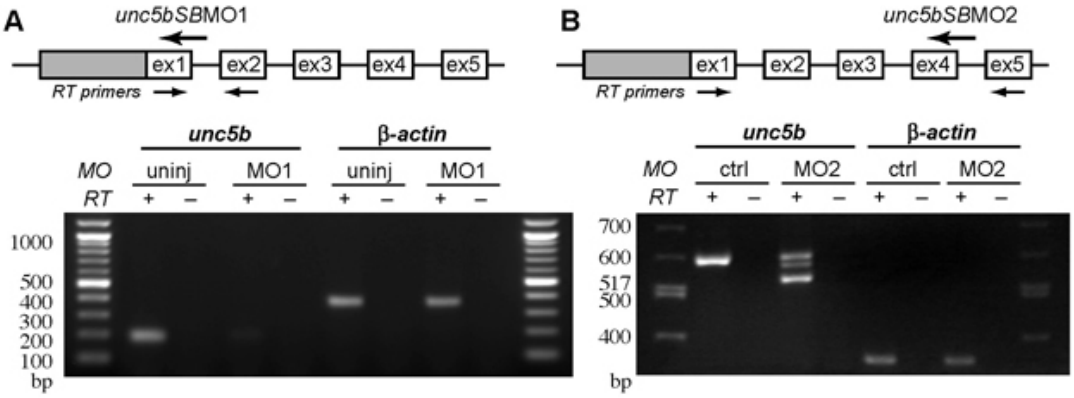

Figure S1. Knockdown of *unc5b* decreases levels of wild-type mRNA. RT-PCR analysis of control and morphant embryos shows that 1 ng *unc5b*SBMO1 or 4 ng *unc5b*SBMO2 significantly reduce levels of wild-type *unc5b* mRNA compared with uninjected embryos or to 8 ng control MO. Diagrams (top) show partial *unc5b* genomic structure (gray box, 5′ UTR; white boxes, coding exons; not to scale), with positions of MO sequences and RT-PCR primers indicated. Agarose gel images (below) show RT-PCR results for *unc5b* message and β-actin as a loading control. *RT*+/−, with or without reverse transcriptase. *unc5b*SBMO1 appears to abolish wild-type mRNA, while *unc5b*SBMO2 reduces wild-type mRNA and yields two additional bands. Sequencing of PCR products confirms that the upper band represents the wild-type product. The lower band corresponds to an in-frame deletion of amino acid residues 162-182, presumably reflecting a cryptic splice donor in exon 4. The middle band is a heteroduplex of the wild type and the alternate splice products. This deletion is in an Ig domain, which has been shown to be required for netrin binding (Kruger et al., 2004). DNA ladder sizes indicated in base pairs.

CHAPTER 3

MOTONEURONS ARE ESSENTIAL FOR VASCULAR PATTERNING

The following chapter was reprinted with permission from The Company of Biologists. In addition to myself, the other authors were Arminda Suli, Karina Yaniv, Brant Weinstein, Chi-Bin Chien and Dean Li. It was originally published in Development, 2011 Sept; 138(17):3847-3857. I participated in the design, execution and interpretation of data related to DCC and motoneuron axons in vascular guidance in zebrafish (Figures 2A, 4A', B', 5, 6, 7, 8; Supplemental Figures 1D-F, 5, 6).

Development 138, 3847-3857 (2011) doi:10.1242/dev.068403

Motoneurons are essential for vascular pathfinding

Amy H. Lim[1,2,*], Arminda Suli[2,*], Karina Yaniv[3], Brant Weinstein[4], Dean Y. Li[1,5,6,†] and Chi-Bin Chien[2]

SUMMARY

The neural and vascular systems share common guidance cues that have direct and independent signaling effects on nerves and endothelial cells. Here, we show that zebrafish Netrin 1a directs Dcc-mediated axon guidance of motoneurons and that this neural guidance function is essential for lymphangiogenesis. Specifically, Netrin 1a secreted by the muscle pioneers at the horizontal myoseptum (HMS) is required for the sprouting of *dcc*-expressing rostral primary motoneuron (RoP) axons and neighboring axons along the HMS, adjacent to the future trajectory of the parachordal chain (PAC). These axons are required for the formation of the PAC and, subsequently, the thoracic duct. The failure to form the PAC in *netrin 1a* or *dcc* morphants is phenocopied by laser ablation of motoneurons and is rescued both by cellular transplants and overexpression of *dcc* mRNA. These results provide a definitive example of the requirement of axons in endothelial guidance leading to the parallel patterning of nerves and vessels in vivo.

KEY WORDS: Netrin, DCC, Lymphatic, Parachordal chain, Motoneuron, Axon guidance, Vascular guidance, Angiogenesis, Zebrafish

INTRODUCTION

There is a striking congruence among the anatomies of nerves, blood vessels and lymphatics. Not surprisingly, the prototypic guidance cues, initially discovered for their roles in axon pathfinding (Dickson, 2002), also guide blood vessels and lymphatics (Adams and Eichmann, 2010; Carmeliet and Tessier-Lavigne, 2005; Larrivee et al., 2009; Melani and Weinstein, 2009; Suchting et al., 2006; Weinstein, 2005). One such family, the Netrins, directly guide both axon outgrowth and vascular sprouting through various receptors. Depending on the receptors expressed, Netrins may be repulsive or attractive (Bouvree et al., 2008; Cirulli and Yebra, 2007; Hong et al., 1999; Larrivee et al., 2007; Lejmi et al., 2008; Lu et al., 2004; Navankasattusas et al., 2008; Park et al., 2004; Rajasekharan and Kennedy, 2009; Wilson et al., 2006). Netrins also act as a survival cue for dependence receptors in shaping the neural and vascular systems during development (Castets et al., 2009; Furne et al., 2008; Tang et al., 2008).

The close alignment of nerves and vessels throughout the body plan could be achieved in one of two ways: either by shared patterning mechanisms or by axons acting to guide vessels (or vice versa). For example, in the developing quail forelimb, nerves and vessels both respond with repulsion to Sema3A/Nrp1 signaling (Bates et al., 2003). By contrast, a subset of axonal projections from the superior cervical ganglion specifically follows Endothelin 3 secreted by the external carotid artery (Makita et al., 2008). Conversely, motoneurons, sensory neurons and/or Schwann cells secrete Vegf that is required for arterial differentiation in the skin (Mukouyama et al., 2005). Therefore, when investigating the effects of axon guidance cues on blood vessels or lymphatic endothelium, it is essential to distinguish a direct effect on endothelial cells from the potential influence on axonal projections, which may subsequently affect the endothelial cells.

The parachordal chain (PAC), a string of endothelial cells located at the horizontal myoseptum (HMS), forms at 2 days post-fertilization (dpf) in zebrafish. Since the PAC bears no evidence of a lumen (Hogan et al., 2009a), we prefer this nomenclature to the previous term ‘parachordal vessel’. The PAC cells eventually migrate ventrally along the trunk vasculature to the space between the dorsal aorta (DA) and the posterior cardinal vein (PCV) to form the main vessel of the lymphatic system: the thoracic duct (TD) (Bussmann et al., 2010; Yaniv et al., 2006). Prior to the formation of the PAC along the HMS, however, motoneurons extend axons along a path parallel to its future trajectory (Beattie, 2000; Eisen et al., 1986; Pike and Eisen, 1990), offering an opportunity to dissect the contribution of neurons and endothelial cells to zebrafish lymphatic patterning and development.

We previously showed that knockdown of *netrin 1a*, a zebrafish ortholog of mammalian netrin 1, disrupts PAC development (Wilson et al., 2006). In the current study, we definitively identify the muscle pioneers (MPs) as the critical source of Netrin 1a for PAC formation. We show that *netrin 1a* and *dcc* are required for three precise events: axonal extension of RoP and secondary motoneurons (SMNs) along the HMS; the turn made by secondary vascular sprouts to follow the HMS; and the formation of the PAC. Furthermore, genetic removal or laser ablation of the motoneurons also prevents secondary sprout turning and PAC formation. These results show that lymphangiogenesis is dependent on choreographed interactions between MPs, axons and endothelial cells. In particular, growth of the RoP axon and associated axons determines the guidance of the PAC lymphendothelial cells.

[1]Molecular Medicine Program, 15 N 2030 East, Room 4140, University of Utah, Salt Lake City, UT 84112, USA. [2]Department of Neurobiology and Anatomy, 20 North 1900 East, Room 401 MREB, University of Utah, Salt Lake City, UT 84132, USA. [3]Department of Biological Regulation, Weizmann Institute of Science, Rehovot, 76100, Israel. [4]Laboratory of Molecular Genetics, National Institute of Child Health and Human Development, National Institutes of Health, Building 6B, Room 309, 6 Center Drive, Bethesda, MD 20892, USA. [5]Division of Cardiology, Department of Medicine, 30 N 1900 East, Room 4A100 SOM, University of Utah, Salt Lake City, UT 84132, USA. [6]Department of Oncological Sciences, 2000 Circle of Hope, University of Utah, Salt Lake City, UT 84112, USA.

*These authors contributed equally to this work
†Author for correspondence (dean.li@u2m2.utah.edu)

Accepted 14 June 2011

MATERIALS AND METHODS

Fish stocks and embryo raising

Zebrafish adults were maintained and bred according to standard procedures. Tg(*fli1a:egfp*)$^{y1/+}$ fish were a gift from Joe Yost (University of Utah). *plcg1*$^{y10/+}$; Tg(*fli1a:egfp*)$^{y1/+}$ and Tg(*fli1a-ep:DsRedEx*)^{um13} fish were a gift from Nathan Lawson (University of Massachusettes). *isl1*$^{sa0029/+}$; Tg(*fli1a:egfp*)$^{y1/+}$ were from the Sanger Institute Zebrafish Mutation Resource. Tg(*hb9:GFP*) fish (official name *mnx1:gfp*^{ml2}) and Tg(*hb9:KikGR*)^{p151}; *fli1a1:egfp* fish were gifts from Michael Granato (Flanagan-Steet et al., 2005). All experiments were carried out subject to NIH guidelines and approved by the University of Utah Institutional Animal Care and Use Committee.

Morpholino oligonucleotide (MO) injections

We injected the following MOs from Gene Tools (Philomath, OR, USA): standard control MO (Control), 5′-CCTCTTACCTCAGTTACAATTTATA-3′; 6-10 ng *netrin 1a* splice-blocking MO (*netrin1a*SBMO), 5′-ATGATGGACTTACCGACACATTCGT-3′ (Wilson et al., 2006); 8.6 ng *dcc* translation-blocking MO (*dcc*TBMO), 5′-GAATATCTCCAGTGACGCAGCCCAT-3′ (Suli et al., 2006) (+1 to +25 bp, reverse strand start codon underlined); 10.2 ng *olig2* splice-blocking MO (*olig2*SBMO), 5′-CGTTCAGTGCGCTCTCAGCTTG-3′ (Park et al., 2002); 15.3 ng *plcg1* MO (*plcg1*SBMO), 5′-ATTAGCATAGGGAACTTACTTTCG-3′ (Lawson et al., 2003); 6.0 ng *isl1*E2 splice-blocking MO, 5′-TTAATCTGCGTTACCTGATGTAGTC-3′ and 6.0 ng *isl1*E3 MO, 5′-GAATGCAATGCCTACCTGCCATTTG-3′ were injected sequentially (Hutchinson and Eisen, 2006). It should be noted that MOs targeted against non-Netrin-related transcripts were injected in other experiments and a PAC and/or axon phenotype at the HMS was not observed: *roundabout 4* (*robo4*), 5′-TTTTTAGCGTACCTATGAGCAGTT-3′ (Bedell et al., 2005); *cardiac troponin T2* (*tnnt2*), 5′-CATGTTTGCTCTGATCTGACACGCA-3′ (Sehnert et al., 2002); *hadp1*, 5′-GATCAACTCTTACCTGCTTGTAAAG-3′ (Wythe et al., 2011); and *microsomal triglyceride transfer protein* (*mtp*) (unpublished).

dcc mRNA injection

Full-length Dcc coding sequence with seven of the first 27 bp mutated (5′-ATGGGaTGtGTaACaGGcGAcATcCGC-3′) was cloned into a Gateway middle clone (Invitrogen) and combined with p5E-CMV-SP6 and p3E-pA (Kwan et al., 2007) in pDestTol2pA2 and used to synthesize RNA. One-cell stage embryos were first injected with 225 pg *dcc* mRNA, using 0.5% Phenol Red as a marker dye. A subset was then re-injected with 8.6 ng *dcc*TBMO.

In situ hybridization (ISH) and immunostaining

ISH for *netrin 1a* and *dcc* was performed as described (Suli et al., 2006). For immunostaining, the following antibodies were used: rabbit anti-GFP primary (1:400; Molecular Probes, Carlsbad, CA, USA) with Alexa 488 anti-rabbit secondary (1:100; Molecular Probes); mouse 4D9 anti-engrailed primary (1:4; Developmental Studies Hybridoma Bank, University of Iowa) with HRP anti-mouse secondary (1:100; Molecular Probes) followed by Alexa 568 tyramide reaction (Molecular Probes); mouse znp-1 (anti-synaptotagmin 2) (1:200; Developmental Studies Hybridoma Bank, University of Iowa).

Sectioning

Following ISH, embryos were dehydrated in methanol, treated with 1:1 Immuno-Bed:methanol for 30 minutes at 4°C and incubated with undiluted infiltrate overnight at 4°C. The embryos were then embedded with a 20:1 mixture of Immuno-Bed:Immuno-Bed Solution B (Electron Microscopy Sciences) and sectioned at 12 μm in a transverse plane for *netrin 1a* or a longitudinal plane for *dcc*.

Cyclopamine treatment

Thirty embryos per well in a 24-well dish were incubated with 1 ml/well 50 μM cyclopamine in 1% DMSO, or 1% DMSO only as a control, from 50% epiboly to 16 hpf at 23°C, then washed several times with E3 embryo medium (5 mM NaCl, 0.17 mM KCl, 0.33 mM $CaCl_2$, 0.33 mM $MgSO_4$).

Cell transplants

One-cell stage *fli1a:egfp*^{y1} embryos were injected with either Rhodamine Dextran (RhDx, 0.5% in water) or 6 ng *netrin1a*SBMO. To target MPs, 5-10 cells were transplanted from 4 hpf RhDx-injected donors into the margin of 3 hpf *netrin 1a* morphant hosts (Halpern et al., 1995). The region between somites 5-15 was scored for PAC defects. The percentage of hemisegments with complete, partial or absent PACs was calculated separately for hemisegments receiving transplanted MPs and those without transplanted MPs, and treated as a paired dataset.

Imaging

z-stack images were acquired (Olympus FV1000 or FV300 confocal microscope) and ImageJ software (Wayne Rasband, NIH) was used to create maximum intensity *z*-projections; these span only one side of the embryo unless otherwise stated. FluoRender (Wan et al., 2009) was used for volume rendering. For PAC analysis in all experiments except cell transplants and motoneuron ablation, 3-5 hemisegments from somites 7-11 were scored.

Time-lapse imaging

z-stack images (2.5 μm step, ~80 slices) were acquired (Olympus FV1000 confocal microscope). Embryos were imaged every 12-15 minutes for 16.5-19 hours, starting at 29-33 hpf. Room temperature was 27±2°C. Time-lapse movies were generated using maximum intensity projections in ImageJ.

Laser ablation

Using *hb9:KikGR* labeling of motoneuron cell bodies and their stereotypical location relative to the somitic boundary to target the laser, motoneuron cell bodies of *hb9:KikGR*; *fli1a:egfp*^{y1} embryos at 18-24 hpf were ablated. A 405 nm laser (Olympus FV1000 or FV300 confocal microscope) was used at 100% intensity at 40 μseconds/pixel for 3000 pulses. The embryos were exposed to UV light from a stereomicroscope for ~5-10 seconds to convert the KikGR protein from green to red at 55 hpf and then imaged.

RESULTS

netrin 1a is required for thoracic duct formation

We previously showed that *netrin 1a* is essential for PAC formation (e.g. Wilson et al., 2006). As the PAC has been shown to be the source of lymphatic endothelial cells (LECs) that populate the TD (Geudens et al., 2010; Yaniv et al., 2006), we next investigated whether *netrin 1a* depletion would affect TD development. Embryos injected with *netrin 1a* splice-blocking MO (*netrin1a*SBMO) were assayed for presence of the TD. Whereas embryos injected with a control MO had a complete or partial TD in 77% of their hemisegments (*n*=200 hemisegments, 16 larvae), *netrin 1a* morphants had a complete or partial TD in only 25% of their hemisegments (*n*=292 hemisegments, 24 larvae) (see Fig. S1A-C in the supplementary material). Thus, *netrin 1a* depletion indeed leads to defects in lymphatic development.

netrin 1a is required for attraction of secondary sprouts at the HMS

The absence of the PAC in *netrin 1a*-depleted embryos could result from impaired angiogenesis from the PCV, from defects in the dorsal extension of secondary intersegmental vessel (ISV) sprouts as they grow from the PCV to the HMS, or from defects in turning upon reaching the HMS (Fig. 1A-C′). To determine which of these three steps is affected in the absence of *netrin 1a* we used *plcg1*^{y10} mutant embryos because in wild-type (WT) embryos the secondary sprouts track very closely with the ventral portion of the primary ISVs and are difficult to distinguish. *plcg1*^{y10} mutants lack primary ISVs but have a normal PCV, secondary sprouts and PAC (Lawson et al., 2003). We injected *plcg1*^{y10}; *fli1a:egfp*^{y1} mutants with

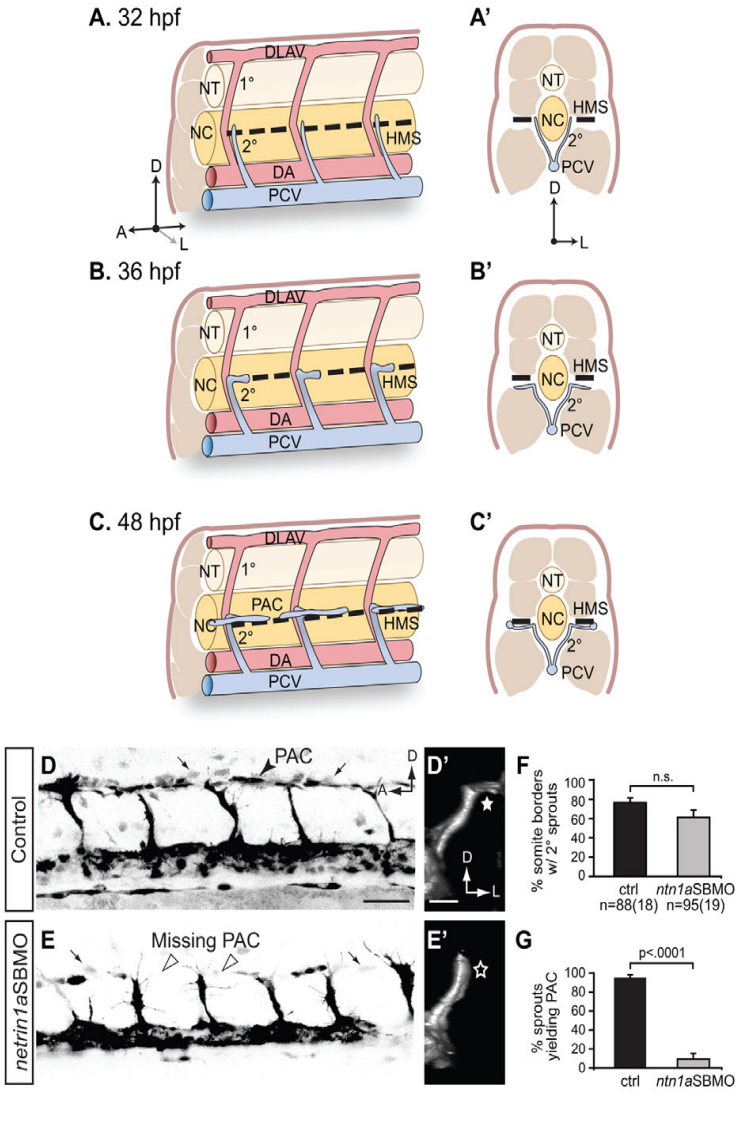

Fig. 1. *netrin 1a* is required for turning of secondary sprouts at the horizontal myoseptum. (**A-C'**) Lateral (A-C) and corresponding transverse views (A'-C') of parachordal chain (PAC) formation, showing dorsal aorta (DA, red), posterior cardinal vein (PCV, blue), horizontal myoseptum (HMS, dashed line), primary intersomitic vessels (1°, red) and secondary sprouts (2°, blue). DA and primary sprouts omitted for clarity. (A,A') Secondary sprouts emerge from the PCV at ~32 hpf and grow dorsally to the HMS. (B,B') Dorsal growth stops at the HMS and sprouts turn and grow laterally. (C') Lateral growth stops at the lateral-most aspect of the muscle, and the sprout then turns anteriorly and posteriorly to form the PAC. (**D-E'**) Removing *netrin 1a* function in 48 hpf *plcg1*^{y10}; *fli1a:egfp*^{y1} zebrafish embryos. (D,E) Lateral views, reversed contrast. (D',E') Transverse view volume renderings of single hemisegments from D,E. (D,D') In uninjected controls, secondary sprouts grow from the PCV and turn at the HMS (star, D') to form the PAC (arrowhead, D). The *fli1a:egfp*^{y1} transgene also labels some dimly fluorescent non-endothelial cells near the HMS (small arrows, D,E). (E,E') In *netrin 1a* morphants, secondary sprouts usually fail to turn laterally (star, E') and form the PAC (arrowheads, E). (**F**,**G**) Secondary sprouts were quantified in five hemisegments per embryo in uninjected controls and *netrin 1a* morphants. (F) The fraction of intersomitic boundaries bearing secondary sprouts is not significantly changed in morphants. Uninjected controls, 75±5%; *netrin 1a* morphants, 61±8%. (G) Fewer secondary sprouts turn to form the PAC in morphants. Uninjected controls, 95±3%; *netrin 1a* morphants, 9±5%. All values are mean±s.e.m.; error bars show s.e.m.; *P*-value determined by Mann-Whitney U test; n.s., not significant; *n*, number of hemisegments (number of embryos). A, anterior; D, dorsal; L, lateral; DLAV, dorsal longitudinal anastomotic vessel; NT, neural tube; NC, notochord; 1°, primary sprouts; 2°, secondary sprouts. Scale bars: 50 μm.

*netrin1a*SBMO and examined secondary sprout formation (Fig. 1D-F). Secondary sprout formation did not differ from that of uninjected controls (75% of hemisegments with secondary sprout; *n*=88 hemisegments, 18 embryos) and *netrin 1a* morphants (61% of hemisegments with secondary sprout; *n*=95 hemisegments, 19 embryos). In uninjected controls, secondary sprouts extended dorsally to the HMS (Fig. 1D), turned laterally (Fig. 1D') and then extended anteroposteriorly to form the PAC (Fig. 1D). In morphants, secondary sprouts extended normally to the HMS (Fig. 1E) but then failed to turn laterally or anteroposteriorly (Fig. 1E'). Whereas in controls 95% of secondary sprouts turned at the HMS to form a PAC, in morphants sprouts only turned at 9% of the somitic boundaries (Fig. 1D-E',G).

We also carried out live imaging in *plcg1*^{y10} mutants, either uninjected or injected with *netrin1a*SBMO (see Fig. S2 and Movies 1 and 2 in the supplementary material), for a period of 16.5-19 hours starting at 29-33 hpf. In control embryos (*n*=4), secondary sprouts grew dorsally, then turned anteroposteriorly upon reaching the HMS. In *netrin 1a* morphants (*n*=3), initial dorsal growth appeared normal. However, upon reaching the HMS, the secondary sprouts usually stalled, ceasing elongation but maintaining active filopodia and failing to turn. These time-lapse data confirmed the conclusion drawn from fixed samples that *netrin 1a* morphants show specific defects in anteroposterior turning by secondary sprouts. Thus, *netrin 1a* is required specifically for secondary sprouts to turn along the HMS, but neither for their initial growth nor their dorsal elongation towards the HMS.

Netrin 1a from the MPs is responsible for PAC formation

To determine when and where Netrin 1a might act to mediate PAC formation, we examined its expression by mRNA in situ hybridization (ISH) at 22 and 32 hpf (Fig. 2A,B). Sectioning revealed *netrin 1a* labeling in the region corresponding to the MPs

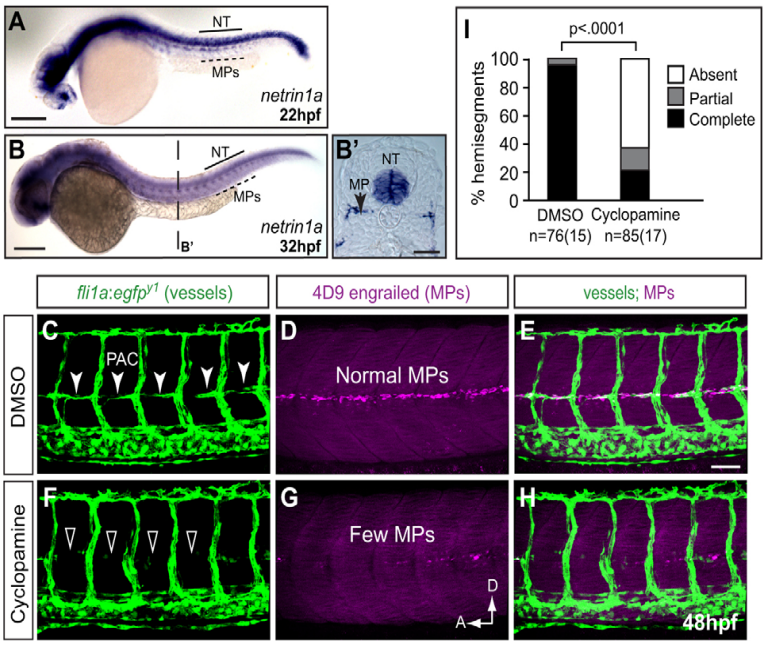

Fig. 2. Muscle pioneers express *netrin 1a* along the HMS prior to and during PAC formation and are required for PAC formation. (**A-B′**) mRNA in situ hybridization (ISH) shows *netrin 1a* expression in MPs and neural tube (NT) at 22 and 32 hpf. (B′) Transverse section of zebrafish embryo in B at the level indicated. (**C-H**) The muscle pioneers (MPs) are the critical source of Netrin 1a for PAC formation. Treatment with 50 μM cyclopamine prevents nearly all MP formation and leads to failure of PAC formation. 48 hpf *fli1a:egfp*^{y1} embryos antibody stained for vessels (GFP, green) and MPs (4D9 anti-engrailed, magenta). Confocal projections. (C-E) In DMSO-treated control embryos, MPs are present at the HMS (D) and the PAC forms normally (C, arrowheads). (F-H) In cyclopamine-treated embryos, very few MPs form (G) and the PAC is missing (F, arrowheads). (**I**) PAC formation was assessed in hemisegments 7-11 in DMSO-treated (97±2% complete; 3±2% partial; 0±0% absent) and cyclopamine-treated (21±6% complete; 15±4% partial; 64±7% absent) embryos. All values are mean±s.e.m.; *P*-value determined by Mann-Whitney U test comparing absent PACs. *n*, number of hemisegments (number of embryos). A, anterior; D, dorsal; NT, neural tube. Scale bars: 200 μm in A-B′; 50 μm in C-H.

at the HMS in addition to the neural tube (Fig. 2B′). Owing to their proximity, we hypothesized that the MPs are the source of the Netrin 1a that guides the PAC, and that Netrin 1a from the neural tube is irrelevant.

To test this hypothesis, we prevented MP formation by treating embryos with the Sonic hedgehog (Shh) inhibitor cyclopamine and examined PAC formation (Fig. 2C-H) (Wolff et al., 2003). We incubated *fli1a:egfp*^{y1} embryos with cyclopamine and examined the presence of MPs at 36 hpf by immunolabeling with the anti-engrailed 4D9 antibody (Wolff et al., 2003). Whereas 4D9 staining was observed at the HMS in DMSO-treated embryos, far less staining was visible in cyclopamine-treated embryos, indicating that the treatment efficiently prevented almost all MP formation. Additionally, *netrin 1a* mRNA could no longer be detected by ISH at the HMS of cyclopamine-treated embryos, whereas its expression in the neural tube was unaffected (see Fig. S3 in the supplementary material). DMSO-treated control embryos had no hemisegments missing the PAC and only 3% with a partial PAC (*n*=76 hemisegments, 15 embryos) (Fig. 2C-E,I). By contrast, in cyclopamine-treated embryos the PAC was absent in 64% of hemisegments and partially formed in 15% (*n*=85 hemisegments, 17 embryos) (Fig. 2F-I). Although cyclopamine can also affect the formation of muscles and vessels, MPs are the most sensitive cells (Wolff et al., 2003). At the carefully titrated cyclopamine dose used here the majority of the MPs are removed, but there is no visible effect on other muscles or other trunk vasculature. Since cyclopamine inhibits the formation of the source of Netrin 1a at the HMS but does not alter *netrin 1a* expression in the spinal cord, we infer that *netrin 1a* expressed by the MPs at the HMS is the critical source of guidance information for the PAC.

To test the sufficiency of MPs for PAC formation we performed heterochronic blastula transplants (Halpern et al., 1995; Suli et al., 2006). We transplanted cells from sphere stage embryos (4 hpf) into blastula embryos (3 hpf), which allows for better targeting of the MPs. Cells from *fli1a:egfp*^{y1} donors injected with Rhodamine Dextran (RhDx) were transplanted into *fli1a:egfp*^{y1} hosts injected with *netrin1a*SBMO (Fig. 3A). RhDx-positive transplanted donor cells contributed to MPs, which were distinguished by their morphology and position at the HMS. Donor cells also contributed to the spinal cord, hypochord, fast and slow muscle cells and endothelial cells. As the donor embryos expressed *fli1a:egfp*^{y1}, endothelial cells derived from the transplanted cells were identified by RhDx and EGFP co-staining (see Fig. S4 in the supplementary material); these embryos were omitted from our analysis. Among *netrin 1a* morphant hemisegments without transplanted WT MPs, only 42% developed a complete or partial PAC (Fig. 3B-H) (*n*=59 hemisegments, 17 embryos). By contrast, 78% of hemisegments that received transplanted WT MPs developed a full or partial PAC (*n*=32 hemisegments, 17 embryos) (Fig. 3B-H). Thus, reintroducing MPs at the HMS, which presumably present the only source of Netrin 1a, is sufficient to restore PAC formation in *netrin 1a* morphants. Together with the cyclopamine experiments, this shows that MPs are the source of Netrin 1a that is responsible for secondary sprout turning at the HMS.

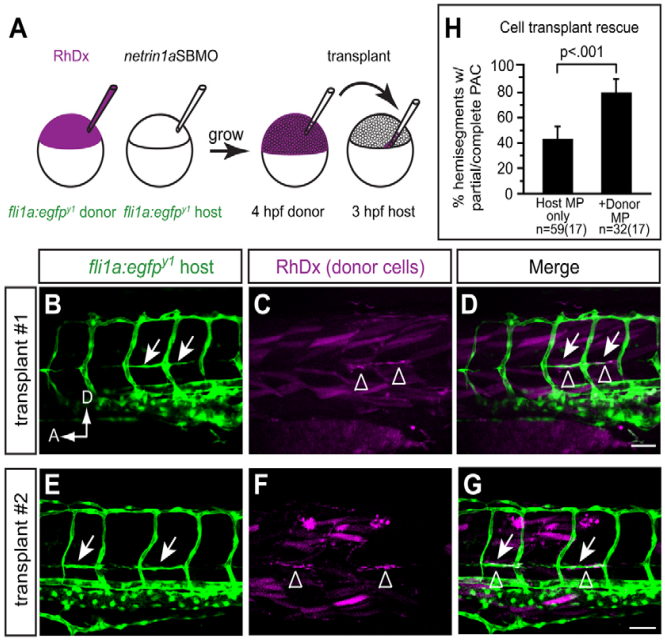

Fig. 3. Transplanting wild-type MPs at the HMS rescues PAC formation in *netrin 1a* morphants. (**A**) Scheme for heterochronic transplants. Rhodamine Dextran (RhDx) is injected into one-cell stage *fli1a:egfp*^{y1} zebrafish embryos (donor). *netrin1a*SBMO is injected into one-cell stage *fli1a:egfp*^{y1} embryos (host). Cells are transferred from the RhDx embryo at 4 hpf to the *netrin 1a* morphant host at 3 hpf at a location fated to include MPs. (**B-G**) Lateral views showing *fli1a:egfp*^{y1} and the lineage marker (RhDx) in two transplanted embryos. The PAC (arrows, B,E) forms in the same hemisegments that receive transplanted wild-type MPs (arrowheads, C,F). Confocal projections. (**H**) Quantitation of rescue in *netrin 1a* morphants showing presence of the PAC (partial or complete) in hemisegments that either received wild-type transplanted MPs or were populated only by morphant host MPs. Host MPs only, 42±9%; transplanted donor MPs, 78±10%. All values are mean±s.e.m.; *P*-value determined by Wilcoxon signed rank test. *n*, number of hemisegments (number of embryos). A, anterior; D, dorsal; MP, muscle pioneer. Scale bar: 50 μm.

dcc is expressed in motoneurons and is required for attraction of secondary sprouts at the HMS and for TD formation

There are several known Netrin 1 receptors: Deleted in colorectal cancer (Dcc), Neogenin, Unc5, Down syndrome cell adhesion molecule (Dscam) and integrin α6β4/α3β1 (Andrews et al., 2008; Cirulli and Yebra, 2007; Liu et al., 2009; Ly et al., 2008; Yebra et al., 2003). Of these, Dcc is the best studied, mediating many Netrin-dependent guidance decisions at the midline and elsewhere.

To test whether *dcc* is necessary for PAC formation, we examined PAC formation under two conditions: single morphants injected only with *plcg1*SBMO, or double morphants injected with *plcg1*SBMO and *dcc*TBMO (Suli et al., 2006). Loss of Dcc gave defects very similar to loss of Netrin 1a: secondary sprouts formed and grew dorsally as normal, but failed to turn laterally and then anteroposteriorly to form the PAC (Fig. 4A-B′). Similar to *netrin 1a* morphants, secondary sprouts formed at 90% of the intersomitic boundaries in the *plcg1 dcc* double morphants (*n*=123 hemisegments, 28 embryos). This is not significantly different from control *plcg1* morphants, where secondary sprouts formed at 97% of boundaries (*n*=96 hemisegments, 22 embryos) (Fig. 4C). However, whereas in *plcg1* single morphants only 17% of the sprouts failed to turn at the HMS, 82% of *plcg1 dcc* double-morphant sprouts failed to turn at the HMS to form a PAC (Fig. 4D). To rule out possible off-target effects of the *dcc*TBMO, we co-injected *dcc* mRNA with its first few codons mutated to prevent it from being targeted by the *dcc*TBMO. This mRNA rescued the PAC phenotype significantly and almost completely (Fig. 4E-G), demonstrating the specificity of the requirement for *dcc*. *netrin 1a* expression and MP formation were not impaired in *dcc* morphants (see Fig. S5 in the supplementary material). Altogether, these results designate Dcc as a receptor required for mediating Netrin 1a signaling in regulating the turning of the secondary sprouts at the HMS to form the PAC.

We next determined whether depletion of *dcc* phenocopies the defects in TD formation. As predicted, *dcc* morphants had impaired TD formation: uninjected controls formed a partial or complete TD in 95% of the hemisegments (*n*=63 hemisegments, 21 embryos), whereas in *dcc* morphants only 45% of hemisegments had a partial or complete TD (*n*=40 hemisegments, 11 embryos) (see Fig. S1D-F in the supplementary material). Thus, *dcc* depletion indeed leads to defects in lymphatic development.

dcc is expressed in the central nervous system but not in endothelial cells

To further understand how Netrin 1a-Dcc signaling mediates PAC formation, we examined *dcc* expression by mRNA ISH. If Netrin 1a-Dcc signaling acts in endothelial cells to guide them to the HMS, we would expect *dcc* expression in the secondary sprouts; however, we were unable to detect *dcc* mRNA in any endothelial cells. Instead, *dcc* is expressed in the brain and ventral spinal cord at 22 and 32 hpf (Fig. 5A,B). These results suggest that Netrin 1a-Dcc-mediated guidance of these sprouts is not endothelial cell autonomous but instead might be acting through neurons. Since Netrin-Dcc signaling is known to mediate axon guidance in many contexts, we hypothesized that in the zebrafish trunk it guides axons that in turn are necessary for PAC formation. If so, we would expect neurons with axons close to the HMS to express *dcc* prior to PAC formation. Single-cell dye labeling has shown that rostral primary motoneuron (RoP) axons extend ventrally along the center of the hemisegment, then turn along the HMS as early as 24 hpf (Eisen et al., 1986), with SMN axons following shortly thereafter. Other primary motoneurons include the caudal primary motoneurons (CaPs) and middle primary motoneurons (MiPs), named for their relative cell body positions in the spinal cord (Fig. 5C,D; Fig. 6A). At 55 hpf, we confirmed that the HMS is contacted by motoneuron axons (Fig. 5D). To determine if these motoneurons express *dcc*, we double labeled *hb9:GFP* embryos with anti-GFP

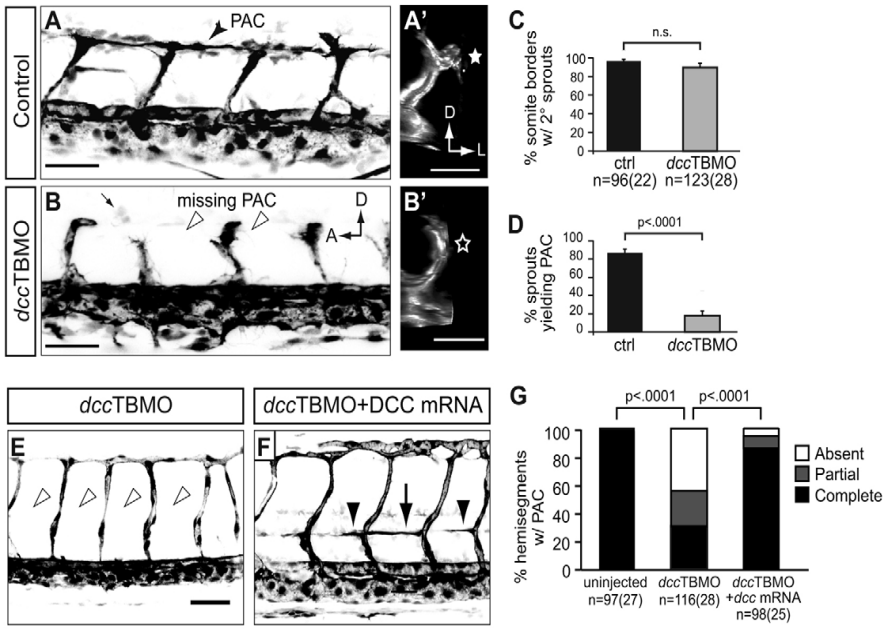

Fig. 4. *dcc* is required for turning of secondary sprouts at the HMS and injection of *dcc* mRNA rescues PAC formation in *dcc* morphants. (**A-B'**) 48 hpf *fli1a:egfp*^{y1} zebrafish embryos injected with (A,A') *plcg1* splice-blocking MO (*plcg1*SBMO) only (control) or (B,B') *plcg1*SBMO plus *dcc* translation-blocking MO (*dcc*TBMO). (A) Lateral view. In *plcg1* morphants, secondary sprouts grow from the PCV and turn at the HMS to form the PAC (arrowhead). (A') Transverse volume rendering of A showing mediolateral turn of secondary sprout. (star). (B) Lateral view. In embryos co-injected with *plcg1*SBMO and *dcc*TBMO, secondary sprouts form but fail to turn and form the PAC (arrowheads). (B') Transverse volume rendering of B showing failure of secondary sprout to turn laterally (star). (**C**) Secondary sprouts formed from the PCV were counted in 4-5 intersomitic boundaries per embryo between segments 7-11 in *plcg1* single morphants (control, 97±3%) and in *plcg1*SBMO/*dcc*TBMO double morphants (*dcc*TBMO, 90±5%), and showed no significant difference (n.s.). (**D**) Secondary sprouts that turned to form the PAC were counted in *plcg1* single morphants (87±5%) and *plcg1*/*dcc* double morphants (18±5%), which showed greatly reduced turning in the absence of Dcc. (**E**,**F**) Lateral views of 48 hpf *fli1a:egfp*^{y1} embryos injected with (E) *dcc*TBMO or (F) *dcc*TBMO and *dcc m*RNA. The PAC is absent in *dcc* morphants (E, arrowheads) and restored when *dcc* morphants are co-injected with *dcc* mRNA (F, arrow and arrowheads indicate complete and partial rescue, respectively). (**G**) Quantification of complete, partial or absent PAC. Uninjected: complete, 99±1%; partial, 1±1%; absent, 0±0%. *dcc* morphant: complete, 31±7%; partial, 25±6%; absent, 44±7%. *dcc* morphant + RNA: complete, 86±5%; partial, 9±4%; absent, 5±3%. All values are mean±s.e.m.; error bars show s.e.m.; *P*-value determined by Mann-Whitney U test (comparing absent PACs in G). *n*, number of hemisegments (number of embryos). A, anterior; D, dorsal; L, lateral; PAC, parachordal chain. Scale bars: 50 μm.

and performed ISH for the *dcc* transcript. Longitudinal sections of these embryos reveal clear localization of *dcc* mRNA in the cell bodies of primary motoneurons, and of RoP in particular (Fig. 5C).

netrin 1a and *dcc* morphants do not form axons at the HMS

Our hypothesis that Netrin 1a-Dcc signaling controls PAC formation indirectly through motoneuron axon guidance predicts these axons to be absent in *netrin 1a* and *dcc* morphants. We injected *netrin 1a* or *dcc* MOs into *hb9:GFP* transgenic embryos. Embryos were imaged at 55 hpf, when the axon fascicle at the HMS, which consists of RoP and secondary motor axons, is reliably visible in this transgenic line. Motoneuron axons were present at the HMS in 98% of uninjected control hemisegments (*n*=97 hemisegments, 32 embryos), but far less often in morphants: 27% of hemisegments in *netrin 1a* morphants (*n*=80 hemisegments, 20 embryos) and 51% of hemisegments in *dcc* morphants (*n*=63 hemisegments, 22 embryos) (Fig. 6B-D). Thus, *netrin 1a* and *dcc* are necessary for primary and secondary motor axon formation at the HMS.

Genetic disruption or laser ablation of motoneurons causes loss of the PAC

To directly test whether motoneuron axons at the HMS are crucial for PAC formation, we inhibited motoneuron formation by knocking down *olig2*, a basic helix-loop-helix (bHLH) transcription factor that is necessary for the development of motoneurons and oligodendrocytes (Lu et al., 2002; Park et al., 2002; Zhou and Anderson, 2002). We confirmed the published observation that *olig2* morphants do not form motor axons (Park et al., 2002) and then scored embryos for the PAC. The PAC was absent in only 6% of uninjected control hemisegments (*n*=71 hemisegments, 23 embryos), whereas in the *olig2* morphants the PAC was absent in 40% of hemisegments (*n*=166 hemisegments, 48 embryos) (Fig. 7A-F,J). We also found that injection of MOs targeting *islet1* (*isl1*), a gene necessary for motoneuron differentiation (Hutchinson and Eisen, 2006), also results in an absence of motoneurons and in a PAC defect, a phenotype also seen in *isl1* mutants (see Fig. S6 in the supplementary material). *isl1* morphants formed MPs normally and expressed *netrin 1a* at the HMS (see Fig. S5 in the supplementary material). Taken together these data provide strong evidence that motor axons are crucial for PAC formation.

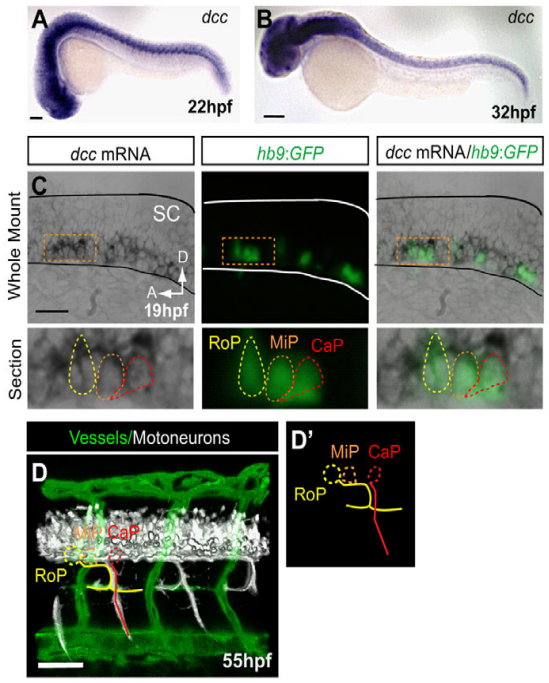

Fig. 5. *dcc* is not detected in endothelial secondary sprouts but is expressed in motoneurons with axons present at the HMS prior to PAC formation. (**A**,**B**) *dcc* mRNA is expressed in the ventral spinal cord at 22 and 32 hpf and is not detectable in the secondary sprouts or other trunk vasculature. (**C**) Whole-mount and longitudinal section of *hb9:GFP* transgenic zebrafish embryo showing *dcc* mRNA ISH (purple), where *hb9:GFP* labels only motoneurons at early stages (green). (**D**) Lateral volume rendering of *fli1a:dsRedEx*; *hb9:GFP* embryo at 55 hpf. Double transgenic labels endothelial cells (green) and motoneuron axons (white) in the trunk. Rostral primary motoneuron (RoP, yellow) axons are present at the HMS adjacent to the PAC. (**D′**) Outline of motoneurons alone. CaP, caudal primary motoneuron (red); MiP, middle primary motoneuron (orange; axon omitted for clarity). SC, spinal cord; A, anterior; D, dorsal. Scale bars: 100 μm.

Finally, we used laser ablation to specifically prevent motoneuron axon formation. We targeted motoneuron cell bodies in a single somite of *hb9:KikGR*; *fli1a:egfp*^{y1} zebrafish embryos (Fig. 7G-I). Since the fine motor axon fascicle at the HMS is not always visible in the *hb9:KikGR* line, we used the CaP axon fascicle projection as a measure of successful motoneuron ablation. Whereas SMNs can pathfind normally (albeit with a delay) after ablation of primary motoneurons (Pike et al., 1992), in successfully ablated segments we saw no secondary motor axons. We analyzed 29 laser-ablated embryos (81 hemisegments) in which the primary and secondary motoneuron axons were completely absent, discarding hemisegments in which the ablation was unsuccessful or partial. Among the 65 hemisegments in which the motoneurons were untreated and formed normally, only 5% had an absent PAC. By contrast, of the 16 hemisegments in which the CaP motoneuron was successfully ablated, 50% had an absent PAC (Fig. 7K). These results provide direct evidence that motoneurons are essential for PAC formation. Additionally, the less penetrant phenotype observed in *olig2* morphants and laser-ablated embryos compared with the *netrin 1a* and *dcc* morphants suggests that *netrin 1a* might act through both motoneuron-dependent and -independent pathways in PAC formation.

DISCUSSION

Our study demonstrates that *netrin 1a* expressed by MPs guides *dcc*-expressing RoP motoneuron axons and associated secondary motor axons to extend along the HMS. These axons at the HMS are required for secondary sprouts to turn, form the PAC, and ultimately develop into the zebrafish lymphatic system. In contrast to previous reports, including our own (Wilson et al., 2006), that focus on Netrin signaling directly to the endothelium to promote or inhibit angiogenesis (Bouvree et al., 2008; Epting et al., 2010; Larrivee et al., 2007; Lu et al., 2004; Park et al., 2004; Wilson et al., 2006), our data support an alternative model whereby *netrin 1a* guides endothelial cells indirectly, via motor axons. This report defines a novel in vivo role for Netrin, which was one of the first neural guidance cues identified, as essential to lymphatic vascular pathfinding and development through its function as an axonal pathfinding cue. We provide in vivo evidence that motor axons are required for endothelial cell guidance. Although it has been shown that motor axons are required for the expression of arterial and smooth muscle markers (Mukouyama et al., 2005), to the best of our knowledge this is the first demonstration of a direct requirement for axons in vascular guidance and lymphangiogenesis.

netrin 1a mRNA is expressed by the MPs from ~15 hpf through 32 hpf at the HMS (Fig. 2A-B′) (Lauderdale et al., 1997). Our cyclopamine and transplantation experiments underscore the necessary and sufficient role of MPs and their expression of *netrin 1a* at the HMS in the ultimate formation of the zebrafish lymphatic system (Figs 2, 3 and see Fig. S1 in the supplementary material). The spatiotemporal expression pattern of *netrin 1a* is coincident with two important events at the HMS: first, motoneuron axon elongation at the HMS at 24 hpf; second, the turning of the secondary sprouts at the HMS to form the PAC, which occurs at ~36 hpf.

We knocked down the Netrin receptor Dcc and showed that the resulting vascular defect phenocopied the *netrin 1a* morphant (Fig. 4). This shared phenotype is characterized by secondary sprouts that fail to turn at the HMS, form a PAC and develop a lymphatic system. However, we were unable to detect *dcc* expression in secondary sprouts by mRNA ISH (Fig. 5). This lack of *dcc* expression in endothelial cells is consistent with previous findings that *dcc* is mostly expressed in the central nervous system (Fricke and Chien, 2005; Gad et al., 1997). The absence of vascular *dcc* expression challenged our initial model in which Dcc mediates a direct pro-angiogenic effect of Netrin 1a, and led us to consider an alternative model. *dcc* is prominently expressed in RoP motoneurons, which project axons laterally and then along the HMS prior to PAC formation (Fig. 5). We therefore hypothesized that *dcc*-expressing RoP motoneuron axons course along the HMS, guided by their attraction to Netrin 1a produced by MPs, and that they, together with the SMNs that follow them, are crucial for directing the endothelial tips of the secondary sprouts to turn and form the PAC. We also recognize that Dcc is one of several Netrin receptors, and do not exclude the possibility that Netrin has a direct effect on the endothelial cells through an as yet undetermined receptor.

Consistent with this alternative model, motoneurons fail to elongate axons along the HMS in both *netrin 1a* and *dcc* morphants (Fig. 6). To demonstrate that motoneurons are crucial for PAC

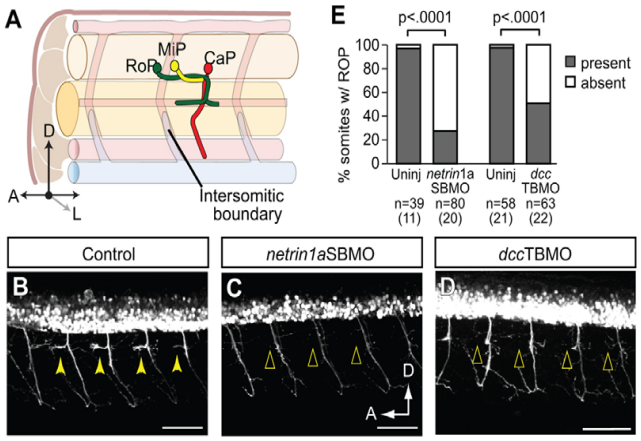

Fig. 6. RoP axons and associated secondary axons at the HMS do not form in *netrin 1a* and *dcc* morphants. (**A**) Diagram of RoP, middle primary (MiP) and caudal primary (CaP) axons at 36 hpf. (**B-D**) Lateral view of 55 hpf *hb9:GFP* zebrafish embryos injected with (B) no MO, (C) *netrin 1a* splice-blocking MO (*netrin1a*SBMO) or (D) *dcc* translation-blocking MO (*dcc*TBMO). Confocal projections. (B) Uninjected controls show axons at the HMS in almost every somite (arrowheads). In embryos injected with (C) *netrin1a*SBMO or (D) *dcc*TBMO, axons fail to form at the HMS (arrowheads). (**E**) Axons at the HMS were counted in 3-4 somites per embryo in segments 7-11 in control, *netrin1a*SBMO- and *dcc*TBMO-injected embryos. Uninjected, 97±3%; *netrin 1a* morphant, 27±7%. Uninjected, 98±2%; *dcc* morphant, 49±7%. All values are mean±s.e.m.; *P*-value determined by Mann-Whitney U test. *n*, number of hemisegments (number of embryos). A, anterior; D, dorsal; L, lateral; RoP, rostral primary motoneuron; MiP, middle primary motoneuron; CaP, caudal primary motoneuron. Scale bars: 50 μm.

formation, we disrupted motoneurons in a *netrin 1a*- and *dcc*-independent fashion. After disrupting motoneurons by *olig2* or *isl1* knockdown or laser ablation, secondary sprouts failed to make the turn along the HMS and form the PAC. Note that SMNs project out of the spinal cord a few hours after RoP and other primary motoneurons, with some of their axons fasciculating with the RoP axon, likely innervating the HMS. Since we are unable to distinguish the behavior of the SMN axons from that of RoP, it is possible that other axons in the RoP fascicle contribute to PAC formation. Thus, MPs and motor axons act in concert to alter the mediolateral and anteroposterior trajectory of secondary sprouts and guide them along the HMS.

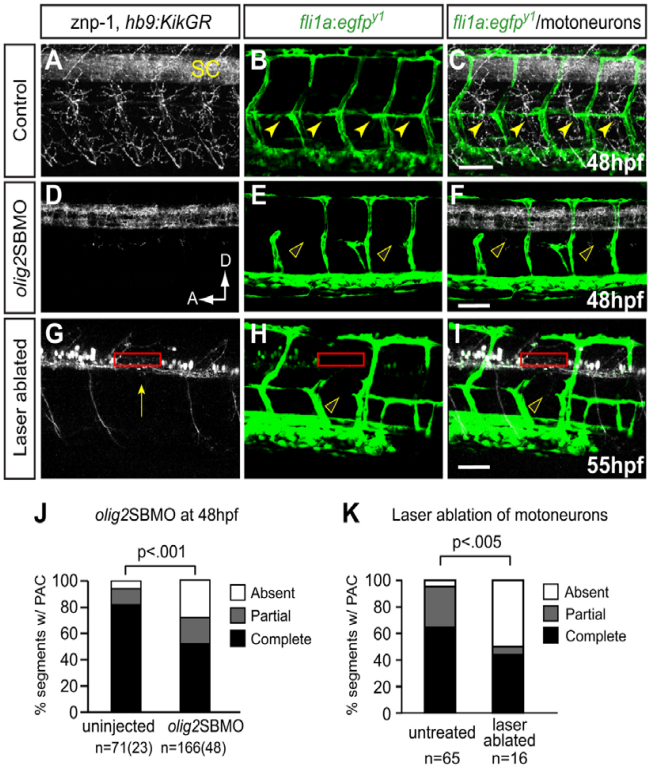

Fig. 7. Preventing differentiation or laser ablation of motoneurons prevents PAC formation. (**A-F**) Lateral views of 48 hpf *fli1a:egfp*^{y1} zebrafish embryos either uninjected or injected with *olig2* splice-blocking MO (*olig2*SBMO) showing labeled vessels (green) and neurons (znp-1 antibody, white). Confocal projection. (A) Motor axons grow ventrally from the spinal cord (SC) in controls. (B,C) The PAC forms normally in controls (arrowheads). (D) Motoneurons and their axons are absent in *olig2* morphants. (E,F) PAC does not form in *olig2* morphants (arrowheads). (**G-I**) Lateral view of 55 hpf *fli1a:egfp*^{y1}; *hb9:KikGR* after photoconversion, with vessels in green and motoneurons in white. Confocal projections. Motoneuron cell bodies were targeted by laser in one somite per embryo (red rectangle), resulting in ablation of motoneurons, (G) missing caudal primary motoneuron (CaP) axon (arrow), and (H,I) missing PAC (arrowhead) in that somite. (**J**) The PAC was scored in 4-5 somites per embryo in uninjected control embryos (complete, 82±6%; partial, 12±6%; absent, 6±4%) and *olig2* morphants (complete, 52±5%; partial, 20±3%; absent, 28±4%). All values are mean±s.e.m.; *P*-value determined by Mann-Whitney U test. *n*, number of hemisegments (number of embryos). (**K**) The number of somites with PACs was quantified in somites that were untreated or successfully laser ablated. Untreated: complete or partial, 95%; absent, 5%. Ablated: complete or partial, 50%; absent, 50%. *n*, number of hemisegments; *P*-value determined by Fischer's exact test. A, anterior; D, dorsal. Scale bars: 50 μm.

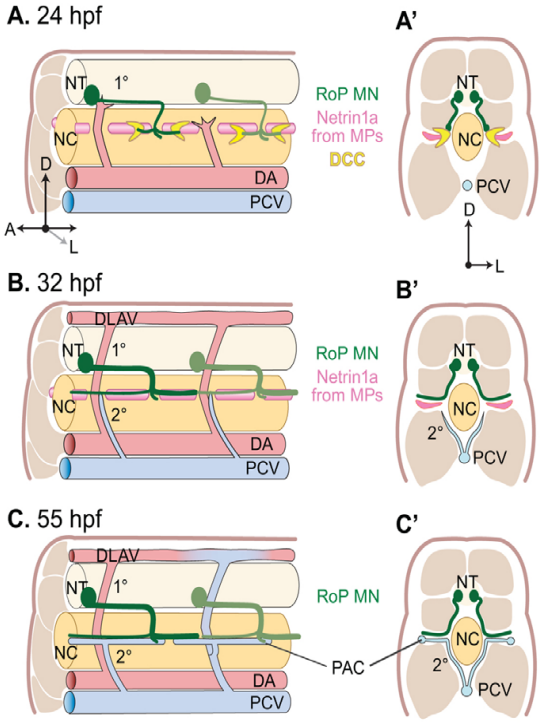

Fig. 8. Model of motoneuron axons and PAC formation. (**A-C'**) Oblique lateral view [A-C, for clarity only the rostral primary motoneuron (RoP) is shown] and transverse view [A'-C', dorsal aorta (DA) and primary sprouts omitted for clarity] of zebrafish trunk. (A,A') RoP motoneuron axons (green) expressing *dcc* (yellow) exit the spinal cord and extend ventrally towards the HMS at 24 hpf. *netrin 1a* (pink) is expressed by the MPs before and during motoneuron axon pathfinding. (B,B') *netrin 1a* expressed by MPs and *dcc* expressed by motoneuron axons are necessary for axon extension along the horizontal myoseptum (HMS). Secondary sprouts (blue) grow dorsally to the HMS. (C,C') The axons at the HMS are required for secondary sprouts to grow laterally at the HMS and then turn anteriorly and posteriorly along the HMS to form the PAC. A, anterior; D, dorsal; L, lateral; MPs, muscle pioneers; DLAV, dorsal longitudinal anastomotic vessel; PCV, posterior cardinal vein; PAC, parachordal chain; NT, neural tube; NC, notochord; 1°, primary sprouts; 2°, secondary sprouts.

We are not aware of any other instance in which a prototypic guidance cue, such as Netrin, is crucial for guiding axons, the subsequent trajectory of which plays an essential function in vascular pathfinding or lymphangiogenesis in vivo. We note that our group and others have proposed direct effects of Netrins on the vascular and lymphatic endothelium in cell culture experiments and in mouse and zebrafish studies (Bouvree et al., 2008; Larrivee et al., 2007; Lauderdale et al., 1997; Park et al., 2004; Wilson et al., 2006). One report suggests an endothelial cell-autonomous role for Netrin 1a-Unc5b signaling in promoting PAC formation (Epting et al., 2010). Since the PAC fails to form in 50% of hemisegments where the motoneuron axon has been ablated, but forms even less often in *netrin 1a* and *dcc* morphants, we do not exclude the possibility that Netrin 1a might have an additional direct effect on the endothelium of secondary sprouts via a non-Dcc receptor.

We have considered the molecular basis by which axons might provide crucial instructions for PAC formation and lymphangiogenesis (Fig. 8). Multiple permutations of potential interactions between the MPs, the RoP motoneuron axons and the endothelium of secondary sprouts are possible. For example, axons may provide either paracrine or juxtacrine cues that have direct effects on the endothelium, or induce MPs to express such endothelial factors. Without knowing whether the requirement for the axonal contribution at the HMS is a direct interaction with the endothelium or an indirect interaction with MPs, it is challenging to devise a rational cellular or biochemical strategy to systematically identify the crucial cell-cell interactions and the molecules that mediate these interactions. Given the essential role of PAC formation in lymphangiogenesis, as emphasized in this study (see Fig. S1 in the supplementary material), and the ease of scoring a loss-of-function phenotype, ongoing mutagenesis screens and future identification of the genes involved might provide valuable insight.

Reports from others have begun to identify the genetic basis for zebrafish with defective lymphangiogenesis (Geudens et al., 2010; Hermans et al., 2010; Hogan et al., 2009a; Hogan et al., 2009b; Kuchler et al., 2006). Most describe zebrafish mutants or morphants that have defects in the earliest step of lymphangiogenesis: secondary sprout formation. This process remains conspicuously intact in the absence of *netrin 1a*, *dcc* or RoP motoneurons. One report implicates Notch signaling as necessary for venous-to-lymphatic differentiation; when Notch signaling is reduced, PAC formation appears to be specifically inhibited (Geudens et al., 2010). This phenotype is strikingly similar to that we observe in the absence of motoneuron axons, in which secondary sprouts form from the PCV but do not turn at the HMS. These investigators suggested that Notch signaling disrupts venous-lymphatic specification, causing flow reversal in the primary sprouts. We found no evidence of flow reversal in the primary sprouts in our case, indicating that the failure of turning is not due to an absence of venous-lymphatic specification.

Our original interest in Netrin signaling and zebrafish lymphangiogenesis was stimulated by the desire to examine whether Netrins were a direct attractive lymphangiogenic cue. Our group has previously shown that Netrin 4 induces lymphangiogenesis in mammalian systems and potentially mediates this effect by directly activating α6β1 integrin receptor expressed by endothelial cells (Larrieu-Lahargue et al., 2010; Larrieu-Lahargue et al., 2011). Although we find that Netrins are required as a positive stimulator of PAC formation and lymphangiogenesis, this study led us to recognize that the requirement for Netrin 1a-Dcc signaling in lymphangiogenesis is through its originally described role as a mediator of axon pathfinding. Furthermore, we implicate Netrin 1a-Dcc signaling in a novel guidance mechanism wherein axons mediate vascular growth.

Acknowledgements

We thank D. Lim for graphical assistance; Hideo Otsuna for help with FluoRender; K. Thomas, F. Poulain, N. London, K. Kwan and A. Chan for critical reading of this manuscript; S. Hutchinson, L. Hale and J. Eisen for helpful discussions; G. King and the Centralized Zebrafish Animal Resource Facility; C. Rodesch, K. Carney and the Cell Imaging Core; Xiaoming Sheng at the Biostatistics Core for help with statistical analysis; M. Granato, J. Yost and N. Lawson for fish; L. Hale and J. Eisen for *isl1* morpholinos; B. Appel for *olig2* morpholino; Uwe Strähle for a partial *netrin 1a* clone; and M. Jurynec and D. Grunwald for the 4D9 antibody and cyclopamine. Funding: D.Y.L. and C.-B.C., NHLBI; B.W., Intramural Research Program of the NIH (NICHD). Deposited in PMC for release after 12 months.

Competing interests statement
The authors declare no competing financial interests.

Supplementary material
Supplementary material for this article is available at
http://dev.biologists.org/lookup/suppl/doi:10.1242/dev.068403/-/DC1

References

Adams, R. H. and Eichmann, A. (2010). Axon guidance molecules in vascular patterning. *Cold Spring Harb. Perspect. Biol.* **2**, a001875.
Andrews, G. L., Tanglao, S., Farmer, W. T., Morin, S., Brotman, S., Berberoglu, M. A., Price, H., Fernandez, G. C., Mastick, G. S., Charron, F. et al. (2008). Dscam guides embryonic axons by Netrin-dependent and -independent functions. *Development* **135**, 3839-3848.
Bates, D., Taylor, G. I., Minichiello, J., Farlie, P., Cichowitz, A., Watson, N., Klagsbrun, M., Mamluk, R. and Newgreen, D. F. (2003). Neurovascular congruence results from a shared patterning mechanism that utilizes Semaphorin3A and Neuropilin-1. *Dev. Biol.* **255**, 77-98.
Beattie, C. E. (2000). Control of motor axon guidance in the zebrafish embryo. *Brain Res. Bull.* **53**, 489-500.
Bedell, V. M., Yeo, S. Y., Park, K. W., Chung, J., Seth, P., Shivalingappa, V., Zhao, J., Obara, T., Sukhatme, V. P., Drummond, I. A. et al. (2005). roundabout4 is essential for angiogenesis in vivo. *Proc. Natl. Acad. Sci. USA* **102**, 6373-6378.
Bouvree, K., Larrivee, B., Lv, X., Yuan, L., DeLafarge, B., Freitas, C., Mathivet, T., Breant, C., Tessier-Lavigne, M., Bikfalvi, A. et al. (2008). Netrin-1 inhibits sprouting angiogenesis in developing avian embryos. *Dev. Biol.* **318**, 172-183.
Bussmann, J., Bos, F. L., Urasaki, A., Kawakami, K., Duckers, H. J. and Schulte-Merker, S. (2010). Arteries provide essential guidance cues for lymphatic endothelial cells in the zebrafish trunk. *Development* **137**, 2653-2657.
Carmeliet, P. and Tessier-Lavigne, M. (2005). Common mechanisms of nerve and blood vessel wiring. *Nature* **436**, 193-200.
Castets, M., Coissieux, M. M., Delloye-Bourgeois, C., Bernard, L., Delcros, J. G., Bernet, A., Laudet, V. and Mehlen, P. (2009). Inhibition of endothelial cell apoptosis by netrin-1 during angiogenesis. *Dev. Cell* **16**, 614-620.
Cirulli, V. and Yebra, M. (2007). Netrins: beyond the brain. *Nat. Rev. Mol. Cell Biol.* **8**, 296-306.
Dickson, B. J. (2002). Molecular mechanisms of axon guidance. *Science* **298**, 1959-1964.
Eisen, J. S., Myers, P. Z. and Westerfield, M. (1986). Pathway selection by growth cones of identified motoneurones in live zebrafish embryos. *Nature* **320**, 269-271.
Epting, D., Wendik, B., Bennewitz, K., Dietz, C. T., Driever, W. and Kroll, J. (2010). The Rac1 regulator ELMO1 controls vascular morphogenesis in zebrafish. *Circ. Res.* **107**, 45-55.
Flanagan-Steet, H., Fox, M. A., Meyer, D. and Sanes, J. R. (2005). Neuromuscular synapses can form in vivo by incorporation of initially aneural postsynaptic specializations. *Development* **132**, 4471-4481.
Fricke, C. and Chien, C. B. (2005). Cloning of full-length zebrafish dcc and expression analysis during embryonic and early larval development. *Dev. Dyn.* **234**, 732-739.
Furne, C., Rama, N., Corset, V., Chedotal, A. and Mehlen, P. (2008). Netrin-1 is a survival factor during commissural neuron navigation. *Proc. Natl. Acad. Sci. USA* **105**, 14465-14470.
Gad, J. M., Keeling, S. L., Wilks, A. F., Tan, S. S. and Cooper, H. M. (1997). The expression patterns of guidance receptors, DCC and Neogenin, are spatially and temporally distinct throughout mouse embryogenesis. *Dev. Biol.* **192**, 258-273.
Geudens, I., Herpers, R., Hermans, K., Segura, I., Ruiz de Almodovar, C., Bussmann, J., De Smet, F., Vandevelde, W., Hogan, B. M., Siekmann, A. et al. (2010). Role of delta-like-4/Notch in the formation and wiring of the lymphatic network in zebrafish. *Arterioscler. Thromb. Vasc. Biol.* **30**, 1695-1702.
Halpern, M. E., Thisse, C., Ho, R. K., Thisse, B., Riggleman, B., Trevarrow, B., Weinberg, E. S., Postlethwait, J. H. and Kimmel, C. B. (1995). Cell-autonomous shift from axial to paraxial mesodermal development in zebrafish floating head mutants. *Development* **121**, 4257-4264.
Hermans, K., Claes, F., Vandevelde, W., Zheng, W., Geudens, I., Orsenigo, F., De Smet, F., Gjini, E., Anthonis, K., Ren, B. et al. (2010). Role of synectin in lymphatic development in zebrafish and frogs. *Blood* **116**, 3356-3366.
Hogan, B. M., Bos, F. L., Bussmann, J., Witte, M., Chi, N. C., Duckers, H. J. and Schulte-Merker, S. (2009a). Ccbe1 is required for embryonic lymphangiogenesis and venous sprouting. *Nat. Genet.* **41**, 396-398.
Hogan, B. M., Herpers, R., Witte, M., Helotera, H., Alitalo, K., Duckers, H. J. and Schulte-Merker, S. (2009b). Vegfc/Flt4 signalling is suppressed by Dll4 in developing zebrafish intersegmental arteries. *Development* **136**, 4001-4009.
Hong, K., Hinck, L., Nishiyama, M., Poo, M. M., Tessier-Lavigne, M. and Stein, E. (1999). A ligand-gated association between cytoplasmic domains of UNC5 and DCC family receptors converts netrin-induced growth cone attraction to repulsion. *Cell* **97**, 927-941.
Hutchinson, S. A. and Eisen, J. S. (2006). Islet1 and Islet2 have equivalent abilities to promote motoneuron formation and to specify motoneuron subtype identity. *Development* **133**, 2137-2147.
Kuchler, A. M., Gjini, E., Peterson-Maduro, J., Cancilla, B., Wolburg, H. and Schulte-Merker, S. (2006). Development of the zebrafish lymphatic system requires VEGFC signaling. *Curr. Biol.* **16**, 1244-1248.
Kwan, K. M., Fujimoto, E., Grabher, C., Mangum, B. D., Hardy, M. E., Campbell, D. S., Parant, J. M., Yost, H. J., Kanki, J. P. and Chien, C. B. (2007). The Tol2kit: a multisite gateway-based construction kit for Tol2 transposon transgenesis constructs. *Dev. Dyn.* **236**, 3088-3099.
Larrieu-Lahargue, F., Welm, A. L., Thomas, K. R. and Li, D. Y. (2010). Netrin-4 induces lymphangiogenesis in vivo. *Blood* **115**, 5418-5426.
Larrieu-Lahargue, F., Welm, A. L., Thomas, K. R. and Li, D. Y. (2011). Netrin-4 activates endothelial integrin $\alpha 6\beta 1$. *Circ. Res.* (in press).
Larrivee, B., Freitas, C., Trombe, M., Lv, X., Delafarge, B., Yuan, L., Bouvree, K., Breant, C., Del Toro, R., Brechot, N. et al. (2007). Activation of the UNC5B receptor by Netrin-1 inhibits sprouting angiogenesis. *Genes Dev.* **21**, 2433-2447.
Larrivee, B., Freitas, C., Suchting, S., Brunet, I. and Eichmann, A. (2009). Guidance of vascular development: lessons from the nervous system. *Circ. Res.* **104**, 428-441.
Lauderdale, J. D., Davis, N. M. and Kuwada, J. Y. (1997). Axon tracts correlate with netrin-1a expression in the zebrafish embryo. *Mol. Cell. Neurosci.* **9**, 293-313.
Lawson, N. D., Mugford, J. W., Diamond, B. A. and Weinstein, B. M. (2003). phospholipase C gamma-1 is required downstream of vascular endothelial growth factor during arterial development. *Genes Dev.* **17**, 1346-1351.
Lejmi, E., Leconte, L., Pedron-Mazoyer, S., Ropert, S., Raoul, W., Lavalette, S., Bouras, I., Feron, J. G., Maitre-Boube, M., Assayag, F. et al. (2008). Netrin-4 inhibits angiogenesis via binding to neogenin and recruitment of Unc5B. *Proc. Natl. Acad. Sci. USA* **105**, 12491-12496.
Liu, G., Li, W., Wang, L., Kar, A., Guan, K. L., Rao, Y. and Wu, J. Y. (2009). DSCAM functions as a netrin receptor in commissural axon pathfinding. *Proc. Natl. Acad. Sci. USA* **106**, 2951-2956.
Lu, Q. R., Sun, T., Zhu, Z., Ma, N., Garcia, M., Stiles, C. D. and Rowitch, D. H. (2002). Common developmental requirement for Olig function indicates a motor neuron/oligodendrocyte connection. *Cell* **109**, 75-86.
Lu, X., Le Noble, F., Yuan, L., Jiang, Q., De Lafarge, B., Sugiyama, D., Breant, C., Claes, F., De Smet, F., Thomas, J. L. et al. (2004). The netrin receptor UNC5B mediates guidance events controlling morphogenesis of the vascular system. *Nature* **432**, 179-186.
Ly, A., Nikolaev, A., Suresh, G., Zheng, Y., Tessier-Lavigne, M. and Stein, E. (2008). DSCAM is a netrin receptor that collaborates with DCC in mediating turning responses to netrin-1. *Cell* **133**, 1241-1254.
Makita, T., Sucov, H. M., Gariepy, C. E., Yanagisawa, M. and Ginty, D. D. (2008). Endothelins are vascular-derived axonal guidance cues for developing sympathetic neurons. *Nature* **452**, 759-763.
Melani, M. and Weinstein, B. M. (2009). Common factors regulating patterning of the nervous and vascular systems. *Annu. Rev. Cell Dev. Biol.* **26**, 639-665.
Mukouyama, Y. S., Gerber, H. P., Ferrara, N., Gu, C. and Anderson, D. J. (2005). Peripheral nerve-derived VEGF promotes arterial differentiation via neuropilin 1-mediated positive feedback. *Development* **132**, 941-952.
Navankasattusas, S., Whitehead, K. J., Suli, A., Sorensen, L. K., Lim, A. H., Zhao, J., Park, K. W., Wythe, J. D., Thomas, K. R., Chien, C. B. et al. (2008). The netrin receptor UNC5B promotes angiogenesis in specific vascular beds. *Development* **135**, 659-667.
Park, H. C., Mehta, A., Richardson, J. S. and Appel, B. (2002). olig2 is required for zebrafish primary motor neuron and oligodendrocyte development. *Dev. Biol.* **248**, 356-368.
Park, K. W., Crouse, D., Lee, M., Karnik, S. K., Sorensen, L. K., Murphy, K. J., Kuo, C. J. and Li, D. Y. (2004). The axonal attractant Netrin-1 is an angiogenic factor. *Proc. Natl. Acad. Sci. USA* **101**, 16210-16215.
Pike, S. H. and Eisen, J. S. (1990). Identified primary motoneurons in embryonic zebrafish select appropriate pathways in the absence of other primary motoneurons. *J. Neurosci.* **10**, 44-49.
Pike, S. H., Melancon, E. F. and Eisen, J. S. (1992). Pathfinding by zebrafish motoneurons in the absence of normal pioneer axons. *Development* **114**, 825-831.
Rajasekharan, S. and Kennedy, T. E. (2009). The netrin protein family. *Genome Biol.* **10**, 239.
Sehnert, A. J., Huq, A., Weinstein, B. M., Walker, C., Fishman, M. and Stainier, D. Y. (2002). Cardiac troponin T is essential in sarcomere assembly and cardiac contractility. *Nat. Genet.* **31**, 106-110.
Suchting, S., Bicknell, R. and Eichmann, A. (2006). Neuronal clues to vascular guidance. *Exp. Cell Res.* **312**, 668-675.
Suli, A., Mortimer, N., Shepherd, I. and Chien, C. B. (2006). Netrin/DCC signaling controls contralateral dendrites of octavolateralis efferent neurons. *J. Neurosci.* **26**, 13328-13337.
Tang, X., Jang, S. W., Okada, M., Chan, C. B., Feng, Y., Liu, Y., Luo, S. W., Hong, Y., Rama, N., Xiong, W. C. et al. (2008). Netrin-1 mediates neuronal

survival through PIKE-L interaction with the dependence receptor UNC5B. *Nat. Cell Biol.* **10**, 698-706.

Wan, Y., Otsuna, H., Chien, C. B. and Hansen, C. (2009). An interactive visualization tool for multi-channel confocal microscopy data in neurobiology research. *IEEE Trans. Vis. Comput. Graph.* **15**, 1489-1496.

Weinstein, B. M. (2005). Vessels and nerves: marching to the same tune. *Cell* **120**, 299-302.

Wilson, B. D., Ii, M., Park, K. W., Suli, A., Sorensen, L. K., Larrieu-Lahargue, F., Urness, L. D., Suh, W., Asai, J., Kock, G. A. et al. (2006). Netrins promote developmental and therapeutic angiogenesis. *Science* **313**, 640-644.

Wolff, C., Roy, S. and Ingham, P. W. (2003). Multiple muscle cell identities induced by distinct levels and timing of hedgehog activity in the zebrafish embryo. *Curr. Biol.* **13**, 1169-1181.

Wythe, J. D., Jurynec, M. J., Urness, L. D., Jones, C. A., Sabeh, M. K., Werdich, A. A., Sato, M., Yost, H. J., Grunwald, D. J., Macrae, C. A. et al. (2011). Hadp1, a newly identified pleckstrin homology domain protein, is required for cardiac contractility in zebrafish. *Dis. Model. Mech.* **4** (in press).

Yaniv, K., Isogai, S., Castranova, D., Dye, L., Hitomi, J. and Weinstein, B. M. (2006). Live imaging of lymphatic development in the zebrafish. *Nat. Med.* **12**, 711-716.

Yebra, M., Montgomery, A. M., Diaferia, G. R., Kaido, T., Silletti, S., Perez, B., Just, M. L., Hildbrand, S., Hurford, R., Florkiewicz, E. et al. (2003). Recognition of the neural chemoattractant Netrin-1 by integrins alpha6beta4 and alpha3beta1 regulates epithelial cell adhesion and migration. *Dev. Cell* **5**, 695-707.

Zhou, Q. and Anderson, D. J. (2002). The bHLH transcription factors OLIG2 and OLIG1 couple neuronal and glial subtype specification. *Cell* **109**, 61-73.

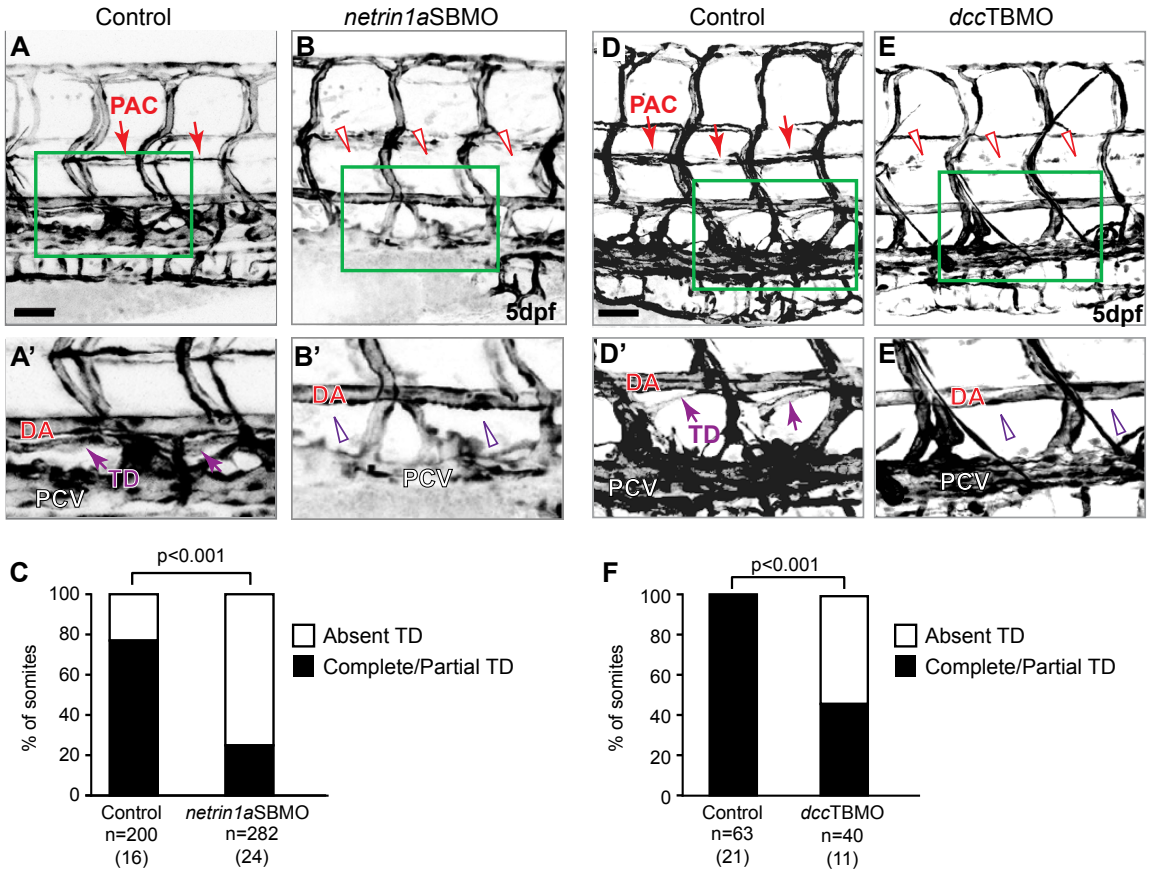

Figure S1. *netrin1a* and *dcc* morphants do not form a complete thoracic duct. (A,B,D,E) 5 dpf *fli1a:egfp*^{y1} larvae; reversed contrast, confocal projections. (A′,B′,D′,E′) Enlargements of the boxed regions from A,B,D,E. (A-A′,D-D′) The thoracic duct (TD) forms normally (arrows) between the dorsal aorta (DA) and posterior cardinal vein (PCV) in uninjected control embryos. (B,B′,E,E′) The TD is absent in *netrin1a*SBMO or *dcc*TBMO morphants (open arrowheads). (C,F) Quantitation of partial or complete TD formation in control embryos (77%), *netrin1a*SBMO morphants (25%) and *dcc*TBMO morphants (45±19%; mean±s.e.m.); *P*-values, Mann-Whitney U test. *n*, number of hemisegments (number of embryos). PAC, parachordal chain; DA, dorsal aorta; PCV, posterior cardinal vein. Scale bars: 50 μm.

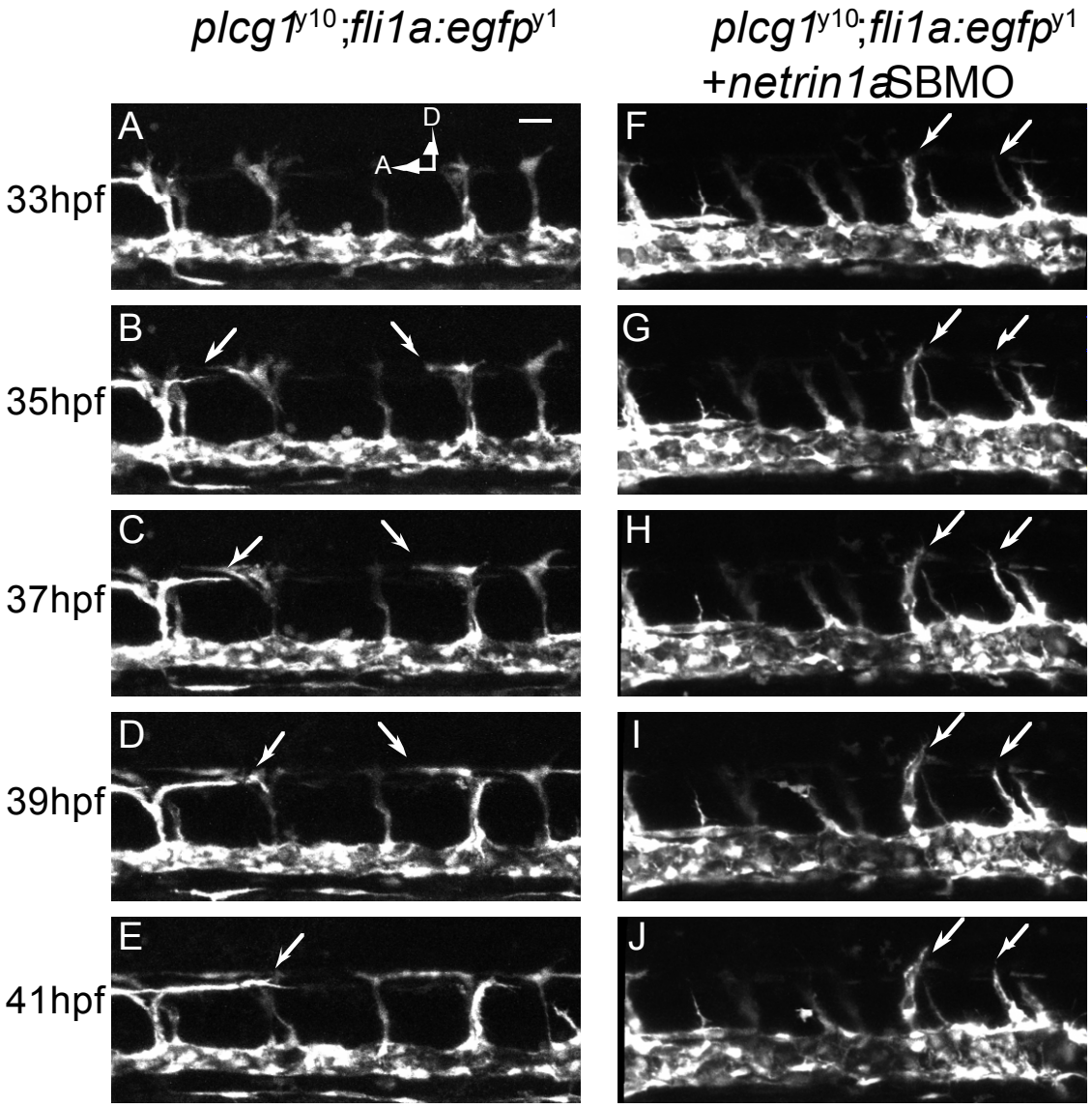

Figure S2. *netrin 1a* is required for secondary sprout elongation along the horizontal myoseptum. Selected frames spanning 8 hours of live time-lapse imaging of (A-E) a *plcg1*^{y10}; *fli1a:egfp*^{y1} embryo and (F-J) a *plcg1*^{y10}; *fli1a:egfp*^{y1} embryo injected with *netrin1a*SBMO1. Lateral views, confocal *z*-projections spanning both left and right sides. (A-E) In uninjected embryos, secondary sprouts have reached the horizontal myoseptum (HMS) and soon thereafter start to elongate along the anterior-posterior axis (arrows). (F-J) In the *netrin 1a* morphant, secondary sprouts have reached the HMS but fail to elongate anteroposteriorly (arrows). A, anterior; D, dorsal. Scale bar: 50 μm.

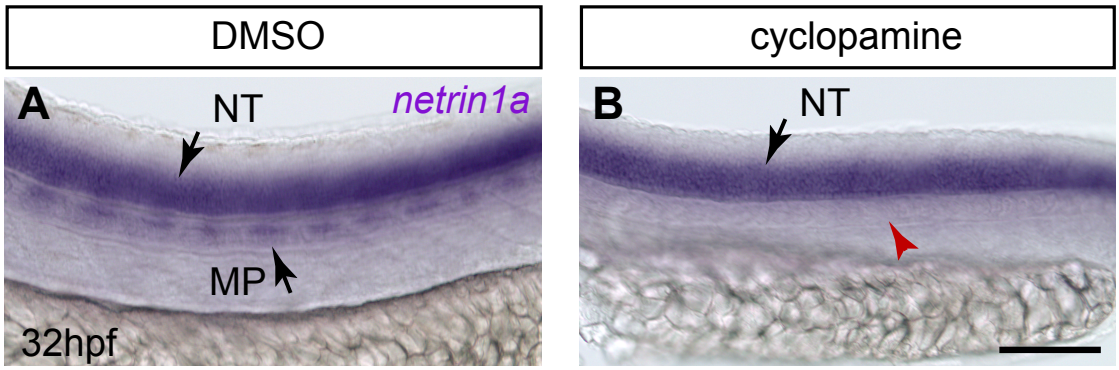

Figure S3. *netrin 1a* expression at the HMS is abolished in embryos treated with 50 *μ*M cyclopamine. Lateral view of in situ hybridizations at 32 hpf. (A) In 1% DMSO-treated controls, *netrin 1a* is expressed in the neural tube (NT) and muscle pioneers (MP) at the HMS (arrows). (B) *netrin 1a* is expressed in the NT but lost at the HMS (red arrowhead) in embryos that lack MPs following cyclopamine treatment. NT, neural tube; MP, muscle pioneer. Scale bar: 100 *μ*m.

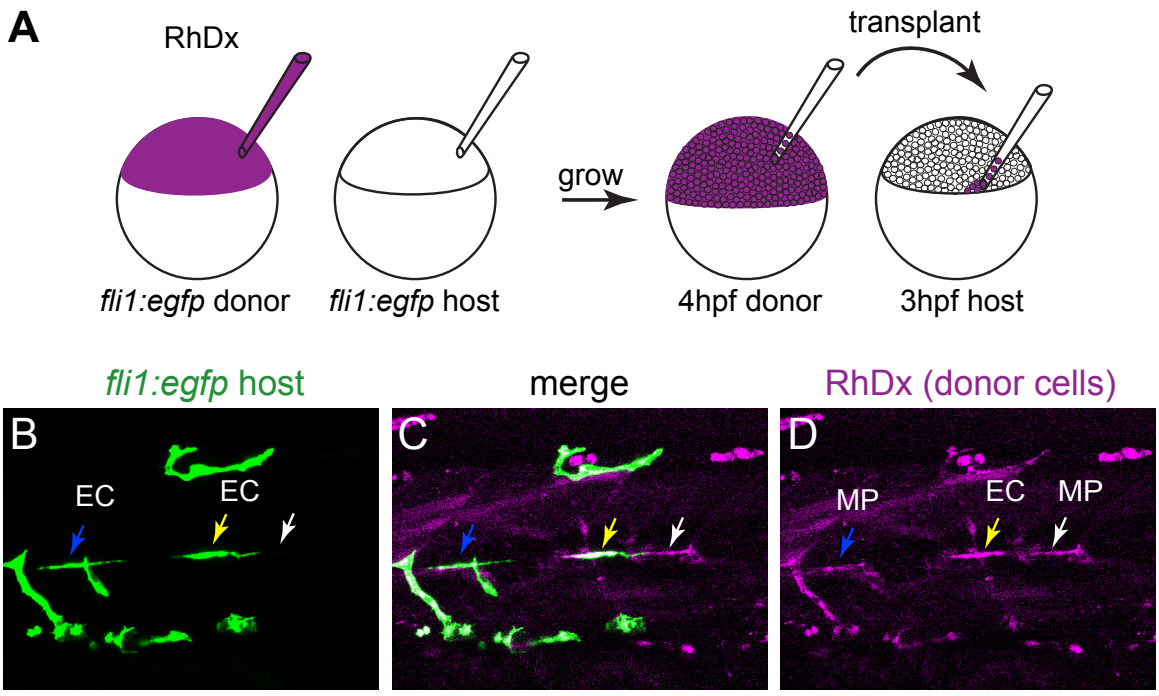

Figure S4. Distinguishing between transplanted muscle pioneers and transplanted endothelial cells. (A) Heterochronic transplant scheme used for this test: donor is labeled with Rhodamine Dextran (RhDx) and both donor and host are marked with *fli1a:egfp*^{y1}. (B-D) Live lateral views of a 48 hpf transplanted embryo. There are three classes of RhDx-positive cells at the HMS. (1) A RhDx^{+} GFP^{-} cell. This is a transplanted muscle pioneer (MP, white arrow). (2) A RhDx^{+} GFP^{+} cell in which the GFP and RhDx fluorescence coincide. This is a transplanted endothelial cell (EC, yellow arrow). (3) A RhDx^{+} cell adjacent to, but not coinciding with, a GFP^{+} cell. This is a transplanted MP adjacent to a host EC (blue arrow). For rescue experiments in which the host was not marked with *fli1a:egfp*^{y1}, class 3 combines with class 1; however, it is still possible to distinguish between transplanted MPs and transplanted ECs by looking for coincident GFP expression from the donor *fli1a:egfp*^{y1} transgene.

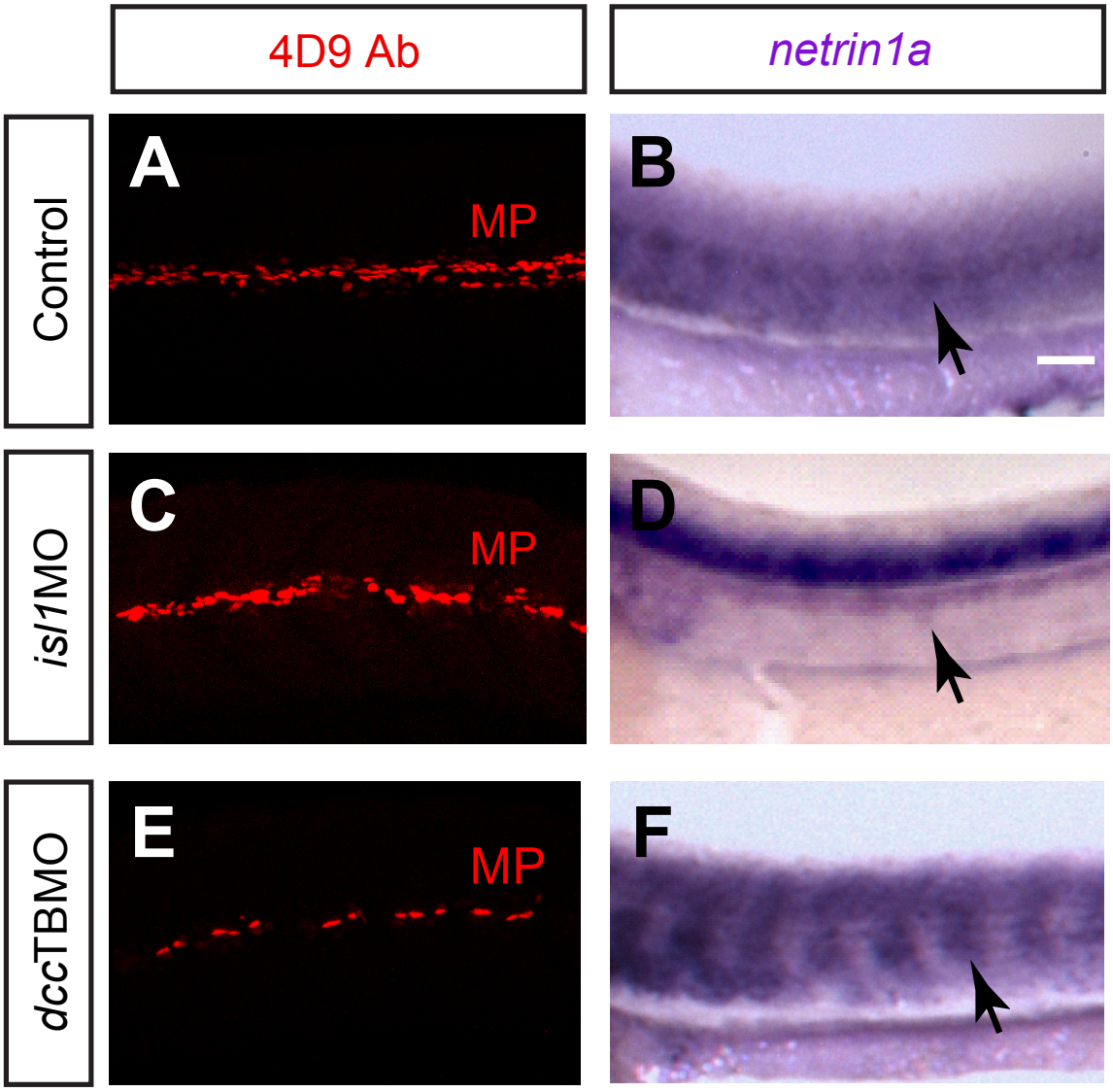

Figure S5. *dcc*TBMO morphants and *isl1* morphants form MPs and express *netrin 1a* at the HMS. (A,C,E) 32 hpf *fli1a:egfp*^{y1} embryos were antibody stained for MPs (4D9 anti-engrailed, red). (B,D,F) mRNA in situ hybridization for *netrin 1a* expression in 32 hpf embryos. (A,C,E) MPs are present at the HMS in (A) uninjected control embryos, (C) *dcc* morphants and (E) *isl1* morphants. (B,D,F) *netrin 1a* mRNA expression is present at the HMS (arrows) in (B) control embryos, (D) *dcc* morphants and (F) *isl1* morphants. MPs, muscle pioneers; A, anterior; D, dorsal. Scale bar: 100 μm.

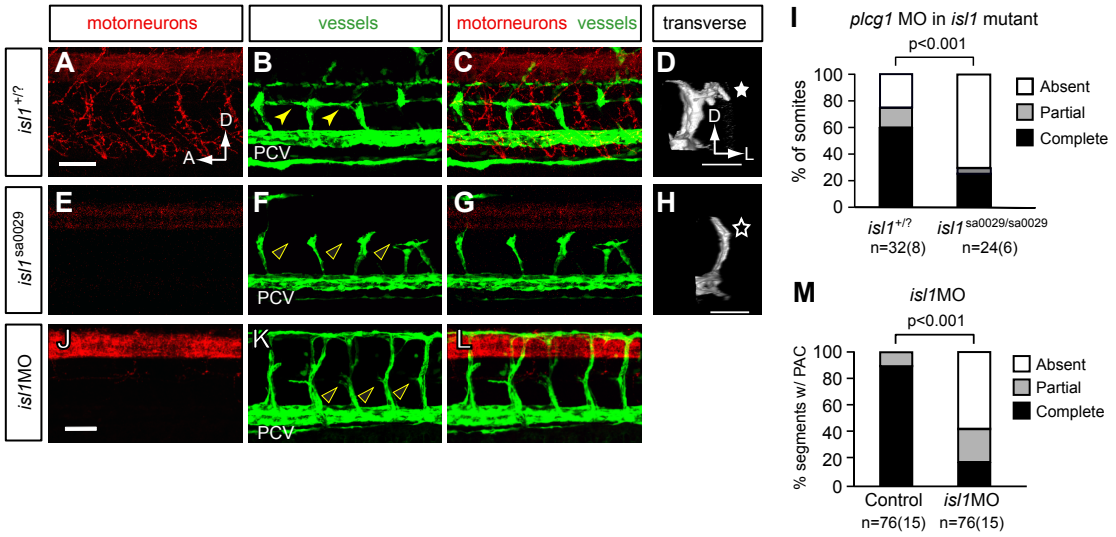

Figure S6. *Isl1* mutants and morphants form secondary sprouts but they do not turn to form a parachordal chain. (A-H) Lateral views of 48 hpf *isl1*$^{+/?}$; *fli1a:egfp*^{y1} or *isl1*$^{-/-}$; *fli1a:egfp*^{y1} embryos injected with *plcg1* morpholino and stained with znp-1 antibody. Confocal projections. (D,H) Volume renderings of a single hemisegment, transverse view. (A-D) In *plcg1* morpholino-injected *isl1*$^{+/?}$ sibs, motoneuron axons form (A), secondary sprouts grow from the posterior cardinal vein (PCV) (B) and turn at the HMS (filled star, D) to form the PAC (parachordal chain, solid yellow arrowheads, B). (E-H) In *plcg1* morpholino-injected *isl1*$^{-/-}$ mutants, secondary sprouts form and extend dorsally (F) but fail to turn (star, H) and form the PAC (arrowheads, F). (I) Quantitation of PAC formation in 4-5 somites per embryo of *plcg1* morpholino-injected *isl1* mutants and siblings. *plcg1*/*isl1*$^{+/?}$: complete, 60±16%; partial, 15±8%; absent, 25±13%. *plcg1*/*isl1*$^{-/-}$: complete, 25±15%; partial, 42±4%; absent, 71±14%. (J-L) Lateral views of 48 hpf *fli1a:egfp*^{y1} embryos injected with *isl1* morpholino and stained with znp-1 antibody. Confocal projections. In *isl1* morphants, motoneuron axons form (J) and the PAC does not form (arrowheads, K). (M) Quantitation of PAC formation in 4-5 somites per embryo. Uninjected control embryos: complete, 91±4%; partial, 9±4%; absent, 0±0%. *isl1* morphants: complete, 26±6%; partial, 32±8%; absent, 42±10%. All values are mean±s.e.m.; *P*-values by Mann-Whitney U test. *n*, number of hemisegments (number of embryos). A, anterior; D, dorsal; L, lateral. Scale bars: 50 μm.

CHAPTER 4

CONCLUDING REMARKS

In studying the mechanism by which Netrin-DCC signaling mediates PAC formation, we have demonstrated for the first time an example of axons guiding vessels. This project was started by Arminda Suli, a former graduate student in Chi-Bin Chien's lab working in collaboration with Dean Li who made the initial observation that Netrin1a and its receptors Unc5b and DCC were required for PAC formation. Together, we collaborated in figuring out the mechanism by which Netrin1a-DCC signaling mediates PAC formation.

First, I would like to address some of the potential mechanisms by which Netrin1a-Unc5b signaling may be acting in PAC formation. One possibility is that Unc5b acts cell autonomously in endothelial cells that form the PAC. However, I was unable to detect expression of Unc5b mRNA by *in situ* hybridization in endothelial cells before or during PAC development. Instead, expression was largely limited to the dorsal eye and fin folds prior to and during PAC development. Unc5b expression has been reported to be in ISVs at 24hpf (Epting et al., 2010), but we have not been able to duplicate this result.

It is possible that our *in situ* assay is not sensitive enough to detect very low levels of Unc5b expression in tissues other than the dorsal eye and fin folds. To definitively address whether or not Unc5b has an endothelial cell autonomous role in turning of the secondary sprouts in PAC formation, the most direct experiment would be to transplant

Unc5b deficient cells fated to become secondary sprouts into *fli1*:GFP host embryos. If these transplanted Unc5b deficient endothelial cells fail to turn at the HMS while the host wild-type cells turn to form a PAC, we can conclude that Netrin1a-Unc5b signaling is acting autonomously in secondary sprouts to mediate PAC turning. Conversely, if the Unc5b-deficient endothelial cells turn at the HMS to form a PAC, then we can conclude that Unc5b is not acting in secondary sprouts, but in another cell type.

Investigation of Netrin1a-DCC signaling in PAC formation revealed a critical role related to what these molecules were first recognized for: axon guidance. We found that Netrin1a-DCC signaling was not acting directly in endothelial cells, but instead, acting to first guide axons, which then subsequently guide PAC formation. In our Netrin1a and DCC depleted embryos, we observe a very specific PAC phenotype in which secondary sprouts form, but do not turn. Most known PAC defects arise instead from the failure of secondary sprouts to form from the PCV (Hermans et al., 2010; Hogan et al., 2009; Kuchler et al., 2006). Failure of secondary sprouts to turn has only been seen in one other case in PAC formation, which was determined to be a venous-lymphatic differentiation defect instead of a guidance defect (Geudens et al., 2010). The turning of the secondary sprouts is of great interest as the PAC is the one of the first lymphatic structures to be formed, and identifying the factors that drive this turn will provide factors important in lymphendothelial guidance, about which relatively little is known.

In mouse and Drosophila, Unc5c is expressed in motor neurons and mediates Netrin-dependent motor axon repulsion (Dillon et al., 2007; Keleman and Dickson, 2001). Interestingly, Unc5b morphants do not form axons at the HMS (data not shown), raising the possibility that Unc5b, like DCC, may be expressed in motor neuron axons

and is required for motor neuron axons to turn at the HMS. In order to test this hypothesis, Unc5b deficient cells fated to be RoPs should be transplanted into wild type embryos and assayed for axon formation at the HMS. If the Unc5 deficient transplanted motor neuron axons fail to turn at the HMS, then it can be concluded that Unc5 is required in motor neuron axons for turning at the HMS. Conversely, if the motor neuron axons form normally, then Unc5 is most likely acting in another cell type to mediate PAC formation.

Another interesting question is what is the mechanism that causes secondary sprouts to stop at the HMS in the absence of Netrin, Unc5 or DCC? In these morphants, the secondary sprouts do not overshoot the HMS by growing dorsally along the ISVs, and instead stall at the HMS. Perhaps there are repulsive cues expressed just dorsal the HMS that prevent further growth of secondary sprouts. Alternatively, the secondary sprouts may be growing away from a repulsive cue near the PCV, the signal at the HMS may be too weak to cause any further dorsal growth of the endothelial cells. In either case, it will be important to examine the expression of other guidance cues for clues as to what may direct these secondary sprouts to the HMS before the axons direct their turning.

To identify factors that are critical for turning of secondary sprouts, we are conducting an F3 mutagenesis screen on a Gal4 line, can be used to drive expression of a fluorescence marker specifically in the PCV, secondary sprouts and parachordal chain. To our knowledge, this is the only transgenic line that allows for clear visualization of these vascular structures without disrupting genes to inhibit primary sprout formation. To identify the factors derived from motor neurons required for PAC formation, we will screen for mutants that form secondary sprouts, but do not turn to form the PAC in order

and other genes important in lymphendothelial cell guidance.

A broader question is whether the requirement axons in vascular guidance is a phenomenon specific to motor neurons and the PAC, or is it a conserved mechanism that can drive parallel axonal and vascular patterning in other parts of the zebrafish and in other organisms? There are many areas in the body plan of several different organisms where axons and vessels follow parallel trajectories. It would not be surprising if axons guided vessels in such circumstances, given the guidance cues are conserved across multiple species.

I have thus far only shown an example where axons are required as a positive guidance structure to endothelial cells. Perhaps there are other instances where axons are required to act as "guard rails" to prevent vessels from growing into specific areas. or during certain times in development. For example, motor neurons in the zebrafish trunk extend in the middle of somites, whereas later growing vessels extend at the somitic boundary. It is conceivable these motor neurons may be important to keep the intersegmental vessels from growing into the somites. We know that they are not absolutely required as intersegmental vessels follow somitic boundaries normally in the absence of motor neurons. Or, axons may be the source of negative guidance factors that prevent vessels from growing into certain areas, for example, during retinal development, but then are down-regulated to later allow vasculature to invade the tissue.

If axons guide vessels, what types of guidance molecules would we expect to be mediating this interaction? It is likely that there are a variety of positive and negative cues, both secreted and expressed on the surface of the axons that function in endothelial cell guidance. It is also likely that the endothelial cells would not passively respond to

cues from the axon, but express different receptors at different times, to temporally regulate their response, just as axons do before and after spinal cord crossing. Axons can alter their response to their environment in many ways, for instance by changing expression of receptors or intracellular calcium levels. It is likely that endothelial cells do so as well. These suppositions stem largely from what is already known about and endothelial cell guidance.

In summary, our current model predicts that Netrin1a-Unc5b signaling is proangiogenic for PAC formation; however, it is unknown through what mechanisms this occurs. Further experimentation should reveal which cell types express Unc5b in order to mediate PAC formation. Additionally, we have determined that Netrin1a-DCC signaling first acts to guide motor neuron axons to the HMS, which then are subsequently required for turning of the secondary sprouts to form the PAC. The screen for mutants that have secondary sprouts that fail to turn will reveal molecules important in endothelial cell guidance and ideally, the factor from motor neuron axons that guides endothelial cells to the HMS. Finally, this work is significant in that this is the first time axons have been shown to be required for vascular patterning.

References

Dillon, A. K., Jevince, A. R., Hinck, L., Ackerman, S. L., Lu, X., Tessier-Lavigne, M. and Kaprielian, Z. (2007). UNC5C is required for spinal accessory motor neuron development. *Mol Cell Neurosci* **35**, 482-9.

Epting, D., Wendik, B., Bennewitz, K., Dietz, C. T., Driever, W. and Kroll, J. (2010). The Rac1 regulator ELMO1 controls vascular morphogenesis in zebrafish. *Circ Res* **107**, 45-55.

Geudens, I., Herpers, R., Hermans, K., Segura, I., Ruiz de Almodovar, C., Bussmann, J., De Smet, F., Vandevelde, W., Hogan, B. M., Siekmann, A. et al. (2010). Role of delta-like-4/Notch in the formation and wiring of the lymphatic network in zebrafish. *Arterioscler Thromb Vasc Biol* **30**, 1695-702.

Hermans, K., Claes, F., Vandevelde, W., Zheng, W., Geudens, I., Orsenigo, F., De Smet, F., Gjini, E., Anthonis, K., Ren, B. et al. (2010). Role of synectin in lymphatic development in zebrafish and frogs. *Blood* **116**, 3356-66.

Hogan, B. M., Bos, F. L., Bussmann, J., Witte, M., Chi, N. C., Duckers, H. J. and Schulte-Merker, S. (2009). Ccbe1 is required for embryonic lymphangiogenesis and venous sprouting. *Nat Genet* **41**, 396-8.

Keleman, K. and Dickson, B. J. (2001). Short- and long-range repulsion by the Drosophila Unc5 netrin receptor. *Neuron* **32**, 605-17.

Kuchler, A. M., Gjini, E., Peterson-Maduro, J., Cancilla, B., Wolburg, H. and Schulte-Merker, S. (2006). Development of the zebrafish lymphatic system requires VEGFC signaling. *Curr Biol* **16**, 1244-8.